

## Technical Report Documentation Page

<b>1. Report No.</b>	<b>2. Government Accession No.</b>	<b>3. Recipient's Catalog No.</b>
<b>4. Title and Subtitle</b> Design and In-situ Load Testing of Bridge No. 1330005 Route 3560 - Phelps County, MO	<b>5. Report Date</b> January 2005	
	<b>6. Performing Organization Code</b> UMR	
<b>7. Author/s</b> A. Rizzo, N. Galati, and A. Nanni	<b>8. Performing Organization Report No.</b>	
<b>9. Performing Organization Name and Address</b> Center for Infrastructure Engineering Studies University of Missouri - Rolla 223 ERL Rolla, MO 65409	<b>10. Work Unit No. (TRAIS)</b>	
	<b>11. Contract or Grant No.</b>	
<b>12. Sponsoring Organization Name and Address</b> University Transportation Center 223 Engineering Research Lab., Rolla, MO 65409-0710  Meramec Regional Planning Commission (MRPC) 4 Industrial Drive, St. James, MO 65559	<b>13. Type of report and period covered</b> Technical Report; 2003-04	
	<b>14. Sponsoring Agency Code</b> UTC, MRPC	
<b>15. Supplementary Notes</b>		
<b>16. Abstract</b> This report presents the use of Mechanically Fastened - Fiber Reinforced Polymers (MF-FRP) pre-cured laminates for the flexural strengthening of a concrete bridge. The system consists of pre-cured FRP laminates bolted onto the concrete surface in order to provide the necessary flexural reinforcement to girders and deck. The advantage of the technique is in the fact that it does not require any surface preparation prior to the installation of the FRP. The bridge selected for this project consists of four Reinforced Concrete (RC) girders monolithically cast with the deck. It can be assumed as simply-supported by the abutments. The bridge is load posted and located on Route 3560 in Phelps County, MO. The bridge analysis was performed for maximum loads determined in accordance to AASHTO Design specification, 17 <sup>th</sup> edition. The strengthening scheme was designed in compliance with the ACI 440.2R-02 design guide and on previous research work on MF-FRP system. The retrofitting of the structure was executed in Spring 2004. The MF-FRP strengthening technique was easily implemented and showed satisfactory performances. Two load tests, one prior to and another after the strengthening, were performed. A Finite Element Method (FEM) analysis was undertaken. The numerical model was able to represent the behavior of the bridge and demonstrated the safety of the proposed posting limit.		
<b>17. Key Words</b> Bridge, carbon fibers, concrete deck, FEM, fiber reinforced polymers, in-situ load test, load rating, Mechanically Fastened FRP pre-cured laminates, reinforced concrete, strengthening, structural evaluation.	<b>18. Distribution Statement</b> No restrictions. This document is available to the public through NTIC, Springfield, VA 22161	
<b>19. Security Classification (of this report)</b> Unclassified	<b>20. Security Classification (of this page)</b> Unclassified	<b>21. No. of Pages</b> 116



# CENTER FOR INFRASTRUCTURE ENGINEERING STUDIES

DESIGN AND IN-SITU LOAD TESTING OF  
OF BRIDGE No. 1330005  
ROUTE 3560 - PHELPS COUNTY, MO

by

**Andrea Rizzo**  
**Nestore Galati**  
**Antonio Nanni**

**January 2005**



### **Disclaimer**

The contents of this report reflect the views of the author(s), who are responsible for the facts and the accuracy of information presented herein. This document is disseminated under the sponsorship of the Center for Infrastructure Engineering Studies (CIES), University of Missouri-Rolla, in the interest of information exchange. CIES assumes no liability for the contents or use thereof.

The mission of CIES is to provide leadership in research and education for solving society's problems affecting the nation's infrastructure systems. CIES is the primary conduit for communication among those on the UMR campus interested in infrastructure studies and provides coordination for collaborative efforts. CIES activities include interdisciplinary research and development with projects tailored to address needs of federal agencies, state agencies, and private industry as well as technology transfer and continuing/distance education to the engineering community and industry.

Center for Infrastructure Engineering Studies (CIES)  
University of Missouri-Rolla  
223 Engineering Research Laboratory  
1870 Miner Circle  
Rolla, MO 65409-0710  
Tel: (573) 341-4497; fax -6215  
E-mail: [cies@umr.edu](mailto:cies@umr.edu)  
<http://www.cies.umr.edu/>

**RESEARCH INVESTIGATION**

**DESIGN AND IN-SITU LOAD TESTING OF BRIDGE No. 1330005**

**ROUTE 3560 – PHELPS COUNTY, MO**

**PREPARED FOR THE  
MISSOURI DEPARTMENT OF TRANSPORTATION**

**IN COOPERATION WITH THE  
UNIVERSITY TRANSPORTATION CENTER**

**Written By:**

Andrea Rizzo, MS Candidate

Nestore Galati, Research Engineer

Antonio Nanni, V. & M. Jones Professor of Civil Engineering

CENTER FOR INFRASTRUCTURE ENGINEERING STUDIES

UNIVERSITY OF MISSOURI – ROLLA

Submitted  
**January 2005**

The opinions, findings and conclusions expressed in this report are those of the principal investigators. They are not necessarily those of the Missouri Department of Transportation, U.S. Department of Transportation, Federal Highway Administration. This report does not constitute a standard, specification or regulation.

## **DESIGN AND IN-SITU LOAD TESTING OF BRIDGE No. 1330005**

### **ROUTE 3560 – PHELPS COUNTY, MO**

#### **Executive Summary**

This report presents the use of Mechanically Fastened - Fiber Reinforced Polymers (MF-FRP) pre-cured laminates for the flexural strengthening of a concrete bridge. The system consists of pre-cured FRP laminates bolted onto the concrete surface in order to provide the necessary flexural reinforcement to girders and deck. The advantage of the technique is in the fact that it does not require any surface preparation prior to the installation of the FRP.

The bridge selected for this project consists of four Reinforced Concrete (RC) girders monolithically cast with the deck. It can be assumed as simply-supported by the abutments. The bridge is load posted and located on Route 3560 in Phelps County, MO. The bridge analysis was performed for maximum loads determined in accordance to AASHTO Design specification, 17th edition. The strengthening scheme was designed in compliance with the ACI 440.2R-02 design guide and on previous research work on MF-FRP system.

The retrofitting of the structure was executed in Spring 2004. The MF-FRP strengthening technique was easily implemented and showed satisfactory performances. Two load tests, one prior to and another after the strengthening, were performed. A Finite Element Method (FEM) analysis was undertaken. The numerical model was able to represent the behavior of the bridge and demonstrated the safety of the proposed posting limit.

## **ACKNOWLEDGMENTS**

The project was made possible with the financial support received from the UMR - University Transportation Center on Advanced Materials, Center for Infrastructure Engineering Studies at the University of Missouri-Rolla and Meramec Regional Planning Commission (MRPC). Master Contractors installed the FRP systems. Strongwell provided the FRP materials.

The authors would like to acknowledge Rick Pilcher, District Liaison Engineer at MoDOT, and Lesley Bennish, Community Development Specialist from Meramec Regional Planning Commission, for their assistance in this project.

# TABLE OF CONTENTS

	Page
<b>TABLE OF CONTENTS</b> .....	<b>VI</b>
<b>LIST OF ILLUSTRATIONS</b> .....	<b>VIII</b>
<b>LIST OF TABLES</b> .....	<b>XIII</b>
<b>LIST OF TABLES</b> .....	<b>XIII</b>
<b>NOMENCLATURE</b> .....	<b>XIV</b>
<b>CONVERSION OF UNITS</b> .....	<b>XX</b>
<b>1. BACKGROUND</b> .....	<b>1</b>
1.1. Delta Regional Authority Program Project .....	1
1.2. Need for the Proposed Project.....	1
1.3. Description of the Project .....	2
1.4. Complementing Existing Regional Plans .....	3
1.5. Impact of the Project.....	4
<b>2. INTRODUCTION</b> .....	<b>5</b>
2.1. Objectives.....	5
2.2. Bridge Conditions.....	6
<b>3. STRUCTURAL ANALYSIS</b> .....	<b>13</b>
3.1. Load Combinations.....	13
3.2. Design Truck and Design Lanes.....	14
3.3. Slab Analysis .....	15
3.4. Girders Analysis .....	17
3.5. Analysis of the Abutments .....	20

<b>4. DESIGN .....</b>	<b>21</b>
4.1. Assumptions .....	21
4.2. Superstructure Design.....	23
4.2.1. Assumptions .....	23
4.2.2. Flexural Strengthening .....	24
4.2.3. Shear Check.....	28
4.2.4. Punching Shear Check .....	29
<b>5. FIELD EVALUATION .....</b>	<b>31</b>
5.1. Introduction .....	31
5.2. Additional Load Test .....	37
5.3. FEM Analysis.....	39
<b>6. LOAD RATING .....</b>	<b>45</b>
<b>7. CONCLUSIONS.....</b>	<b>49</b>
<b>8. REFERENCES .....</b>	<b>50</b>
<b>APPENDICES.....</b>	<b>52</b>
A. Prior to Strengthening Test Results.....	53
B. After Strengthening Test Results.....	62
C. Comparison between prior to and after Strengthening Normalized Results.....	83
D. Dynamic Test Results .....	87
E. Installation of the MF-FRP Strengthening System.....	92

## LIST OF ILLUSTRATIONS

Figure	Page
2.1. Bridge No. 1330005 .....	5
2.2. Condition of the Superstructure .....	7
2.3. Condition of Deck and Abutments.....	7
2.4. Material Characterization of the Concrete.....	8
2.5. Material Characterization of the Steel Bars .....	9
2.6. Longitudinal View of the Bridge .....	10
2.7. Plan View of the Bridge .....	11
2.8. Details of the Inspected Sections .....	11
2.9. Shear Reinforcement in the Outer Girders (G1 and G4).....	12
2.10. Shear Reinforcement in the Inner Girders (G2 and G3).....	12
3.1. Truck Load and Truck Lanes .....	14
3.2. Loading Conditions .....	15
3.3. Slab Load Conditions .....	16
3.4. Slab Transversal Bending Moment Distribution .....	16
3.5. Girders Load Conditions for Analysis and Design .....	17
3.6. Interior Girder Bending Moment Diagrams Envelopes .....	19
3.7. Interior Girder Shear Diagrams Envelopes.....	19
4.1. Details of the Connection Concrete-FRP .....	22
4.2. Girder Strengthened Section .....	26
4.3. Strengthening of the Deck .....	26
4.4. Pattern of the Bolts.....	27

4.5. Diagram of the Capacity of the Beam at the Ultimate Load Conditions.....	28
5.1. Load Tests prior to and after Strengthening on Bridge No.1330005 .....	31
5.2. Legal Trucks Used in the Load Tests .....	33
5.3. LVDT Positions in the Load Test Prior to Strengthening .....	34
5.4. LVDT and Strain Gage Positions in the Load Test after Strengthening .....	35
5.5. Mid-span Displacement, Pass #3 and Rear Axle in the Mid-span .....	36
5.6. Mid-span Strain in the FRP Laminates, Pass #3 Stop #3 .....	36
5.7. After Strengthening Displacements at 13.4 <i>m/s</i> (30 <i>MPH</i> ) .....	38
5.8. Live Load Impact Factor <i>I</i> versus Truck Speed .....	38
5.9. FEM Model Geometry (I).....	41
5.10. FEM Model Geometry (II).....	42
5.11. Comparison of Experimental and Analytical Results for Mid-span Displacement, Pass #3 and Rear Axle in the Mid-span.....	43
5.12. Comparison of Experimental and Analytical Results for Strain in the FRP Fastened on the Girders at Mid-span, Pass #3 and Stops #1, #2 and #3 .....	44
5.13. Comparison of Experimental and Analytical Results for Strain in the Longitudinal Direction in the FRP Fastened on the Girders, Pass #3 Stop #3.....	44
A. 1. Prior to Strengthening Mid-span Displacement, Pass #1 .....	54
A. 2. Prior to Strengthening Mid-span Displacement, Pass #2 .....	54
A. 3. Prior to Strengthening Mid-span Displacement, Pass #3 .....	55
A. 4. Prior to Strengthening Mid-span Displacement, Pass #4 .....	55
A. 5. Prior to Strengthening Mid-span Displacement, Pass #5 .....	56
A. 6. Prior to Strengthening Displacement Distribution, Pass #1 Stop #1.....	56
A. 7. Prior to Strengthening Displacement Distribution, Pass #1 Stop #2.....	57
A. 8. Prior to Strengthening Displacement Distribution, Pass #2 Stop #1.....	57

A. 9. Prior to Strengthening Displacement Distribution, Pass #2 Stop #2.....	58
A. 10. Prior to Strengthening Displacement Distribution, Pass #3 Stop #1.....	58
A. 11. Prior to Strengthening Displacement Distribution, Pass #3 Stop #2.....	59
A. 12. Prior to Strengthening Displacement Distribution, Pass #4 Stop #1.....	59
A. 13. Prior to Strengthening Displacement Distribution, Pass #4 Stop #2.....	60
A. 14. Prior to Strengthening Displacement Distribution, Pass #5 Stop #1.....	60
A. 15. Prior to Strengthening Displacement Distribution, Pass #5 Stop #2.....	61
B. 1. After Strengthening Mid-span Displacement, Pass #1 .....	63
B. 2. After Strengthening Mid-span Displacement, Pass #2 .....	63
B. 3. After Strengthening Mid-span Displacement, Pass #3 .....	64
B. 4. After Strengthening Mid-span Displacement, Pass #4 .....	64
B. 5. After Strengthening Mid-span Displacement, Pass #5 .....	65
B. 6. After Strengthening Displacement Distribution, Pass #1 Stop #1 .....	65
B. 7. After Strengthening Displacement Distribution, Pass #1 Stop #2 .....	66
B. 8. After Strengthening Displacement Distribution, Pass #1 Stop #3 .....	66
B. 9. After Strengthening Displacement Distribution, Pass #2 Stop #1 .....	67
B. 10. After Strengthening Displacement Distribution, Pass #2 Stop #2.....	67
B. 11. After Strengthening Displacement Distribution, Pass #2 Stop #3.....	68
B. 12. After Strengthening Displacement Distribution, Pass #3 Stop #1.....	68
B. 13. After Strengthening Displacement Distribution, Pass #3 Stop #2.....	69
B. 14. After Strengthening Displacement Distribution, Pass #3 Stop #3.....	69
B. 15. After Strengthening Displacement Distribution, Pass #4 Stop #1.....	70
B. 16. After Strengthening Displacement Distribution, Pass #4 Stop #2.....	70
B. 17. After Strengthening Displacement Distribution, Pass #4 Stop #3.....	71

B. 18. After Strengthening Displacement Distribution, Pass #5 Stop #1.....	71
B. 19. After Strengthening Displacement Distribution, Pass #5 Stop #2.....	72
B. 20. After Strengthening Displacement Distribution, Pass #5 Stop #3.....	72
B. 21. Strain in the FRP Strengthening on the Girders at Mid-span, Pass #1 .....	73
B. 22. Strain in the FRP Strengthening on the Girders at Mid-span, Pass #2 .....	73
B. 23. Strain in the FRP Strengthening on the Girders at Mid-span, Pass #3 .....	74
B. 24. Strain in the FRP Strengthening on the Girders at Mid-span, Pass #4 .....	74
B. 25. Strain in the FRP Strengthening on the Girders at Mid-span, Pass #5 .....	75
B. 26. Strain Distribution in the FRP along the Girders, Pass #1 Stop #1 .....	75
B. 27. Strain Distribution in the FRP along the Girders, Pass #1 Stop #2.....	76
B. 28. Strain Distribution in the FRP along the Girders, Pass #1 Stop #3.....	76
B. 29. Strain Distribution in the FRP along the Girders, Pass #2 Stop #1 .....	77
B. 30. Strain Distribution in the FRP along the Girders, Pass #2 Stop #2.....	77
B. 31. Strain Distribution in the FRP along the Girders, Pass #2 Stop #3.....	78
B. 32. Strain Distribution in the FRP along the Girders, Pass #3 Stop #1 .....	78
B. 33. Strain Distribution in the FRP along the Girders, Pass #3 Stop #2.....	79
B. 34. Strain Distribution in the FRP along the Girders, Pass #3 Stop #3.....	79
B. 35. Strain Distribution in the FRP along the Girders, Pass #4 Stop #1 .....	80
B. 36. Strain Distribution in the FRP along the Girders, Pass #4 Stop #2.....	80
B. 37. Strain Distribution in the FRP along the Girders, Pass #4 Stop #3.....	81
B. 38. Strain Distribution in the FRP along the Girders, Pass #5 Stop #1 .....	81
B. 39. Strain Distribution in the FRP along the Girders, Pass #5 Stop #2.....	82
B. 40. Strain Distribution in the FRP along the Girders, Pass #5 Stop #3.....	82
C. 1. Mid-span Displacement prior to and after the Strengthening, Pass #1 and Rear Axle	

in the Mid-span .....	84
C. 2. Mid-span Displacement prior to and after the Strengthening, Pass #2 and Rear Axle in the Mid-span .....	84
C. 3. Mid-span Displacement prior to and after the Strengthening, Pass #3 and Rear Axle in the Mid-span .....	85
C. 4. Mid-span Displacement prior to and after the Strengthening, Pass #4 and Rear Axle in the Mid-span .....	85
C. 5. Mid-span Displacement prior to and after the Strengthening, Pass #5 and Rear Axle in the Mid-span .....	86
D. 1. After Strengthening Displacements at 2.2 <i>m/s</i> (5 <i>MPH</i> ) .....	88
D. 2. After Strengthening Displacements at 4.5 <i>m/s</i> (10 <i>MPH</i> ) .....	88
D. 3. After Strengthening Displacements at 8.9 <i>m/s</i> (20 <i>MPH</i> ) .....	89
D. 4. After Strengthening Displacements at 13.4 <i>m/s</i> (30 <i>MPH</i> ) .....	89
D. 5. After Strengthening Strain in the FRP Laminates at 2.2 <i>m/s</i> (5 <i>MPH</i> ) .....	90
D. 6. After Strengthening Strain in the FRP Laminates at 4.5 <i>m/s</i> (10 <i>MPH</i> ) .....	90
D. 7. After Strengthening Strain in the FRP Laminates at 8.9 <i>m/s</i> (20 <i>MPH</i> ) .....	91
D. 8. After Strengthening Strain in the FRP Laminates at 13.4 <i>m/s</i> (30 <i>MPH</i> ) .....	91
E. 1. Drilling of the Pre-cured FRP Laminates.....	93
E. 2. Positioning of the Pre-cured FRP Laminates .....	93
E. 3. Drilling of the Holes in the Concrete .....	93
E. 4. Fastening Procedure.....	94
E. 5. Bridge No. 1330005 after Strengthening .....	94

## LIST OF TABLES

Table	Page
2.1. Geometry of the Bridge .....	10
3.1. Distribution Coefficient for the Girders .....	18
3.2. Interior Girder Bending Moments and Shear Forces .....	18
4.1. Material Properties .....	21
4.2. Geometrical Properties and Internal Steel Reinforcement .....	24
4.3. Strengthening Summary .....	25
4.4. Superstructure Shear Capacity .....	29
6.1. Maximum Shear and Moment due to Live Load for the Deck .....	46
6.2. Maximum Shear and Moment due to Live Load for the Girders.....	47
6.3. Rating Factor for the Deck (Bending Moment) .....	47
6.4. Rating Factor for the Deck (Shear) .....	47
6.5. Rating Factor for the Girders (Bending Moment).....	48
6.6. Rating Factor for the Girders (Shear).....	48

## NOMENCLATURE

$ADT$	Annual Daily Traffic
$A_g$	Gross Area of a Section
$A_s$	Area of the Generic Tensile Non-prestressed Steel Reinforcement
$A_{s,slab\ long.}$	Area of the Longitudinal Tensile Non-prestressed Steel Reinforcement of the Deck
$A_{s,slab\ transv.}$	Area of the Transverse Tensile Non-prestressed Steel Reinforcement of the Deck
$A_{s,web}$	Area of the Longitudinal Tensile Non-prestressed Steel Reinforcement of the Girders Web
$A_{tire}$	Area of the Print of a Wheel according to AASHTO (2002): $A_{tire} = l_{tire} w_{tire}$
$A_1$	Factor for Dead Loads
$A_2$	Factor for Live Loads
$b_0$	Perimeter of Critical Section
$b_w$	Web Width
$B$	Design Flange Width for a Girder according to AASHTO (2002) Section 4.6.2.6.1
$B^{Ext}$	Design Flange Width for an Interior Girder according to AASHTO (2002) Section 4.6.2.6.1
$B^{Int}$	Design Flange Width for an Exterior Girder according to AASHTO (2002) Section 4.6.2.6.1
$c.o.v._c$	Coefficient of Variation for the Compressive Strength $f'_c$ of Concrete: $c.o.v._c = \frac{SD_c}{f'_c}$
$c.o.v._y$	Coefficient of Variation for the Specified Yield Strength $f_y$ of Non-

prestressed Steel Reinforcement:  $c.o.v._y = \frac{f_y}{SD_y}$

$C$	Capacity of the Member
$C_E$	Environmental Reduction Factor according to ACI 440 Table 7.1: for Carbon Plate Exposed in Exterior Aggressive Ambient $C_E = 0.85$
$d$	Effective Depth of the Steel Reinforcement for a Generic Section
$d_c$	Length of the Cantilever Deck
$d_g$	Spacing between Girders on Center
$d_{slab\ long.}$	Effective Depth of the Longitudinal Tensile Non-prestressed Steel Reinforcement of the Deck
$d_{slab\ transv.}$	Effective Depth of the Transverse Tensile Non-prestressed Steel Reinforcement of the Deck
$d_{web}$	Effective Depth of the Longitudinal Tensile Non-prestressed Steel Reinforcement of the Girders Web
$D$	Dead Load of the Bridge
$D_i$	Part of Deck between the Girders No. $i$ and $i+1$ with $i=1,2,3$
$D_L$	Distribution Length of the Lane Lad in the Transverse Direction
$D_p$	Distance between Two Wheels of the Truck in the Transverse Direction
$E_c$	Modulus of Elasticity of Concrete according ACI 318-02 Section 8.5.1: $E_c = 57000\sqrt{f'_c}$ $psi$ with $[f'_c] = [psi]$
$E_f$	Modulus of Elasticity of the Pre-cured FRP Laminate
$E_s$	Modulus of Elasticity of Non-prestressed Steel Reinforcement
$f'_c$	Specified Compressive Strength of Concrete
$f_{fu}$	Design Tensile Strength of the Pre-cured FRP Laminate: $f_{fu} = C_E f_{fu}^*$
$f_{fu}^*$	Guaranteed Tensile Strength of the Pre-cured FRP Laminate as Reported by the Manufacturer

$f_y$	Specified Yield Strength of Non-prestressed Steel Reinforcement
$F_{FRP}$	Maximum Axial Load that the Pre-cured FRP Laminate Experiences at Ultimate Conditions
$G_i$	Girder No. $i$ with $i = 1, 2, 4$
$h$	Overall Thickness of Member
$h_b$	Embedment Depth of the Anchor
$h_c$	Vertical Distance between Supports of the Wall
$H_d$	Height of the Deck
$H_g$	Height of the Girders Web
$H_o$	Height of the Deck Overlay
$I$	Live Load Impact Factor: $I = \frac{50}{l_d + 125} \leq 0.30$ where $[l_d] = [ft]$
$I_{experimental, i}$	Live Load Impact Factor Measured during the Load Test after Strengthening in the Pass No. $i$ with $i = Pass \#1, Pass \#2..Pass \#5$
$k$	Effective Length Factor according to ACI 318-02 Section 14.5.2: $k = 2.0$ for Walls Not Braced against Lateral Translation
$K_a$	Generalized Stiffness of the Bridge after Strengthening
$K_p$	Generalized Stiffness of the Bridge Prior to Strengthening
$l_c$	Clear Span of the Bridge
$l_d$	Design Length of the Bridge
$l_{tire}$	Size of the Print of a Wheel in the Longitudinal Direction according to AASHTO (2002)
$L$	Live Load Applied on the Bridge. The Same Symbol is Used in Some Figures to Indicate the Design Span of the Bridge
$M_n$	Nominal Moment Strength at Section
$M_s$	Unfactored Moment due to the Most Demanding Load Condition for a Structural Element

$M_u$	Ultimate (Factored) Moment due to the Most Demanding Load Condition for a Structural Element
$n_{b,\min}$	Minimum Number of Fastener to Anchor a Pre-cured FRP laminate so that Failure in Tension Controls: $n_{b,\min} = \frac{F_{FRP}}{R_b}$
$P$	Generic Concentrated Load Applied to a Structure
$P_{front-axle}$	Total Load corresponding to the Truck Front Axle
$P_{rear-axle}$	Total Load corresponding to the Truck Rear Axles
$P_{H15-44}$	Weight of a Rear Axle Wheel of the <i>H15-44</i> Truck
$P_n$	Nominal Axial Capacity of the Concrete Walls for Unit of Length
$q$	Generic Uniform Distributed Load Applied to the Structure
$q_{DL}$	Uniform Distributed Load due to Dead Loads
$q_{LL}$	Uniform Distributed Load due to Live Loads
$R_{ab}$	Ultimate (Factored) Axial Load due to the Most Demanding Load Condition for the Two Walls
$R_b$	Design Shear Capacity of the Connection
$R_i$	Reaction of the Girder $G_i$ . The Same Symbol is Used to Indicate the LVDT No. $i$ with $i = 1, 2, \dots, 13$
$RF$	Rating Factor
$RT$	Rating of the Bridge: $RT = RF \cdot W$
$SD_c$	Standard Deviation for the Specified Compressive Strength $f'_c$ of Concrete
$SD_y$	Standard Deviation for the Specified Yield Strength $f_y$ of Non-prestressed Steel Reinforcement
$SG_i$	Strain Gauge No. $i$ with $i = 1, 2, \dots, 5$
$t_f$	Thickness of the Pre-cured FRP Laminate
$T_b$	Shear Capacity of the Connection

$T_c$	Shear Capacity of the Anchor Embedded in Concrete
$V_c$	Concrete Contribution to the Shear Capacity
$V_n$	Nominal Shear Strength at Section
$V_{c,i}$	Nominal Shear Strength at Section for Punching Shear Check: $i = 1, 2, 3$
$V_s$	Unfactored Shear due to the Most Demanding Load Condition for a Structural Element
$V_u$	Ultimate (Factored) Shear due to the Most Demanding Load Condition for a Structural Element
$w_f$	Width of the Pre-cured FRP Laminate
$w_{tire}$	Size of the Print of a Wheel in the Transverse Direction according to AASHTO (2002)
$W$	Weight of the Nominal Truck Used to Determine the Live Load Effect
$W_g$	Width of the Girders Web
$W_r$	Width of the Roadway
$W_{rc}$	Width of the Roadway between Curbs
$x$	Generic Position of the Truck in the Transverse Direction of the Bridge
$a_s$	Coefficient Used in the Punching Shear Check according to ACI 318-02: $a_s = 40$ for Interior Load; $a_s = 30$ for Edge Load; $a_s = 20$ for Corner Load
$b_c$	Ratio of Long Side to Short Side of the Area over Which the Load is Distributed for Punching Shear Check
$b_d$	Coefficient as per AASHTO (2002) Table 3.22.1A: $b_d = 1.0$ for Ultimate Conditions and $b_d = 1.0$ for Service Conditions
$b_L$	Coefficient as per AASHTO (2002) Table 3.22.1A: $b_L = 1.67$ for Ultimate Conditions and $b_L = 1.00$ for Service Conditions
$g$	Coefficient as per AASHTO (2002) Table 3.22.1A: $g = 1.3$ for Ultimate Conditions and $g = 1.0$ for Service Conditions

$d_{\max}$	Maximum Displacement Experienced during Load Tests
$e_{fu}$	Design Tensile Strain of the Pre-cured FRP Laminate: $e_{fu} = C_E e_{fu}^*$
$e_{fu}^*$	Guaranteed Tensile Strain of the Pre-cured FRP Laminate as Reported by the Manufacturer
$f$	Strength Reduction Factor according to ACI 318-02 Section 9.3: $f = 0.70$ for Axial Load and Axial Load with Flexure for Member without Spiral Reinforcement conforming to ACI 318-02 Section 10.9.3. The Same Symbol is Applied to Indicate the Factors Used to Convert Nominal Values to Design Capacities of Member
$f_{punch}$	Strength Reduction Factor for Punching Shear Check according to ACI 318-02 Section 9.3: $f_{punch} = 0.85$
$r_w$	Ratio of Tensile Non-prestressed Steel Reinforcement: $r_w = \frac{A_s}{b_w d}$
$w_u$	Ultimate Value of Stresses due to Moments and Shear Forces

## CONVERSION OF UNITS

$$1 \text{ Inch (in)} = 8.333 \cdot 10^{-2} \text{ Feet (ft)}$$

$$1 \text{ Inch (in)} = 2.54 \cdot 10^{-2} \text{ Meters (m)}$$

$$1 \text{ Foot (ft)} = 12 \text{ Inches (in)}$$

$$1 \text{ Foot (ft)} = 3.048 \cdot 10^{-1} \text{ Meters (m)}$$

$$1 \text{ Kip (kip)} = 4.448222 \text{ Kilonewton (kN)}$$

$$1 \text{ Kip (kip)} = 4.448222 \cdot 10^3 \text{ Newton (N)}$$

$$1 \text{ Kip (kip)} = 10^3 \text{ Pounds-Force (lbf)}$$

$$1 \text{ Kip per Square Inch (ksi)} = 6.894757 \text{ Mega Pascal (MPa)}$$

$$1 \text{ Kip per Square Inch (ksi)} = 6.894757 \cdot 10^6 \text{ Pascal (Pa)}$$

$$1 \text{ Mile per Hour (MPH)} = 4.470 \text{ Meter per Second (m/s)}$$

$$1 \text{ Pound-Force (lbf)} = 4.448222 \text{ Newton (N)}$$

$$1 \text{ Pound-Force (lbf)} = 4.448222 \cdot 10^{-3} \text{ Newton (kN)}$$

$$1 \text{ Pound-Force per Square Inch (psi)} = 6.894757 \cdot 10^{-3} \text{ Megapascal (MPa)}$$

$$1 \text{ Pound-Force per Square Inch (psi)} = 6.894757 \cdot 10^3 \text{ Pascal (Pa)}$$

$$1 \text{ Ton-Force (ton)} = 2 \cdot 10^3 \text{ Pounds-Force (lbf)}$$

$$1 \text{ Ton-Force (ton)} = 2 \text{ Kips (kip)}$$

# **1. BACKGROUND**

## **1.1. Delta Regional Authority Program Project**

In December 2002, as a result of its partnership with University of Missouri, Rolla – University Transportation Center (UMR-UTC), the Meramec Regional Planning Commission (MRPC) received a \$193895 grant award from the Delta Regional Authority for bridge improvement projects in Crawford, Dent, Phelps, and Washington Counties.

## **1.2. Need for the Proposed Project**

Transportation infrastructure is one of the major economic development needs for the Meramec Region. Local roads and bridges affect the economic welfare of the region by providing links to the major routes. Local roads and bridges are the collector systems into the larger state highway system for the transport of manufactured products and agricultural goods, accessing employment centers, and bringing travelers and tourists to the region. While many residents are engaged in agriculture and use the roads for farm-to-market routes, a growing number of people are working in cities and living in unincorporated areas relying on rural roads to commute to work. Aging bridges prohibit growth in much of the region because they severely limit access to many communities.

According to the National Bridge Inventory in 1995, 29 percent of county bridges do not meet minimum tolerable conditions to be left as-is. Nationwide, 40 percent of rural bridges are posted as to weight or other travel restrictions. Load postings are defined as the safe loads to cross a bridge. Loads over the posted limit cause damage to the structure and shorten the life of the bridge. Examples of vehicles affected would be school buses, fire trucks and ambulances, commercial truck traffic and large farm equipment. Dump trucks are affected by all load postings according to the Missouri Department of Transportation (MoDOT) and emergency vehicles are affected by most postings. The Federal Highway Administration (FHWA) classifies 32 percent of rural bridges as structurally deficient. Over one-third of the rural bridges in Crawford, Dent, Phelps and Washington counties are considered deficient by MoDOT standards. Much of the problems with local bridges are due to age and obsolete design.

The high cost associated with bridge replacement keeps communities from addressing many bridges. Even the cost to repair bridges is high when using conventional technologies. Maintaining and upgrading transportation infrastructure is a challenge for rural regions because of the sparse density of residents and number of roads and bridges running throughout the area. The low Average Daily Traffic (ADT) on most rural bridges seems to make the cost for bridge replacement ineffective. Low-volume bridges make it difficult for rural areas to compete for grant funding to assist with bridge replacements because rural areas are in competition with larger metropolitan areas. Rural areas are at a disadvantage because more populated areas can incorporate additional aspects of transportation, such as public transit and major economic impact, in grant proposals.

### **1.3. Description of the Project**

Fiber-reinforced polymer (FRP) materials have recently emerged as a practical alternative for construction and renovation of bridges. Advantages of FRP materials are that they resist corrosion, long outlive conventional materials, and have high strength-to-weight ratio. Placement of FRP material is in two forms, near-surface mounted bars and externally-bonded laminates, and the materials are applied on the underside of bridges. UMR has been working with FRP technology on projects around the state and in the Meramec Region. Projects have included strengthening of bridges in Boone County, Phelps County, and St. Louis. Bridges constructed with FRP materials were installed in the city of St. James, MO. FRP strengthening of bridges has had significant cost and time savings over conventional methods.

MRPC is working with local elected officials, UMR and MoDOT to identify and develop 31 bridge strengthening projects in the four-county area of Crawford, Dent, Phelps and Washington. Counties provide MRPC a list of bridge needs and MRPC staff reviews the list with UMR and MoDOT representatives to determine bridges that would be prime candidates for FRP strengthening technology. MoDOT will also review the bridges to determine those that have previously been inspected and found to be structurally deficient or require a load posting. MoDOT will also help determine if projects can help the counties earn soft-match credit towards larger projects using Bridge Replacement Off-system (BRO) funds. MRPC will then determine the economic development impact each bridge has on the region and prioritize projects based on this ranking. The University will

prepare design specifications for applying FRP material to each bridge. Contractors will be competitively procured to install the FRP material and those contractors will be required to have or receive certification from UMR for FRP technology training. The University will monitor the application of FRP material to each bridge. Each county may use a third party engineering firm to seal the design and monitor the contractor's activity to ensure that the results of the FRP technology are accurate and valid. Bridges may be tested for load posting before and after the strengthening process to determine the effect of the activity on the strength of each bridge. It is anticipated that strengthening will allow for the load postings to be removed or significantly raised for the structures subjected to such limitations.

#### **1.4. Complementing Existing Regional Plans**

Through MRPC, each county completed a Strategic Plan in 2000-2001 to identify current needs and develop a plan of action. This information became part of the region's Comprehensive Economic Development Strategy. Transportation infrastructure was a common need found in all counties. A top priority for economic development was determined to be the need for a better transportation system. Each county identified an objective to improve existing infrastructure. Activities proposed to address the transportation system included encouraging transportation development to enhance economic growth. Most counties found that tourism is directly related to the transportation system and if the tourism industry is to be promoted in the region, the transportation system must be addressed. Counties determined that activities must include improvements to local roads and bridges as well as state routes.

Each community will be required to cover 30 percent of the cost to reinforce each bridge addressed in their jurisdiction. Communities are also responsible for using a third party engineering firm to seal the University's design work and inspect the work of contractor(s) hired to apply the FRP reinforcement. The bridges to be addressed are not deficient due to poor maintenance, but to age and structural obsolescence. Once strengthened, the bridges will have an increased life by removing or upgrading the current load postings. Each community budgets for road and bridge maintenance and this will not change with the proposed project. Strengthening is the only alternative to replacement, and should not require additional maintenance from the community's road

crews.

An improved transportation system is a severe need all across the state, including these four Delta counties of the Meramec Region. The transportation system, bridges in particular, was found to be a top priority in the strategic plans for each county as part of the Comprehensive Economic Development Strategy developed for the region. Transportation was directly related to economic development in each county and for the region. The transportation infrastructure of the region has a direct impact on economic development by providing the means necessary to transport raw materials and products, employees to/from work and consumers to/from business centers.

### **1.5. Impact of the Project**

Strengthening bridges will allow for communities to open bridges to more traffic and facilitate the movement of freight, farm equipment and products, and commuter traffic. Counties will add new strength to bridges that otherwise would need to be replaced or closed due to posting limits. Major employment centers are located in each of the four counties. The industries are dependent upon moving their goods and, in the Meramec Region, goods move only via the road system. Major employment centers rely on the local transportation system to allow access for employees and connecting with larger transportation systems for moving materials and products. Such industries include Doe Run Inc., Salem Memorial District Hospital and US Food Service in Dent County, Dana Brake Parts Inc., Meramec Industries Inc., and Missouri Baptist Hospital in Crawford County, Briggs & Stratton Corp., Boys & Girls Town of Missouri and Wal-Mart Distribution Center in Phelps County and Red Wing Shoe Co., Georgian Gardens Nursing Home and YMCA of the Ozarks in Washington County.

Up to 31 county bridges may be strengthened using the FRP technology. Strengthening will remove load postings or significantly increase postings so that bridges will be open to more traffic. These bridges will allow for more access from county roads to major routes running through the area, directly impacting the economic development potential of the region.

## 2. INTRODUCTION

This report summarizes the procedures used for the upgrade of the bridge No. 1330005 (see Figure 2.1), located in Phelps County (Route 3560), MO. The bridge is actually load posted to a maximum weight of 10 *ton*.



Figure 2.1. Bridge No. 1330005

The total length of the bridge is  $7925\text{ mm}$  ( $26\text{ ft}$ ) and the total width of the deck is  $6680\text{ mm}$  ( $21\text{ ft } 11\text{ in}$ ). The span of the bridge consists of four reinforced concrete (RC) girders monolithically cast with a  $152\text{ mm}$  ( $6\text{ in}$ ) deep deck. It can be assumed as simply-supported by the abutments.

### 2.1. Objectives

The primary objectives of this document are to analyze the bridge superstructure and to provide the design calculations for its strengthening using a Mechanically Fastened Fiber-Reinforced Polymer system (MF-FRP). The advantage system consists of pre-cured FRP laminates bolted onto the concrete surface in order to provide the necessary flexural reinforcement to girders and deck. The strength of the technique is in the fact that it does

not require any surface preparation prior to the installation of the FRP.

## 2.2. Bridge Conditions

Prior to the strengthening of the bridge, a detailed investigation was required to determine the initial conditions of the bridge and the properties of the constituent materials.

From visual observations, some concrete spalling along the longitudinal edges of the bridge was observed. The girders and deck showed traces of steel rebar corrosion (see Figure 2.2-a). As a consequence of the insufficient amount of longitudinal reinforcement, all the girders were visibly cracked at mid-span (see Figure 2.2-b). In addition, due to the inadequate transversal reinforcement, the deck also presented a longitudinal crack halfway between adjacent girders (see Figure 2.3-a). The abutments appeared to be in good condition except for some vertical cracks running down from the edges of the girders across the entire height of the abutment (see Figure 2.3-b).

The details of the bridge reinforcement and material properties were unknown due to the unavailability of the bridge plans. As a consequence, at the onset of the project, these properties were determined in-situ, based on visual and Non Destructive Testing (NDT) evaluation.

In particular, three concrete cores were drilled from the deck (see Figure 2.4-a), and they were tested in compliance with ASTM C39/C39M-1 and ASTM C42/C42M-99 (see Figure 2.4-b). The following results were found:

§ Average Compression Strength:  $f'_c = 46.6 \text{ MPa}$  (6760 psi);

§ Standard Deviation:  $SD_c = 3.9 \text{ MPa}$  (560 psi);

§ Variance:  $c.o.v._c = 100 \frac{SD_c}{f'_c} = 8.3\%$ .

Concrete cover and size of longitudinal and transverse steel bars in the deck were determined from the concrete cores (see Figure 2.5-a) as follows:

Ø Transverse Direction

#4 (12.7 mm (0.5 in) diameter) steel bars

average spacing: 432 mm (17 in) on center

clear concrete cover: 63.5 mm (2½ in);

Ø Longitudinal Direction

#4 (12.7 mm (0.5 in) diameter) steel bars

average spacing: 330 mm (13 in) on center

clear concrete cover: 50.4 mm (2 in).



a) Girders and Deck



b) Bending Cracks in the Girders

Figure 2.2. Condition of the Superstructure



a) Longitudinal Crack in the Deck



b) Vertical Crack in the Abutment

Figure 2.3. Condition of Deck and Abutments



a) Coring



b) Compression Tests

Figure 2.4. Material Characterization of the Concrete

Concrete cover, number and size of flexural and shear reinforcement for the girders were determined by chipping off concrete at different locations (see Figure 2.5-b). The reinforcement consisted of:

Ø Flexural Reinforcement

3 #6 (19 mm ( $\frac{6}{8}$  in) diameter) steel bars

clear concrete cover: 76.2 mm (3 in);

Ø Shear Reinforcement

1 #4 (12.7 mm (0.5 in) diameter) steel bars @ 355 mm (14 in) on center at the mid-span

2 #4 (12.7 mm (0.5 in) diameter) steel bars @ 355 mm (14 in) on center (close to the abutments)

clear concrete cover: 57 mm ( $2\frac{1}{4}$  in).

The location of the steel reinforcement for the deck and girders was accurately detected with a rebar locator. Using the same equipment it was also possible to determine that all girders were reinforced with the same amount of steel.

The mechanical properties of the steel reinforcement were determined by testing three

specimens cut from an exposed bar found in one of the abutments. They were tested according to ASTM A615 and ASTM A955 (see Figure 2.5-c). The following results were found:

§ Average Yield Strength:  $f_y = 377.1 \text{ MPa}$  ( $54690 \text{ psi}$ );

§ Standard Deviation:  $SD_y = 28.7 \text{ MPa}$  ( $4170 \text{ psi}$ );

§ Variance:  $c.o.v._y = 100 \frac{SD_y}{f_y} = 7.6\%$ .

Based on the experimental results, a Grade 50 steel was assumed for design.

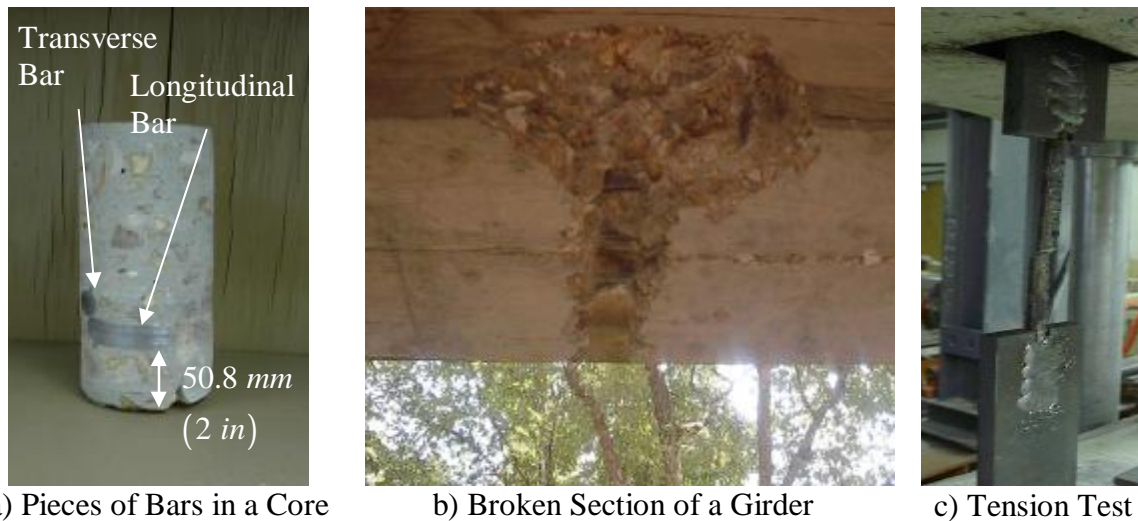


Figure 2.5. Material Characterization of the Steel Bars

The geometry of the bridge is summarized in Table 2.1. Figure 2.6 and Figure 2.7 show the longitudinal and plan view of the bridge. Figure 2.7 also draws the position from where the concrete cores were extracted and the longitudinal and transverse steel reinforcement of the deck.

Cross section and steel reinforcement for the girders are summarized in Figure 2.8, Figure 2.9 and Figure 2.10. In particular, Figure 2.8 summarizes cross-section and longitudinal reinforcement for all the girders while Figure 2.9 and Figure 2.10 show the shear reinforcement for the outer and the inner girders respectively.

Table 2.1. Geometry of the Bridge

Clear Span	$l_c = 7315 \text{ mm}$ (24 ft)
Design Length	$l_d = 7620 \text{ mm}$ (25 ft)
Deck Height	$H_d = 152 \text{ mm}$ (6 in)
Girder Web Height	$H_g = 406 \text{ mm}$ (16 in)
Girder Width	$W_g = 366 \text{ mm}$ (14 in)
Spacing between Girders On Center	$d_g = 1803 \text{ mm}$ (5 ft 11 in)
Cantilever Deck	$d_c = 457 \text{ mm}$ (1 ft 6 in)
Roadway Width	$W_r = 6680 \text{ mm}$ (21 ft 11 in)
Curb to Curb Roadway Width	$W_{rc} = 6172 \text{ mm}$ (20 ft 3 in)
Overlay Height (Compact Gravel)	$H_o = 152 \text{ mm}$ (6 in)

The analysis and design of the bridge was performed according to the MoDOT Bridge Manual, to the experimental results attained at the University of Wisconsin-Madison (Bank et al., 2002) and at the University of Missouri-Rolla. The assumed load configurations were consistent with the AASHTO Specifications (AASHTO, 2002).

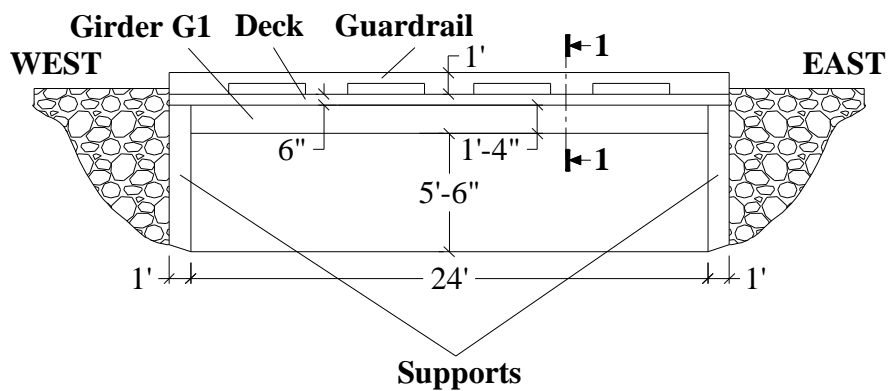


Figure 2.6. Longitudinal View of the Bridge

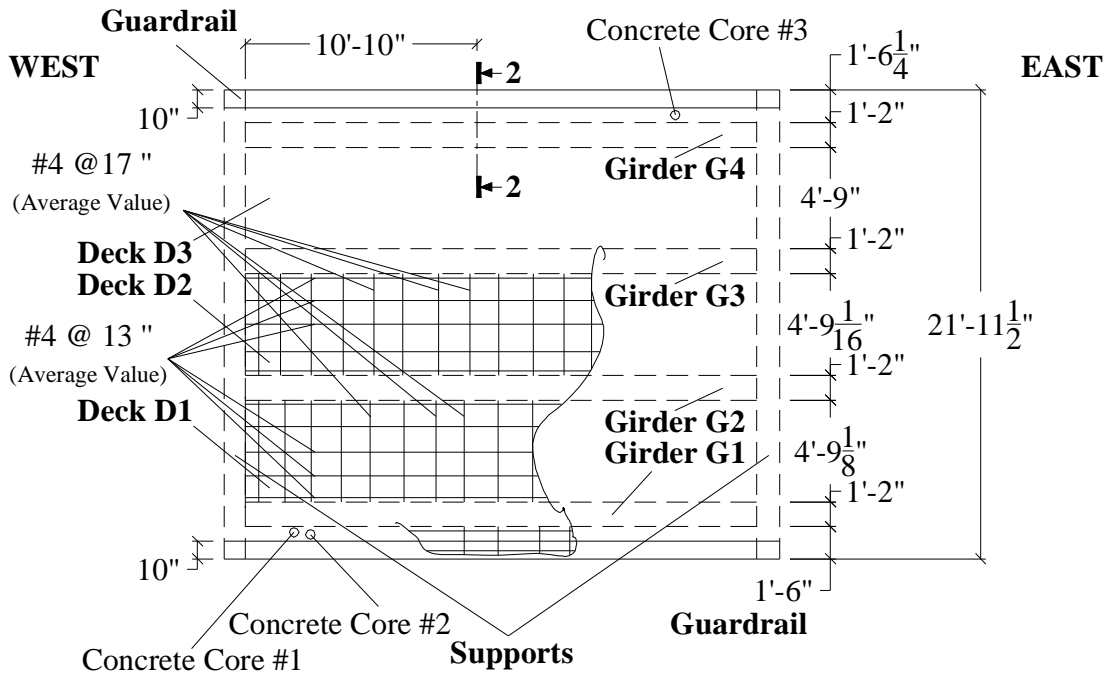


Figure 2.7. Plan View of the Bridge

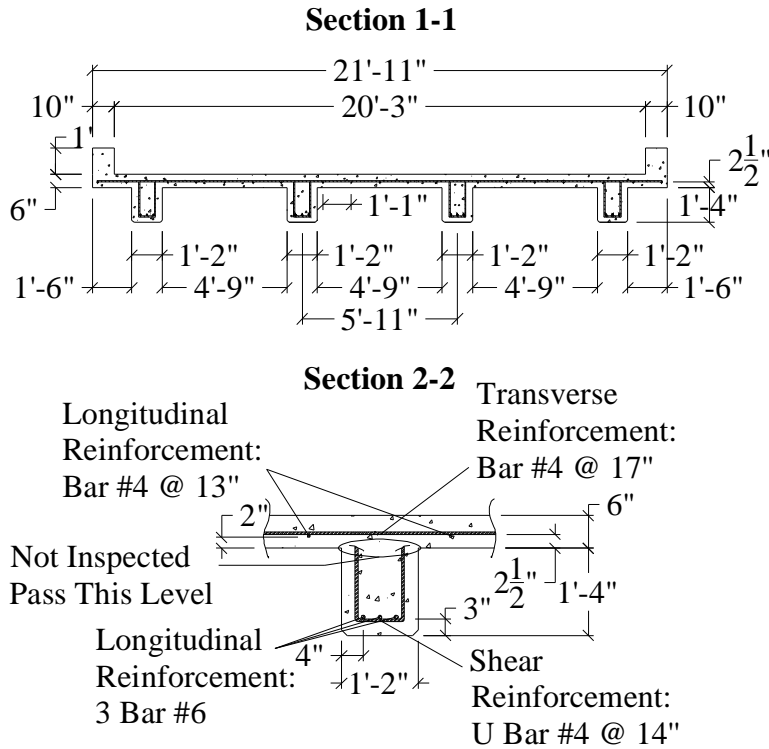


Figure 2.8. Details of the Inspected Sections

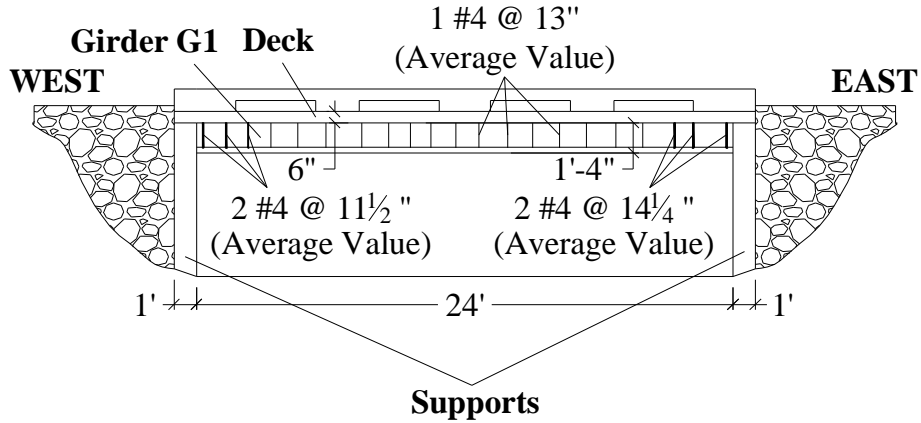


Figure 2.9. Shear Reinforcement in the Outer Girders (G1 and G4)

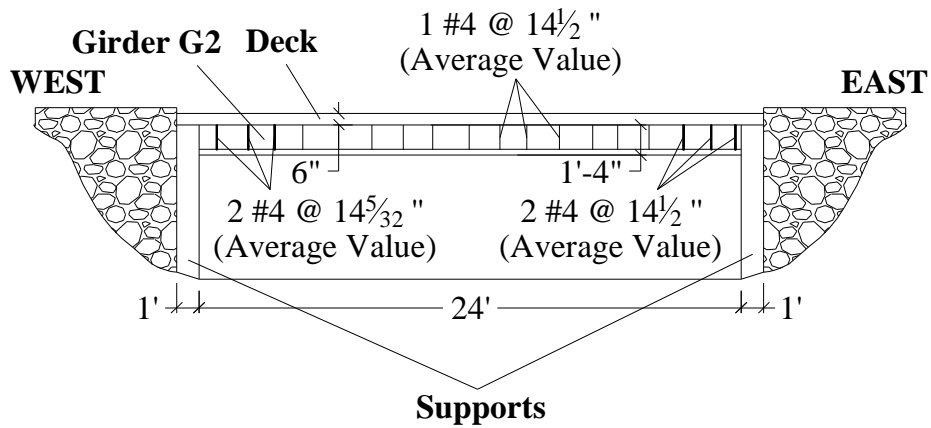


Figure 2.10. Shear Reinforcement in the Inner Girders (G2 and G3)

### 3. STRUCTURAL ANALYSIS

#### 3.1. Load Combinations

For the structural analysis of the bridge, the definitions of design truck and design lane are necessary. This will be addressed in the next section.

Ultimate values of bending moments and shear forces are obtained by multiplying their nominal values with the dead and live load factors and by the impact factor according to AASHTO (2002) as shown in equation (3.1):

$$w_u = g [b_d D + b_L (1 + I) L] \quad (3.1)$$

where

$D$  is the dead load;

$L$  is the live load;

$g, b_d, b_L$  are coefficients as per AASHTO (2002) Table 3.22.1A:

ultimate conditions  $\Rightarrow g = 1.3, b_d = 1.0, b_L = 1.67$ ;

service conditions  $\Rightarrow g = 1.0, b_d = 1.0, b_L = 1.00$ ;

$I$  is the live load impact calculated as follows:

$$I = \frac{50}{l_d + 125} = \frac{50}{25.0 + 125} = 0.33 \leq 0.30 \quad (3.2)$$

and  $l_d = 25 \text{ ft}$  (7620 mm) represents the span length from center to center of support. The impact factor should not be larger than 0.30, and therefore the latter value is assumed for the design.

### 3.2. Design Truck and Design Lanes

Prior to the design of the strengthening, the analysis of the bridge was conducted by considering a H15-44 truck load (which represents the design truck load as per AASHTO, 2002 Section 3.7.4) having geometrical characteristics and weight properties shown in Figure 3.1.

According to AASHTO Section 3.6.3 (2002), roadway widths between 6096 and 7315 mm (20 and 24 ft) shall have two design lanes, each one equal to one-half of the roadway width. However, in this case, the low value of the Annual Daily Traffic ( $ADT = 35$ ) of the bridge allows to deal just with one design lane. To be noted that the centerline of the wheels of the rear axle shown in Figure 3.1 is located 305.0 mm (1.0 ft) away from the curb as specified in AASHTO (2002) for slab design.

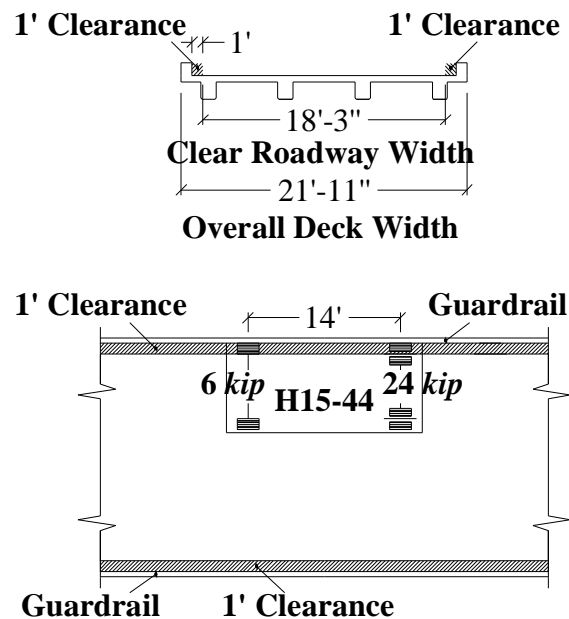
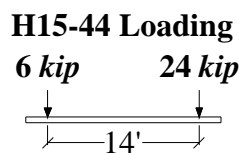


Figure 3.1. Truck Load and Truck Lanes

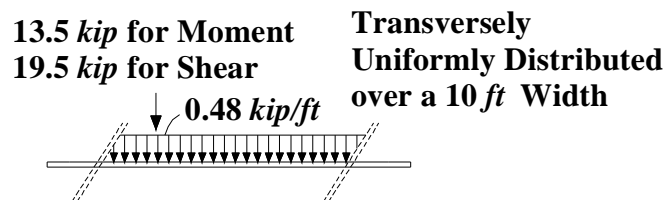
Two loading conditions are required to be checked as laid out in Figure 3.2.

The H15-44 design truck load (Figure 3.2-a) has a front axle load of 26.7 kN (6.0 kip) and rear axle load located 356 mm (14 ft) behind the drive axle.

The design lane loading condition consists of a load of  $2.1 \text{ kN}$  ( $0.48 \text{ kip}$ ) per linear foot, uniformly distributed in the longitudinal direction with a single concentrated load so placed on the span as to produce maximum stress. The concentrated load and uniform load are considered to be uniformly distributed over a  $3048 \text{ mm}$  ( $10.0 \text{ ft}$ ) width on a line normal to the center of the lane. The intensity of the concentrated load is represented in Figure 3.2-b for both bending moments and shear forces. This load shall be placed in such positions within the design lane as to produce the maximum stress in the member.



a) Design Truck (H15-44)



b) Design Lane

Figure 3.2. Loading Conditions

### 3.3. Slab Analysis

Since it was not possible to detect the presence of longitudinal reinforcement in the negative moment regions, the continuity of the deck over the girders was conservatively neglected. This led to model the deck as a slab simply-supported between two girders (see Figure 3.3).

Figure 3.3 shows the worst loading condition for the slab between girders G2 and G3. The design value was determined from the truck design condition when the wheel is in the middle of the slab. The load of the wheel was spread over a surface  $508 \times 254 \text{ mm}$  ( $20 \times 10 \text{ in}$ ) as prescribed in the AASHTO (2002) Section 4.3.30. A

commercial finite elements program (SAP 2000) was used to analyze the structure. The ultimate moment found from this analysis was (see Figure 3.4):

$$M_u = 37.4 \frac{kN \cdot m}{m} \left( 8.4 \frac{kip \cdot ft}{ft} \right).$$

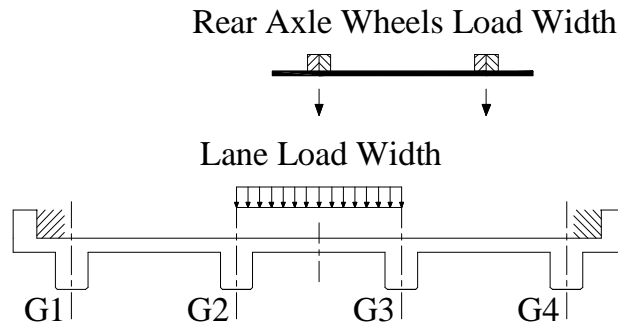


Figure 3.3. Slab Load Conditions

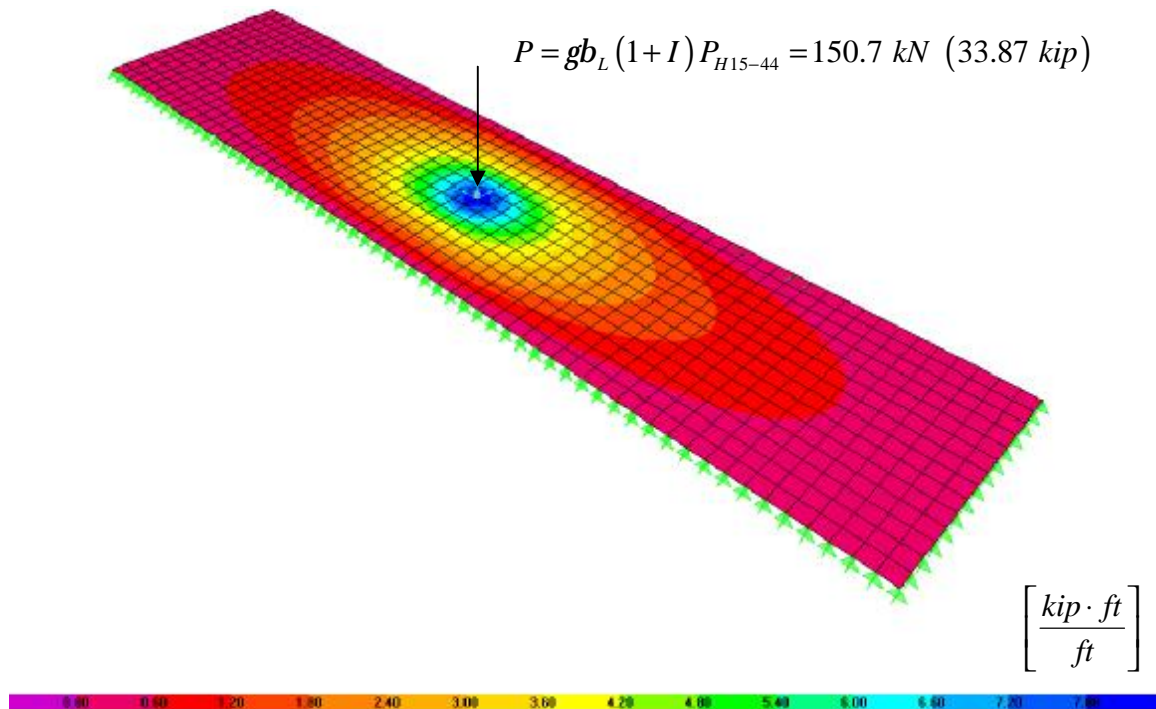


Figure 3.4. Slab Transversal Bending Moment Distribution

### 3.4. Girders Analysis

The transverse load distribution was found by analyzing the structure represented in Figure 3.5, where a generic axle of unit weight  $P = 1 \text{ kN}$  ( $0.225 \text{ kip}$ ) and a unitary uniform distributed load  $q = 1 \frac{\text{kN}}{\text{m}}$  ( $0.068 \frac{\text{kip}}{\text{ft}}$ ) have been assumed. As mentioned, the continuity of the slab was neglected and therefore the scheme to be considered for the structural analysis is the one shown in Figure 3.5. From Figure 3.5 it can be observed that by increasing the value of  $x$  the design lanes move from the left to the right portion of the bridge slab.

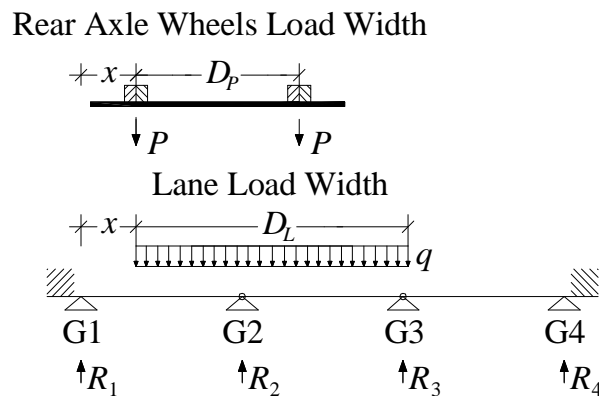


Figure 3.5. Girders Load Conditions for Analysis and Design

Table 3.1 summarizes the results of the analysis, where  $q_{DL}$  is related to a uniform distributed load over all the spans (like the dead load),  $q_{LL}$  to a uniform distributed load over the two spans next to the support (like the lane design load) and  $P$  to the truck design load.

Table 3.2 summarizes the results in terms of unfactored and factored bending moments ( $M_s$  and  $M_u$ ) and shear forces ( $V_s$  and  $V_u$ ). The maximum values, found considering the positions of the load that produces the worst condition for the structure (i.e., varying the position of the truck along the length of the bridge), are adopted for design.

Figure 3.6 and Figure 3.7 show respectively the bending moment  $M_u$  and the shear  $V_u$  envelopes due to the load obtained, taking for each section (at the distance  $x$  from the

left support) the maximum value given by the two loading conditions: the worst load condition is that one related to the truck load design.

Table 3.1. Distribution Coefficient for the Girders

<i>Load Combination</i>	<i>Girder Reaction</i>	$R_1$	$R_2$	$R_3$	$R_4$
		[kN] ([kip])	[kN] ([kip])	[kN] ([kip])	[kN] ([kip])
$q_{DL}$ over all the spans in kN/m (kip/ft)		78.92 (5.408)	81.00 (5.550)	81.00 (5.550)	78.92 (5.408)
$q_{LL}$ over the two spans next to the support in kN/m (kip/ft)		46.90 (3.214)	86.26 (5.911)	86.26 (5.911)	46.90 (3.214)
$P$ in kN (kip)		15.61 (1.070)	14.55 (0.997)	14.55 (0.997)	15.61 (1.070)

Table 3.2. Interior Girder Bending Moments and Shear Forces

<i>Loading Condition</i>	<i>Unfactored Moment<sup>a)</sup></i> $M_s$ [kN·m] ([kip·ft])	<i>Factored Moment<sup>a)</sup></i> $M_u$ [kN·m] ([kip·ft])	<i>Unfactored Shear<sup>b)</sup></i> $V_s$ [kN] ([kip])	<i>Factored Shear<sup>b)</sup></i> $V_u$ [kN] ([kip])
<i>Dead Load</i>	103.0 (76.0)	134.1 (98.9)	16.5 (12.2)	21.4 (15.8)
<i>H15-44 Load Design Condition</i> <i>Number of Lanes = 1</i>				
<i>Truck Design</i>	101.4 (74.8)	286.1 (211.0)	18.0 (13.3)	50.84 (37.5)
<i>Total</i>	204.5 (150.8)	420.2 (309.9)	34.4 (25.4)	72.3 (53.3)
<i>Lane Design</i>	97.8 (72.1)	275.9 (203.5)	20.5 (15.1)	57.8 (42.6)
<i>Total</i>	201.0 (148.2)	346.2 (255.3)	37.0 (27.3)	79.2 (58.4)
<i>a) Computed at a cross-section in the middle of the span.</i> <i>b) Computed at a cross-section in the middle of the support.</i>				

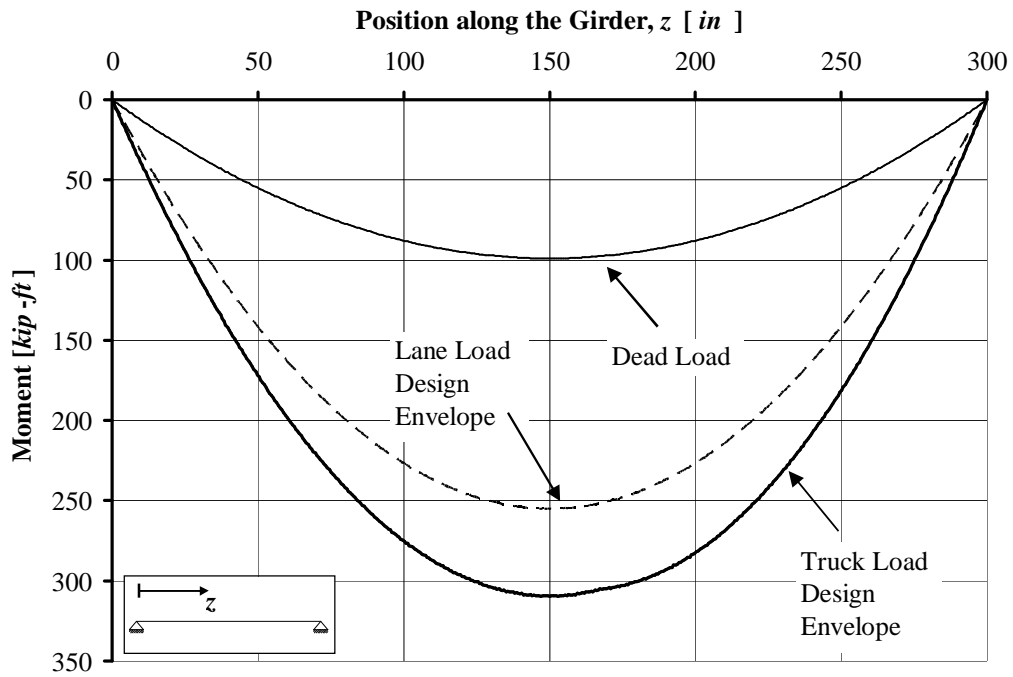


Figure 3.6. Interior Girder Bending Moment Diagrams Envelopes

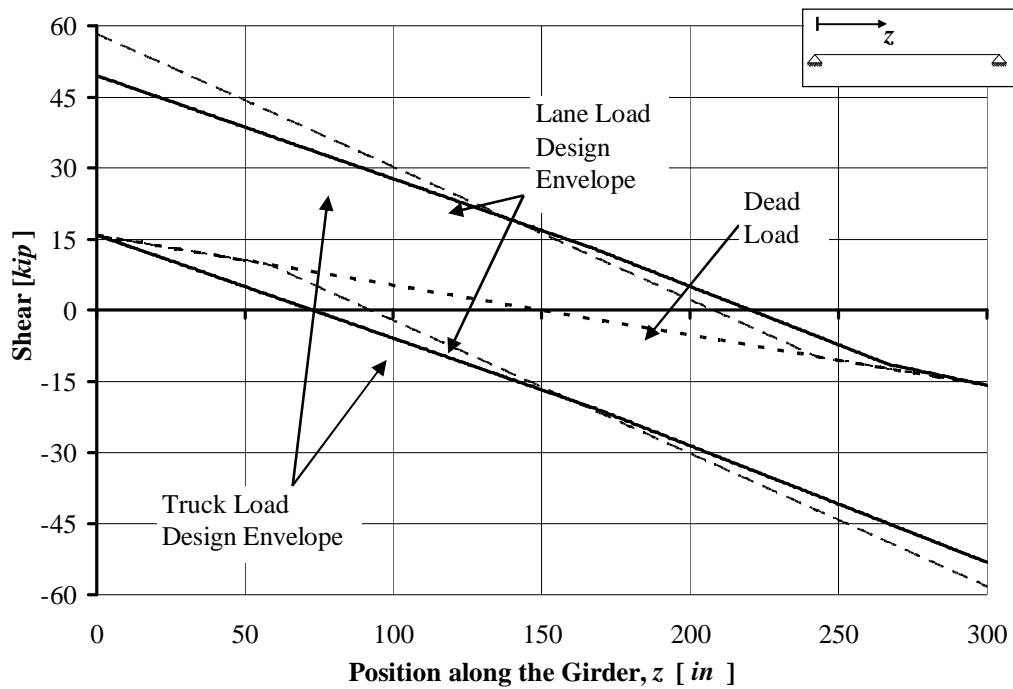


Figure 3.7. Interior Girder Shear Diagrams Envelopes

### 3.5. Analysis of the Abutments

The abutment can be analyzed as a wall loaded in its plane. According to ACI 318-02 Section 14.5.2, design axial load strength  $fP_n$  for a wall of solid rectangular cross section with resultant of all factored loads located within the middle third of the overall thickness of the wall is given by

$$fP_n = 0.55f'f_c A_g \left[ 1 - \left( \frac{kh_c}{32h} \right)^2 \right] \cong 1713 \text{ kN} \quad (385 \text{ kip}) \quad (3.3)$$

where

$f = 0.70$  is the strength reduction factor;

$A_g$  is the gross area of the section;

$k$  is the effective length factor ( $k = 2.0$  for walls not braced against lateral translation);

$h_c$  is the vertical distance between supports;

$h$  is the overall thickness of member.

The worst loading condition comes out by considering the maximum shear demand of the girders:

$$R_{ab} = V_u = 58.4 \text{ kip} .$$

Since  $R_{ab} < fP_n$ , the supports do not need further analysis.

## 4. DESIGN

### 4.1. Assumptions

Mechanically-Fastened FRP laminate design is carried out according to the principles of ACI 440.2R-02 (ACI 440 in the following). The properties of concrete, steel and FRP laminates used in the design are summarized in Table 4.1. The concrete and steel properties are obtained by testing of samples while the FRP properties are guaranteed values.

The  $f$  factors used to convert nominal values to design capacities are obtained as specified in AASHTO (2002) for the as-built and from ACI 440 for the strengthened members.

Table 4.1. Material Properties

<i>Concrete</i>	<i>Steel</i>		<i>FRP - SAFSTRIP</i>			
Compressive Strength	Yield Strength	Modulus of Elasticity	Tensile Strength	Modulus of Elasticity	Thickness	Width
$f'_c$	$f_y$	$E_s$	$f_{fu}^*$	$E_f$	$t_f$	$w_f$
[MPa]	[MPa]	[GPa]	[MPa]	[GPa]	[mm]	[mm]
([psi])	([ksi])	([ksi])	([ksi])	([ksi])	([in])	([in])
46.6 (6760)	344.7 (50)	200.0 (29000)	588.8 (85.4)	60.7 (8800)	3.175 (0.125)	101.6 (4.00)

Material properties of the FRP reinforcement reported by manufacturers, such as the ultimate tensile strength, typically do not consider long-term exposure to environmental conditions, and should be considered as initial properties. FRP properties to be used in all design equations are given as follows (ACI 440):

$$\begin{aligned}
 f_{fu} &= C_E f_{fu}^* \\
 e_{fu} &= C_E e_{fu}^*
 \end{aligned}
 \tag{4.1}$$

where  $f_{fu}$  and  $e_{fu}$  are the FRP design tensile strength and ultimate strain considering the

environmental reduction factor  $C_E$  as given in Table 7.1 (ACI 440), and  $f_{fu}^*$  and  $e_{fu}^*$  represent the FRP guaranteed tensile strength and ultimate strain as reported by the manufacturer (see Table 4.1).

The maximum strength that the MF-FRP strengthening can develop depends on the capacity of the connection bolt-strip and, therefore, on the number of fasteners used.

In order to mechanically fasten the FRP laminate to the concrete, the optimal solution in terms of mechanical behavior of the connection was found as a result of an experimental program conducted at UMR. The chosen fastening system consisted of:

- Ø Concrete wedge anchor (diameter  $9.525\text{ mm}$  ( $\frac{3}{8}\text{ in}$ ) and total length  $57.15\text{ mm}$  ( $2\frac{1}{4}\text{ in}$ ) - Figure 4.1). The shear capacity  $T_c$  of the anchor embedded in the concrete depends upon the embedment depth  $h_b$  and the strength of the concrete  $f'_c$ . The shear strength of the anchor,  $T_b$ , becomes equal to  $T_c$  with a value of  $26.7\text{ kN}$  ( $6.0\text{ kip}$ ) when  $f'_c = 41.4\text{ MPa}$  ( $6000\text{ psi}$ ) and  $h_b = 38.1\text{ mm}$  ( $1\frac{1}{2}\text{ in}$ );
- Ø Steel washer (inner diameter  $11.112\text{ mm}$  ( $\frac{7}{16}\text{ in}$ ), outer diameter  $25.4\text{ mm}$  ( $1\text{ in}$ ) and thickness  $1.587\text{ mm}$  ( $\frac{1}{16}\text{ in}$ ) - Figure 4.1);
- Ø Epoxy between the washer and the FRP and throughout the hole on the FRP.

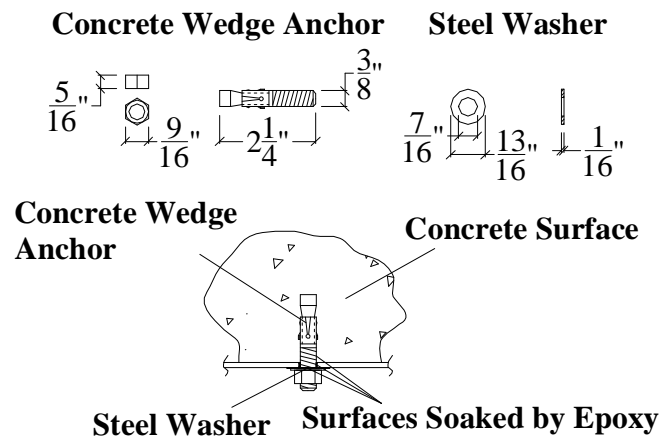


Figure 4.1. Details of the Connection Concrete-FRP

Bond tests on the connection FRP-fastener showed that at the ultimate conditions, the applied load is uniformly distributed between all the fasteners. In addition, it was observed that for concrete having an  $f'_c \geq 27.6 \text{ MPa}$  (4000 *psi*), the failure mode of the connection is due to the bearing of the FRP. The experimental ultimate load supported by this connection was found to be 14.0 *kN* (3.15 *kip*). For design purposes a safety factor equal to 1.25 was assumed and therefore the design capacity of the connection is  $R_b = 11.1 \text{ kN}$  (2.5 *kip*).

Under these assumptions, the minimum number of fasteners  $n_{b,\min}$  to anchor each FRP strip so that failure of the FRP controls, is given by:

$$n_{b,\min} = \frac{F_{FRP}}{R_b} \quad (4.2)$$

where  $F_{FRP}$  is the maximum load that the FRP strip experiences at ultimate conditions. Assuming  $C_E = 0.85$  (i.e., carbon plate exposed in exterior aggressive ambient) and taking into account the net area of the strip (i.e., subtraction of the area lost to insert the bolt), from equation (4.2) the minimum number of bolts to reach the ultimate capacity of the FRP strip is 26. If fewer bolts are used, the failure would occur at the connection (i.e. bearing of the FRP strip).

## 4.2. Superstructure Design

### 4.2.1. Assumptions

The geometrical properties and the internal steel flexural reinforcement of the design cross section are summarized in Figure 2.8 and Table 4.2. The expression for the flange width  $B$ , is given by the equation (4.3), according to AASHTO (2002) Section 4.6.2.6.1 for interior and exterior girders, respectively:

$$\begin{cases} B^{Int} = \min\left(\frac{l_d}{4}, 12H_s + W_g, d_g\right) \\ B^{Ext} = \min\left(\frac{l_d}{4}, 12h_s + W_g, \frac{d_g + W_g}{2} + d_c\right) \end{cases} \quad (4.3)$$

where  $l_d$ ,  $H_s$ ,  $W_g$ ,  $d_g$  and  $d_c$  are defined in Table 2.1. It results:

$$B^{Int} \cong 1803 \text{ mm (71 in)}$$

$$B^{Ext} \cong 1549 \text{ mm (61 in)}$$

Table 4.2. Geometrical Properties and Internal Steel Reinforcement

Slab Thickness	Web Width	Flange Width	Slab Longitudinal Tensile Steel Area	Effective Depth	Slab Transverse Tensile Steel Area	Effective Depth	Web Tensile Steel Area	Effective Depth
$H_d$ [mm] ([in])	$W_g$ [mm] ([in])	$B$ [mm] ([in])	$A_{s,slab \text{ long.}}$ [mm <sup>2</sup> ] ([in <sup>2</sup> ])	$d_{slab \text{ long.}}$ [mm] ([in])	$A_{s,slab \text{ transv.}}$ [mm <sup>2</sup> /m] ([in <sup>2</sup> /ft])	$d_{slab \text{ transv.}}$ [mm] ([in])	$A_{s,web}$ [mm <sup>2</sup> ] ([in <sup>2</sup> ])	$d_{web}$ [mm] ([in])
152.4 (6.0)	355.6 (14)	1803.4 (71)	506.4 (0.785)	95.2 (3¾)	292.1 (0.138)	108.0 (4¼)	854.2 (1.324)	473.1 (18⅝)

#### 4.2.2. Flexural Strengthening

Table 4.3 summarizes the strengthening recommendations for the superstructure of the bridge. It can be observed that for the longitudinal direction the new moment capacity is slightly smaller than the demand. The value can be accepted because of the high safety factors used for design.

Figure 4.2 details the longitudinal flexural strengthening, while Figure 4.3 shows the transverse one. Finally, the pattern of the bolts for longitudinal and transversal reinforcement is shown in Figure 4.4.

The bolt pattern was verified at the ultimate condition in order to avoid having any

section in which the moment demand is greater than the moment capacity. During this step, the position of the bolts is optimized. Figure 4.5 details the moment capacity of the beam along its length for the chosen bolt pattern. Appendix E contains some pictures of the FRP strengthening installation.

Table 4.3. Strengthening Summary

Section	Strengthening Scheme	Design Capacity		Moment Demand
		$fM_n$		$M_u$
		[kN · m] ([kip · ft])		[kN · m] ([kip · ft])
		Un-strengthened	Strengthened	
Longitudinal Direction	Bottom of each girder: 3 Plates Sides of each girder: 2 Plates	158.0 (116.5)	408.1 (301.0)	420.2 (309.9)
Transversal Direction	Each span of the deck: 15 Plates @ 457.2 mm (18 in) o/c	3.4 <sup>a)</sup> (2.5) <sup>a)</sup>	17.4 <sup>a)</sup> (12.8) <sup>a)</sup>	17.1 <sup>a)</sup> (12.6) <sup>a)</sup>

a) Value corresponding to a 457.2 mm (18 in) wide stripe of the deck.

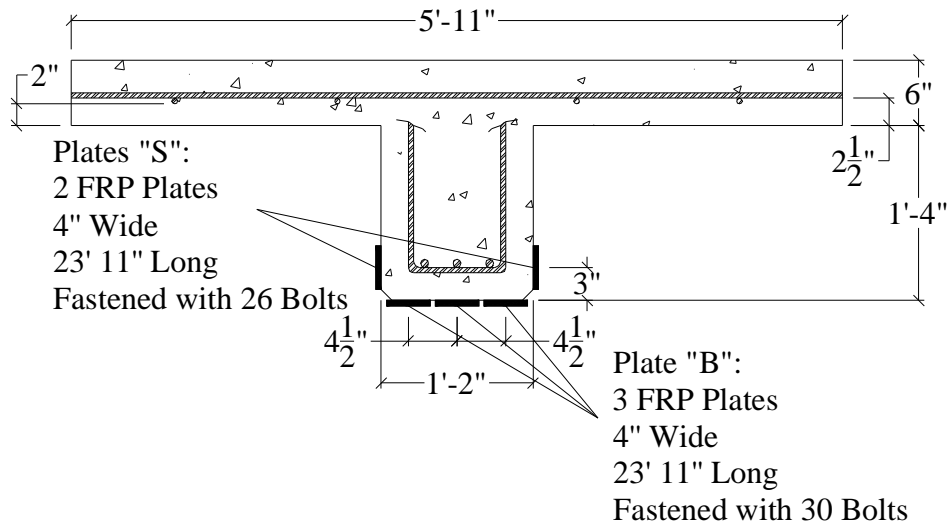


Figure 4.2. Girder Strengthened Section

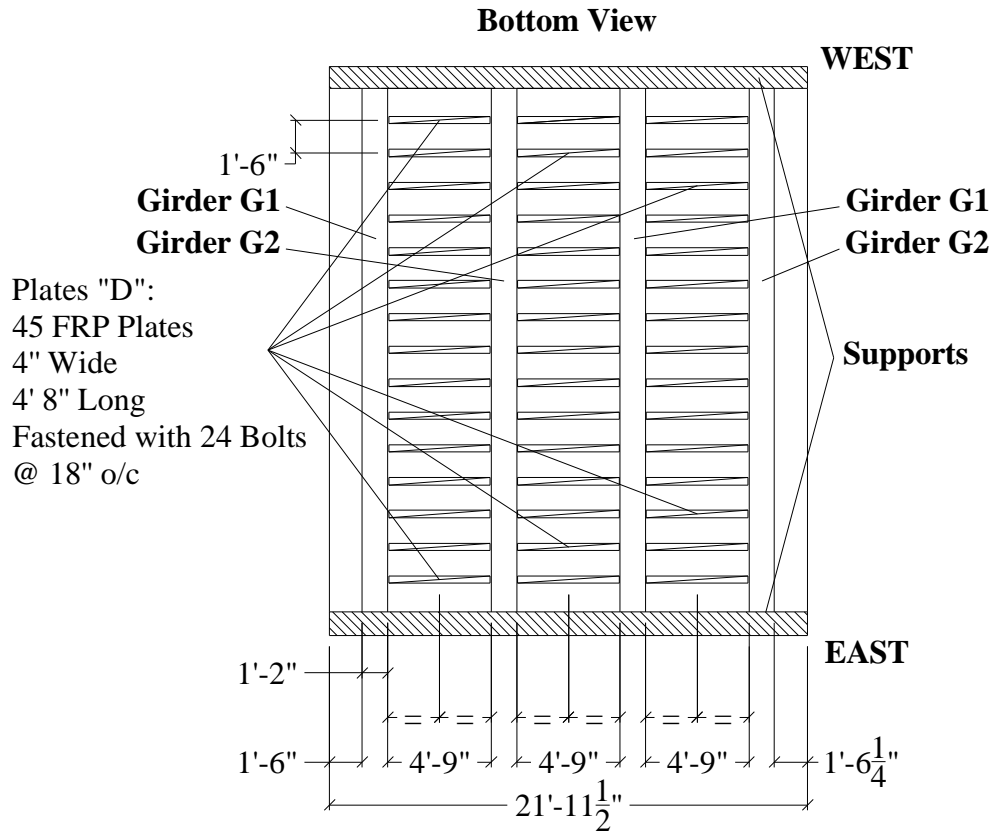


Figure 4.3. Strengthening of the Deck

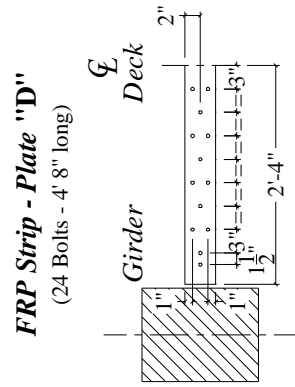
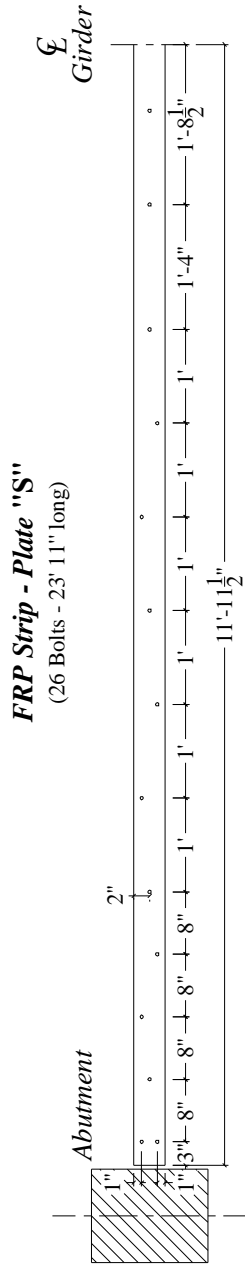
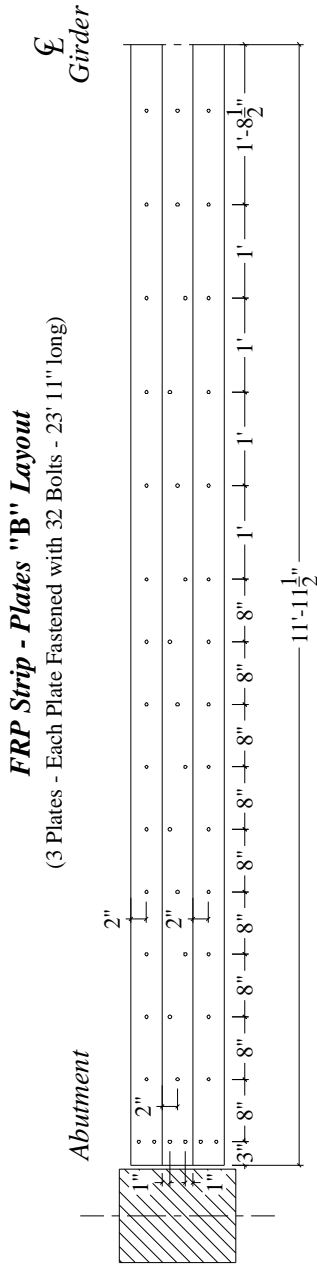


Figure 4.4. Pattern of the Bolts

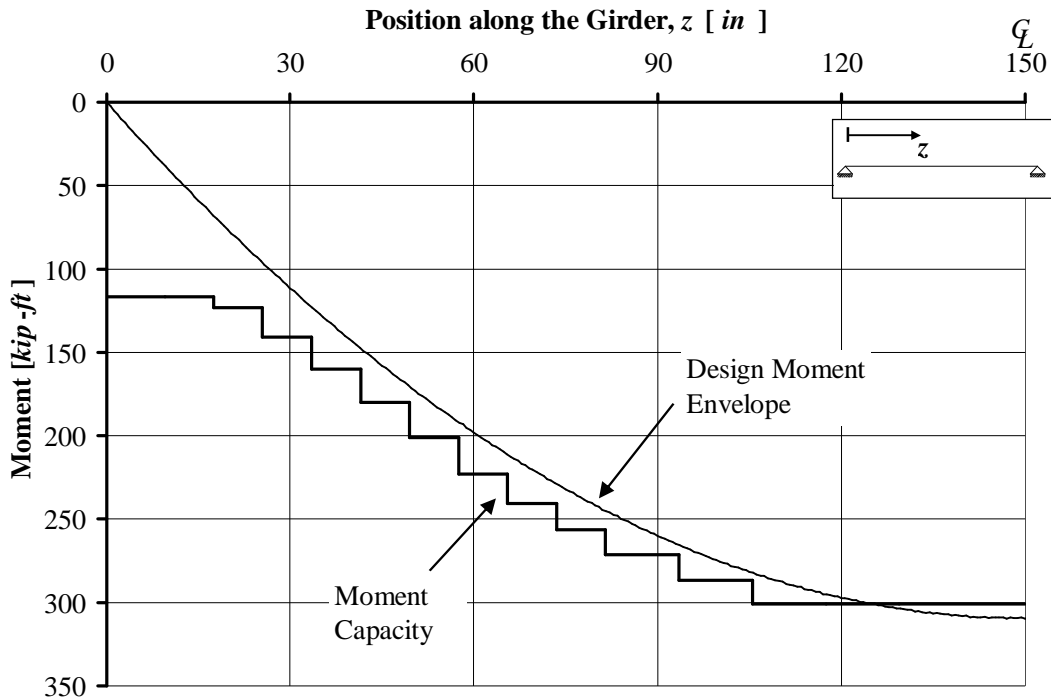


Figure 4.5. Diagram of the Capacity of the Beam at the Ultimate Load Conditions

#### 4.2.3. Shear Check

The concrete contribution to the shear capacity was calculated based on equation (11-5) of ACI 318-02 as follows:

$$\begin{cases} V_c = \left( 1.9\sqrt{f'_c} + 2500r_w \frac{V_u d}{M_u} \right) b_w d \leq 3.5\sqrt{f'_c} b_w d \\ [f'_c] = [psi] \end{cases} \quad (4.4)$$

The as-built shear capacity is then computed by adding the concrete contribution to the one due to the shear reinforcement. Table 4.4 summarizes the findings for the superstructure. Since the capacity is higher than the demand, it can be concluded that no shear reinforcement is required.

Table 4.4. Superstructure Shear Capacity

<i>Element</i>	<i>Shear Capacity</i> $fV_n$	<i>Shear Demand</i> $V_u$
<i>Slab</i> $\left[ \frac{kN}{m} \right] \left( \left[ \frac{kip}{ft} \right] \right)$	87.6 (6.0)	51.1 (3.5)
<i>Interior Girder</i>		
Close to the Supports $[kN]$ ( $[kip]$ ) Stirrups 2#4 @ 356 mm (14 in)	381.7 (85.8)	260.0 (58.4)
914 mm (3 ft) from the Abutments $[kN]$ ( $[kip]$ ) Stirrups 1#4 @ 356 mm (14 in)	245.5 (55.2)	209.1 (47.0)

#### 4.2.4. Punching Shear Check

The deck must also be checked for punching shear. This check was based on ACI 318-02 requirements. ACI 318-02 Sec. 11.12.2.1 prescribes that for non-prestressed slabs and footings,  $V_c$  shall be the smallest of the following expressions:

$$\left\{ \begin{array}{l} V_{c,1} = \left( 2 + \frac{4}{b_c} \right) \sqrt{f'_c} b_0 d \\ V_{c,2} = \left( \frac{a_s d}{b_0} + 2 \right) \sqrt{f'_c} b_0 d \\ V_{c,3} = 4 \sqrt{f'_c} b_0 d \end{array} \right. \quad \text{with } [f'_c] = [psi] \quad (4.5)$$

where:

- $b_c$  is the ratio of long side to short side of the area over which the load is distributed;
- $a_s$  is 40 for interior load, 30 for edge load and 20 for corner load;
- $b_0$  is the perimeter of critical section;
- $d$  is the distance from the extreme compression fiber to centroid of tension reinforcement.

By using a tire contact area as given by AASHTO (2002):

$$\begin{cases} l_{tire} = 254 \text{ mm} \text{ (10 in)} \\ w_{tire} = 508 \text{ mm} \text{ (20 in)} \\ A_{tire} = l_{tire} w_{tire} = 129032 \text{ mm}^2 \text{ (200 in}^2\text{)} \end{cases} \quad (4.6)$$

the following shear capacity can be found:

$$f_{punch} V_c = f_{punch} \min(V_{c,01}, V_{c,02}, V_{c,03}) \cong 0.85(307 \text{ kN}) \cong 258 \text{ kN} \text{ (58.0 kip)}$$

which is smaller than the ultimate punching shear capacity given by:

$$g b_L (1 + I) P_{H15-44} \cong 151.2 \text{ kN} \text{ (34.0 kip)}.$$

## 5. FIELD EVALUATION

### 5.1. Introduction

Although in-situ bridge load testing is recommended by the AASHTO (2002) Specification as an “effective means of evaluating the structural performance of a bridge”, no guidelines currently exist for bridge load test protocols. In each case, the load test objectives, load configuration, instrumentation type and placement, and analysis techniques are to be determined by the organization conducting the test.

In order to validate the behavior of the bridge prior to and after strengthening, static load tests were performed with H15 and H20 legal trucks, respectively, on bridge No.1330005 (see Figure 5.1): the first test was conducted in December 2003 while the second one was conducted in June 2004, one month after the installation of the strengthening. Figure 5.2 shows the distribution of the load between the axles of each truck and the loading configurations that maximize the stresses and deflections at mid-span of deck panels and girders under a total of five passes, one central and four laterals. For each pass, two and three stops were executed respectively for the load test prior to and after the strengthening. For each stop, the truck rear axle was centered over the marks on the deck. During each stop, the truck was stationary for at least two minutes before proceeding to the next location in order to allow stable readings.



Figure 5.1. Load Tests prior to and after Strengthening on Bridge No.1330005

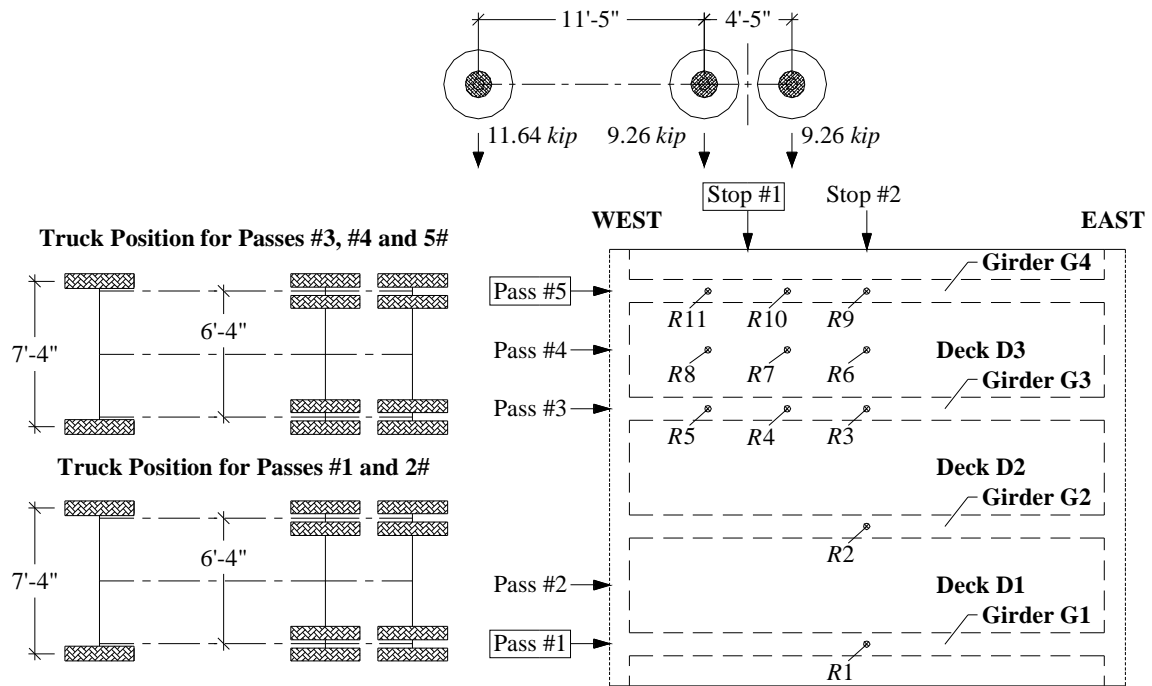
Displacements in the longitudinal and transverse directions were measured using Linear Variable Differential Transducers (LVDTs). Strains in the strengthening material were monitored by means of strain gages. Figure 5.3 and Figure 5.4 show the details of the instrumentation whose layout was designed to gain the maximum amount of information about the structure. It was assumed that the bridge acted symmetrically, therefore the instrumentation was concentrated on one half of the bridge.

Figure 5.5 compares the results prior to and after strengthening relative to Pass #3 corresponding to the rear axle of the truck at the mid-span (Stop #2 and Stop #3 for the load test prior to and after strengthening, respectively). The experimental results were normalized by dividing displacements to the weight of the truck used for testing. The performance of the structure prior to and after the strengthening was determined by comparing the normalized experimental results prior to and after strengthening. In both cases, the bridge performed well in terms of overall deflection. In fact, the maximum deflection measured during the load test is below the allowable deflection prescribed by AASHTO, 2002 Section 8.9.3 ( $d_{\max} \leq L/800 = 9.525 \text{ mm} (0.375 \text{ in})$ ).

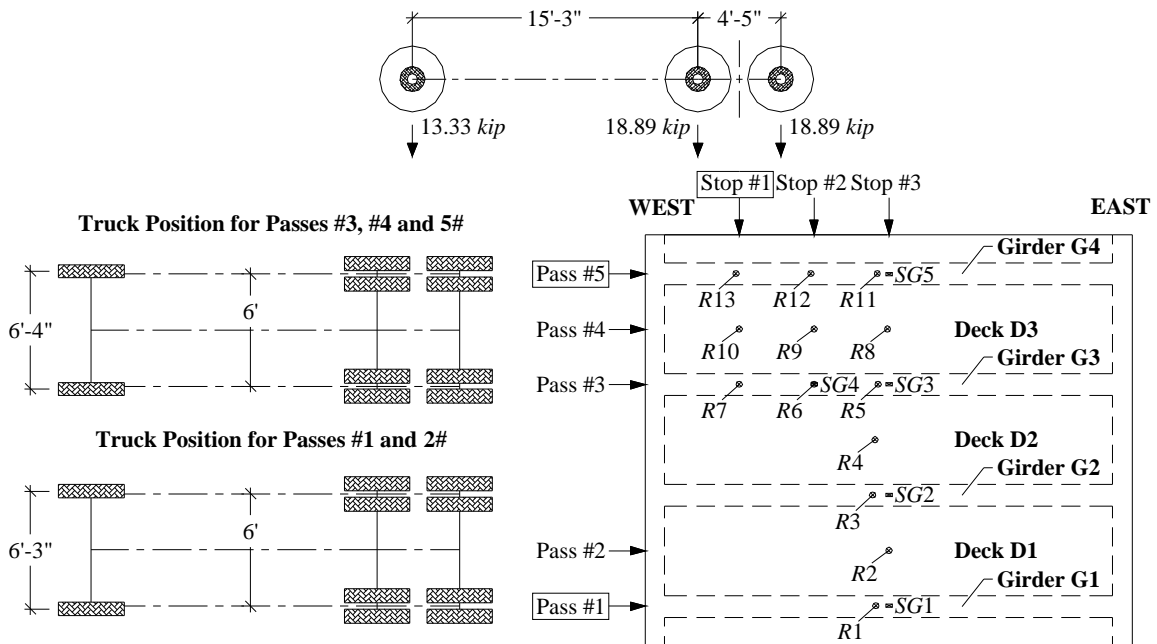
As one can see from Figure 5.5, the strengthening provided a slight increase of the stiffness of the bridge while the slope of the deformation line remains unchanged. For these reasons, the ratio between the stiffness  $K_p$  and  $K_a$ , prior to and after the strengthening respectively, could be estimated as the ratio between the normalized displacements prior to and after the strengthening: on average, it results  $K_a/K_p \cong 1.23$ .

Figure 5.6 reports the reading of the strain gages applied to the FRP strengthening, relative to Pass #3 Stop #3. The strain readings (between 120 and 170  $\mu\epsilon$ ) for the most loaded girders indicate a satisfactory performance of the FRP laminates. The distribution of the strain is not symmetric as one might expect from a symmetric load condition as that one shown in Figure 5.6. The difference between the strain readings in girders G2 and G3 can be attributed to the fact that the laminate on girder G3 was less engaged. This kind of behavior is typical of the non-bond critical strengthening systems where the strengthening needs relatively large deformations of the structure before being completely engaged.

Results for the other load configurations are summarized in Appendices A, B and C together with the theoretical values obtained with the Finite Element Method (FEM) model described in the next section.



a) H15 Legal Truck Prior to Strengthening



b) H20 Legal Truck after Strengthening

Figure 5.2. Legal Trucks Used in the Load Tests

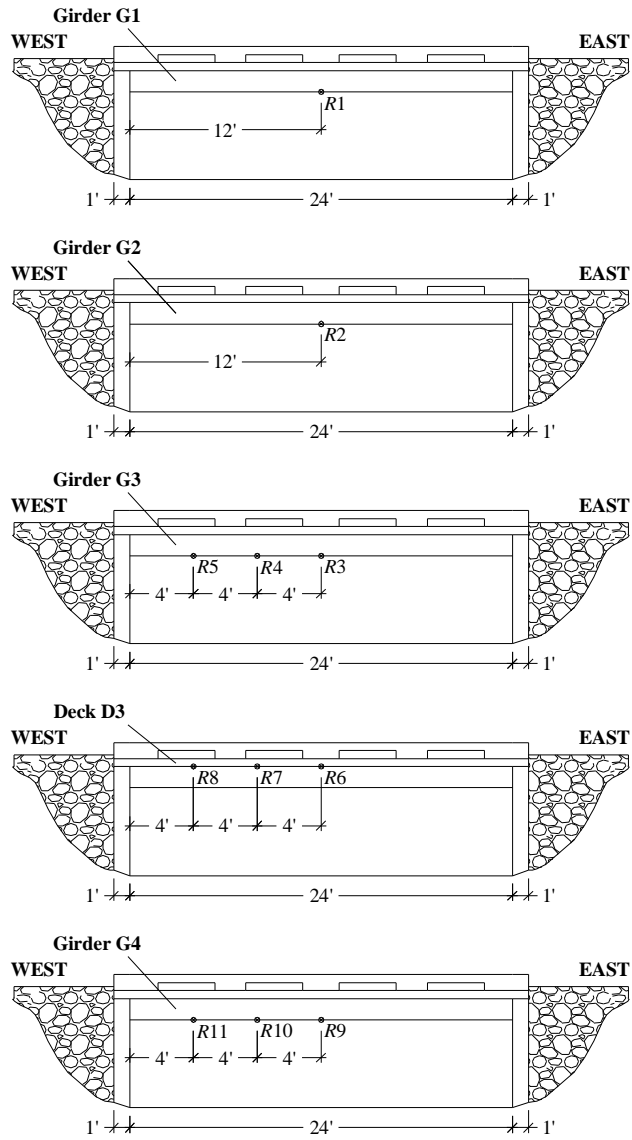


Figure 5.3. LVDT Positions in the Load Test Prior to Strengthening

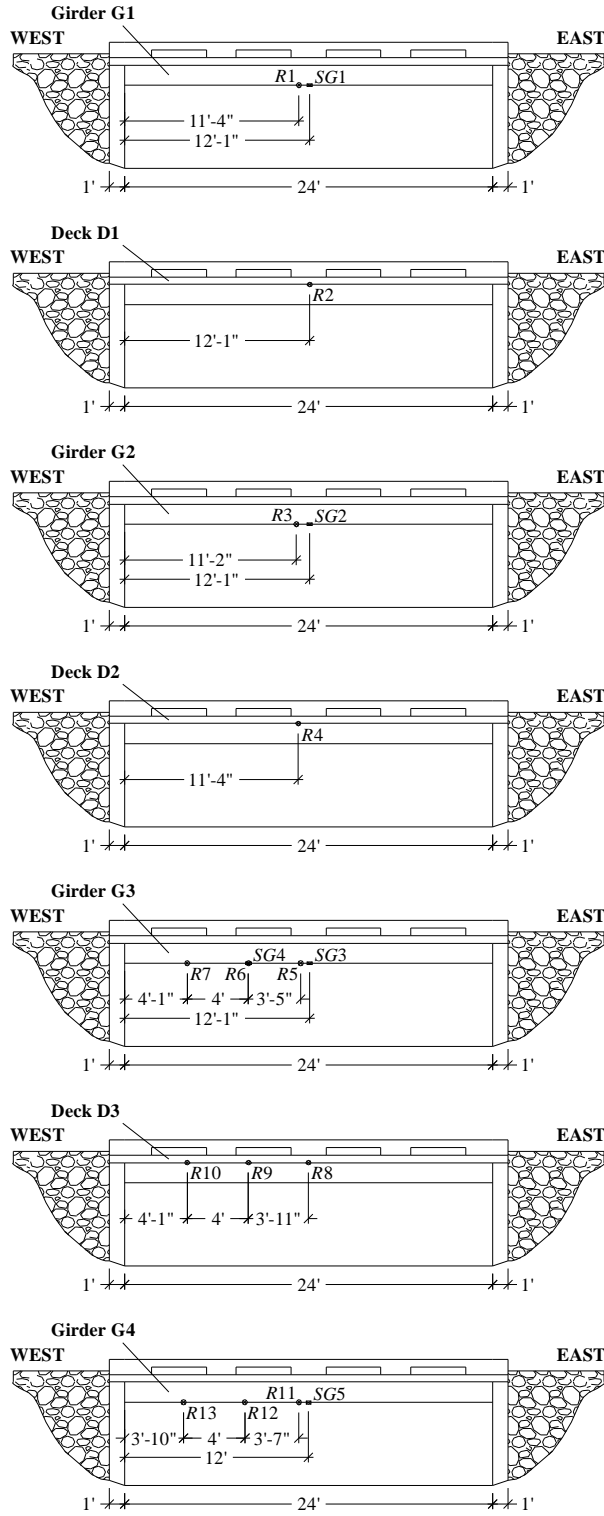


Figure 5.4. LVDT and Strain Gage Positions in the Load Test after Strengthening

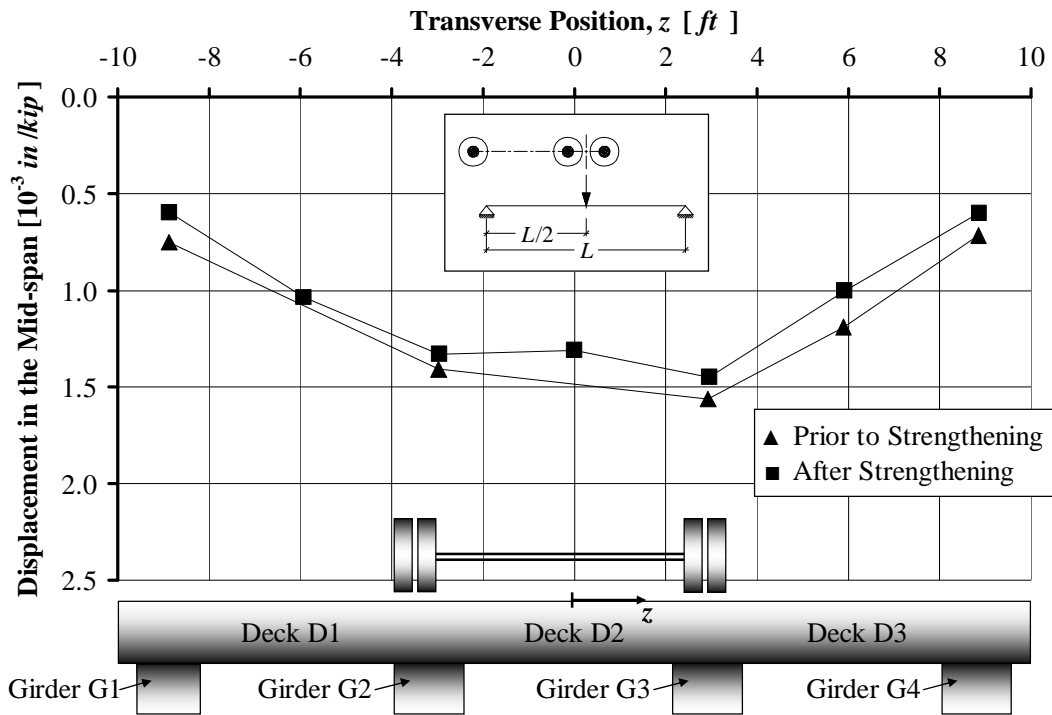


Figure 5.5. Mid-span Displacement, Pass #3 and Rear Axle in the Mid-span

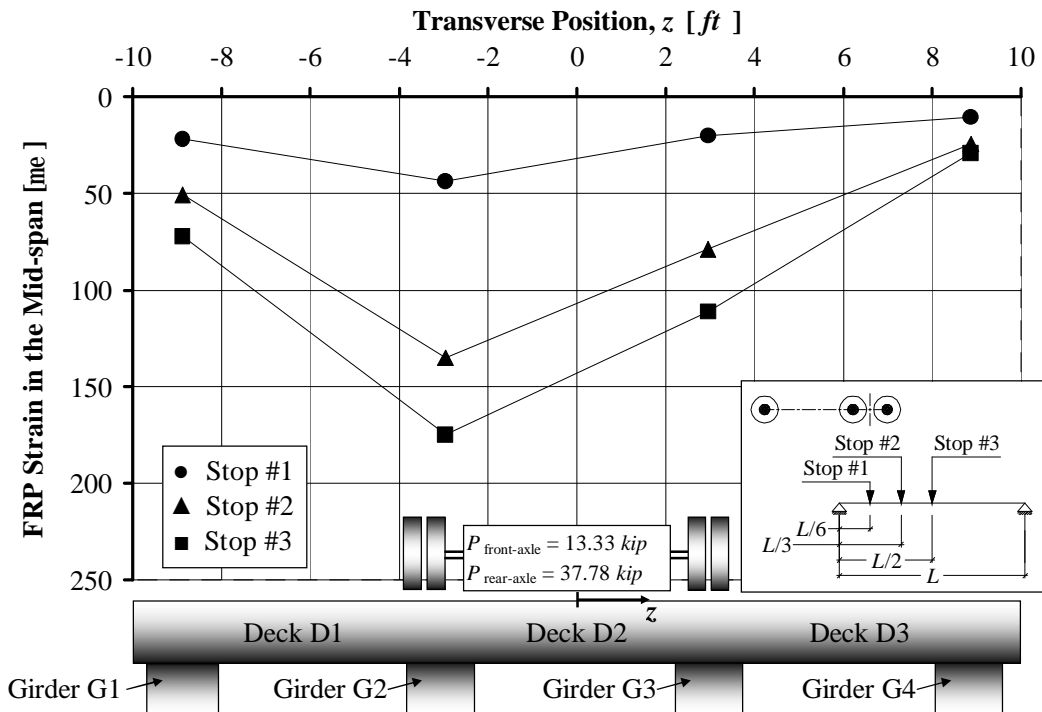


Figure 5.6. Mid-span Strain in the FRP Laminates, Pass #3 Stop #3

## 5.2. Additional Load Test

A dynamic test was conducted on the strengthened bridge in order to determine the impact factor by moving the truck on Pass #3 at speeds equal to 2.2, 4.5, 8.9 and 13.4  $m/s$  (5, 10, 20 and 30  $MPH$ ). The dynamic test was performed acquiring the data at a frequency of 22  $Hz$ . The live load impact factor  $I$  was computed as the ratio between the difference between the maximum dynamic and static displacements to the maximum static deflection (i.e. Pass #3 Stop #3). As an example, Figure 5.7 shows the dynamic deflections as a function of time at a 13.4  $m/s$  (30  $MPH$ ) speed. Figure 5.8 plots the live load impact factor  $I$  for displacements and strains for different truck speeds. In most cases, it is possible to determine the truck speed above which the impact factor decreases. This is due to the fact that by increasing the speed, the time of application of the load on the bridge is reduced and, consequently, the corresponding deflection is reduced due to bridge hysteretic behavior. From Figure 5.8., it is possible to state that the maximum impact factor related to this test was  $I_{experimental, Pass \#3} \cong 0.23$  which is smaller than that one used for design according to AASHTO (2002) ( $I = 0.30$ ).

Appendix D reports all the results obtained at different truck speeds.

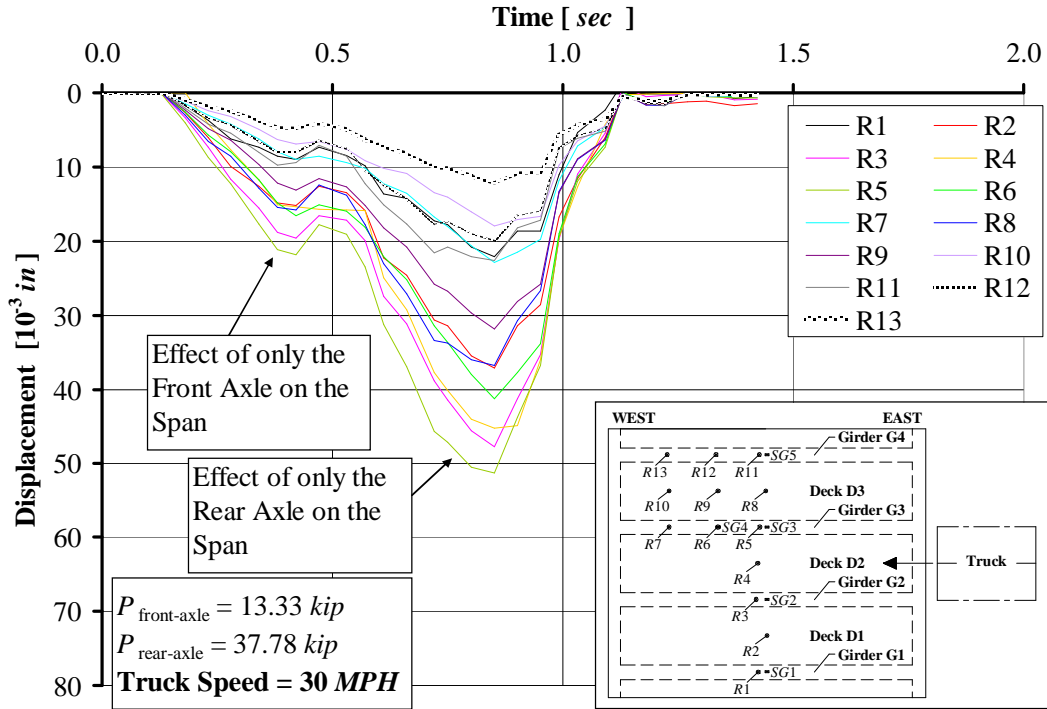


Figure 5.7. After Strengthening Displacements at 13.4 m/s (30 MPH)

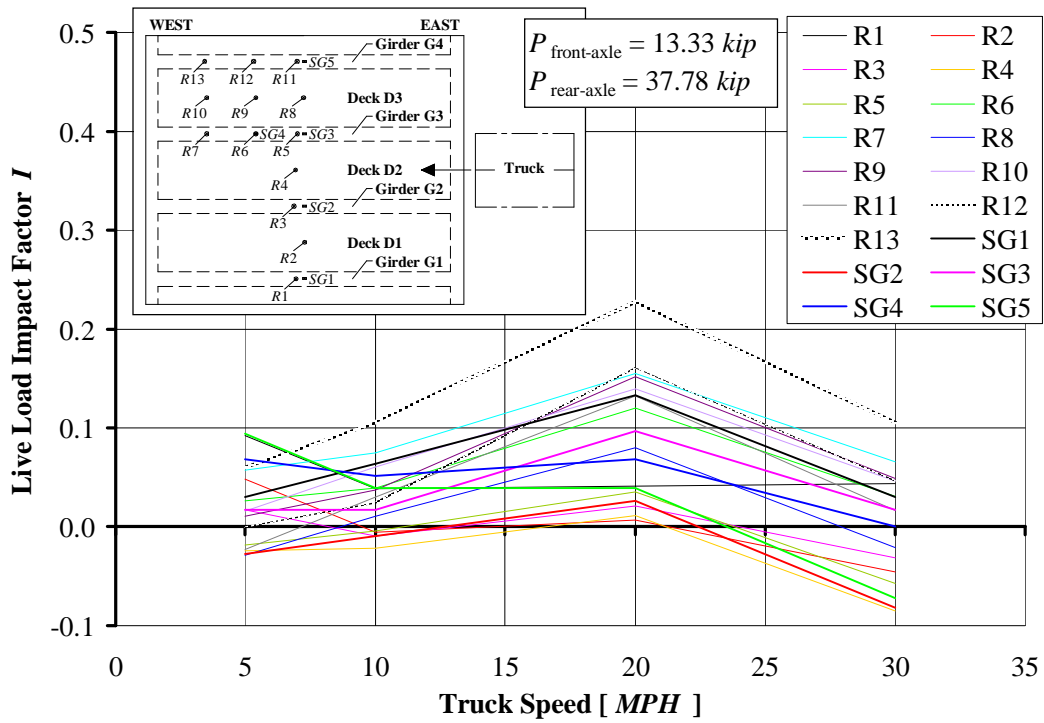


Figure 5.8. Live Load Impact Factor  $I$  versus Truck Speed

### 5.3. FEM Analysis

In this section, a FEM analysis model is described. This model was developed in order to interpret the experimental data prior to and after the strengthening. For this purpose, a commercially available finite element program ANSYS 7.1 was used. Details of the geometry can be found in Figure 5.9 and Figure 5.10.

The element SOLID65 was chosen to model the concrete and the FRP laminates. SOLID65 is used for the three-dimensional modeling of solids with or without reinforcing bars. The solid is capable of cracking in tension and crushing in compression. In addition, up to three different rebar specifications may be defined. The element is defined by eight nodes having three degrees of freedom at each node: translations in the nodal  $x$ ,  $y$  and  $z$  directions. SOLID65 is subject to the following assumption and restrictions:

- cracking is permitted in three orthogonal directions at each integration point;
- if cracking occurs at an integration point, the cracking is modeled through an adjustment of material properties which effectively treats the cracking as a “smeared band” of cracks, rather than discrete cracks;
- the concrete material is assumed to be initially isotropic;
- whenever the reinforcement capability of the element is used, the reinforcement is assumed to be “smeared” throughout the element;
- in addition to cracking and crushing, the concrete may also undergo plasticity, with the Drucker-Prager failure surface being most commonly used. In this case, the plasticity is done before the cracking and crushing checks.

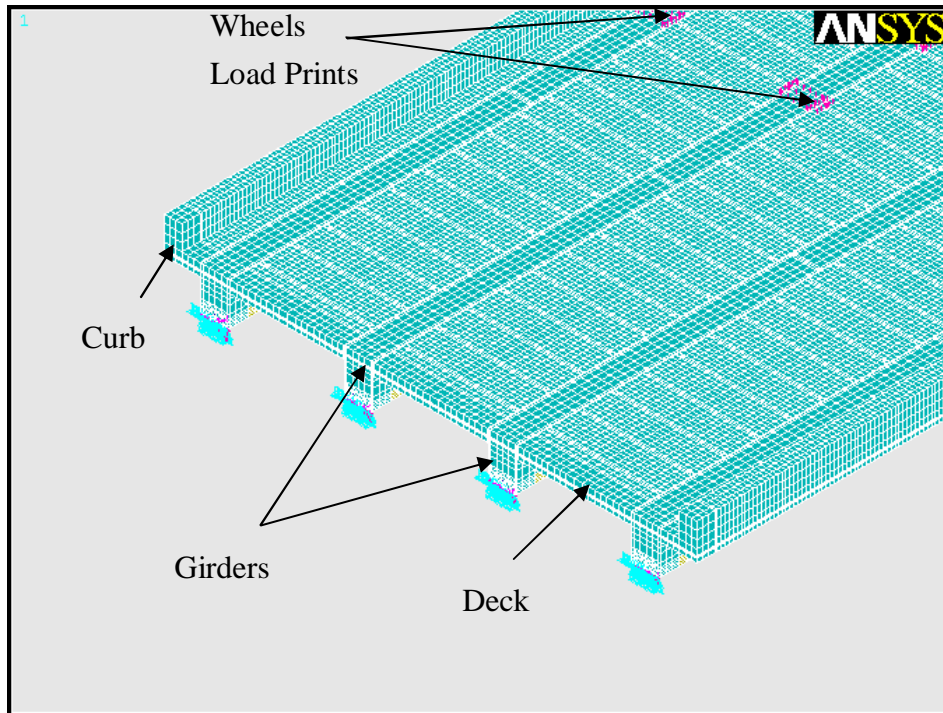
For this project, the material properties of concrete were assumed to be isotropic and linear elastic, since the applied load was relatively low with respect to the ultimate load condition. The modulus of elasticity of the concrete was based on the measured compressive strength of the cores obtained from the slab according to the standard equation ACI 318-02 Section 8.5.1:  $E_c = 57000\sqrt{f'_c} \text{ psi} \approx 32.6 \text{ GPa} (4738 \text{ ksi})$  with  $[f'_c] = [\text{psi}]$ .

In order to take into account the presence of the cracks in the girders and in the deck, as a

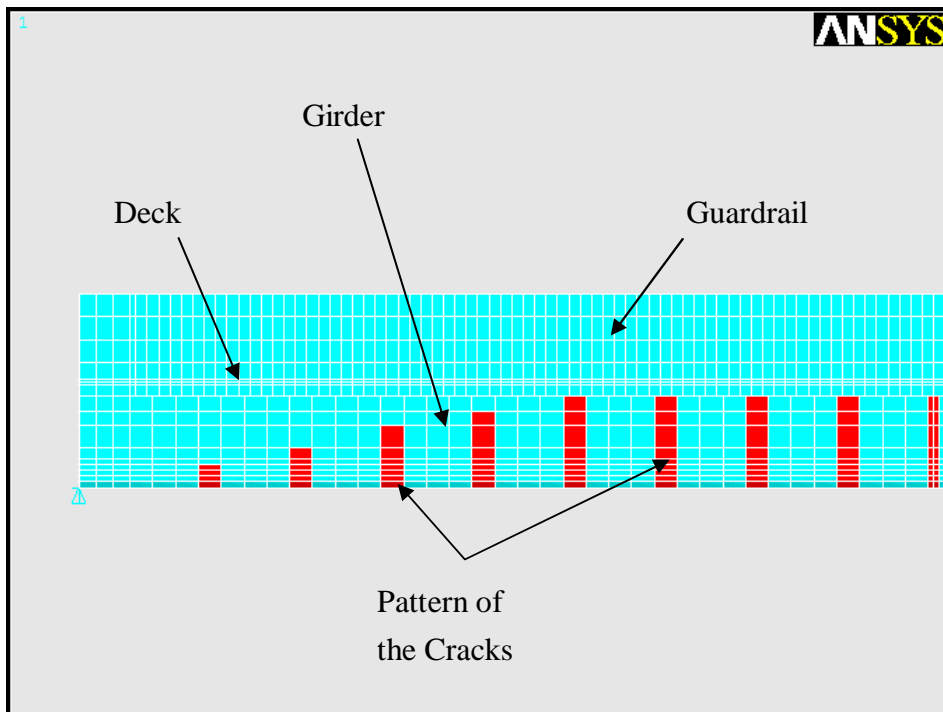
result of a parametric analysis, the modulus of elasticity was reduced to  $16.3 \text{ GPa}$  ( $2369 \text{ ksi}$ ) in the elements corresponding to the cracks as shown in Figure 5.9b. The depth of the cracks was chosen according to the data collected during the in-situ inspection while the width was assumed to be equal to the elements dimensions. The concrete Poisson's ratio was set to 0.19. Different elements were used to optimize the model and decrease the computation time. The chosen shape and size in the longitudinal and transverse cross sections allowed to locate more accurately the steel rebars (see Figure 5.10a), to properly connect the FRP laminates to the surface of the concrete (see Figure 5.10b) and to reduce the number of the elements in the "secondary" parts of the model, such as the curbs (see Figure 5.10a). The modulus of the elasticity and the Poisson's ratio for the steel reinforcement were assumed as  $200.0 \text{ GPa}$  ( $29000 \text{ ksi}$ ) and 0.3, respectively.

The connections between the FRP laminates and the concrete surface were modeled as rigid, neglecting any form of non-linearity due to a potential initial non-perfect engagement of the strengthening. Modulus of the elasticity and the Poisson's ratio for the FRP laminates were assumed to be  $60.6 \text{ GPa}$  ( $8800 \text{ ksi}$ ) and 0.3, respectively.

The bridge was vertically restrained at both ends while the longitudinal displacement was fixed to zero at one end only (see Figure 5.10a). The loads were assumed as uniformly distributed over  $508 \times 254 \text{ mm}$  ( $20 \times 10 \text{ in}$ ) areas as specified in AASHTO (2002) Section 4.3.30. Such loads were applied at the top of the deck simulating, in such way, the truck wheel prints (see Figure 5.9a). The uniform load was concentrated at the nodes corresponding to the truck wheel print and each force was determined by dividing the total load for the number of nodes.

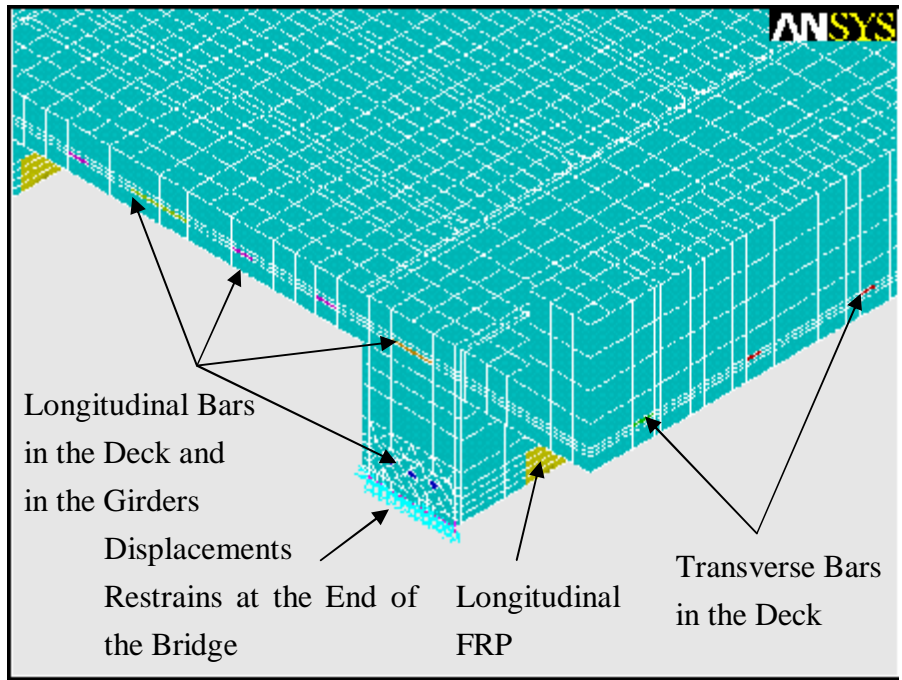


a) Global View of the Model

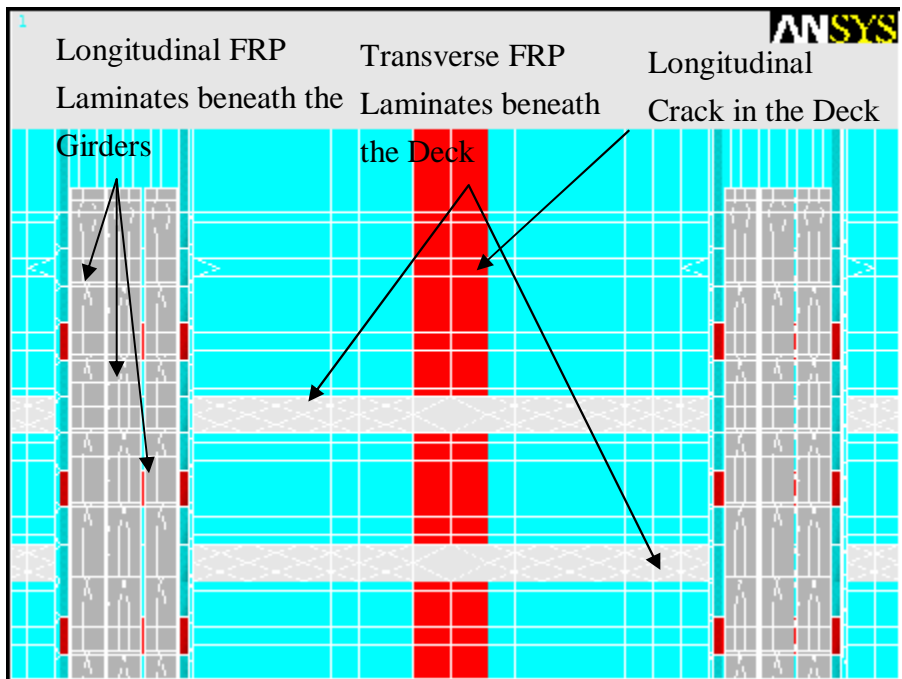


b) Details of the Cracks Modeling

Figure 5.9. FEM Model Geometry (I)



a) Details of the Steel Reinforcement and Boundary Conditions



b) Details of the FRP Strengthening (Bottom View)

Figure 5.10. FEM Model Geometry (II)

Figure 5.11 reports the experimental and analytical mid-span displacements, relative to Pass #3 when the rear axle of the truck is in the mid-span (Stop #2 and Stop #3 for the load test prior to and after strengthening, respectively). The graph shows a good match in deflections between experimental and analytical results.

Figure 5.12 compares experimental and analytical strains on the FRP, relative to the Pass #3 and Stops #1, #2 and #3. The graph shows a good match in strains between experimental and analytical results for girders G1 and G2. The mismatch for girders G3 and G4 can be explained with the incomplete engagement of the FRP laminates to the concrete.

Figure 5.13 plots the longitudinal distribution of the strain in the middle of the central laminates present in each girder. It is important to note that there is stress concentration in a small area of the laminates around each fastener. The peak in the mid-span is emphasized by the presence of the crack in the concrete.

Appendices A, B and C report all the analysis developed for the bridge prior to and after the strengthening.

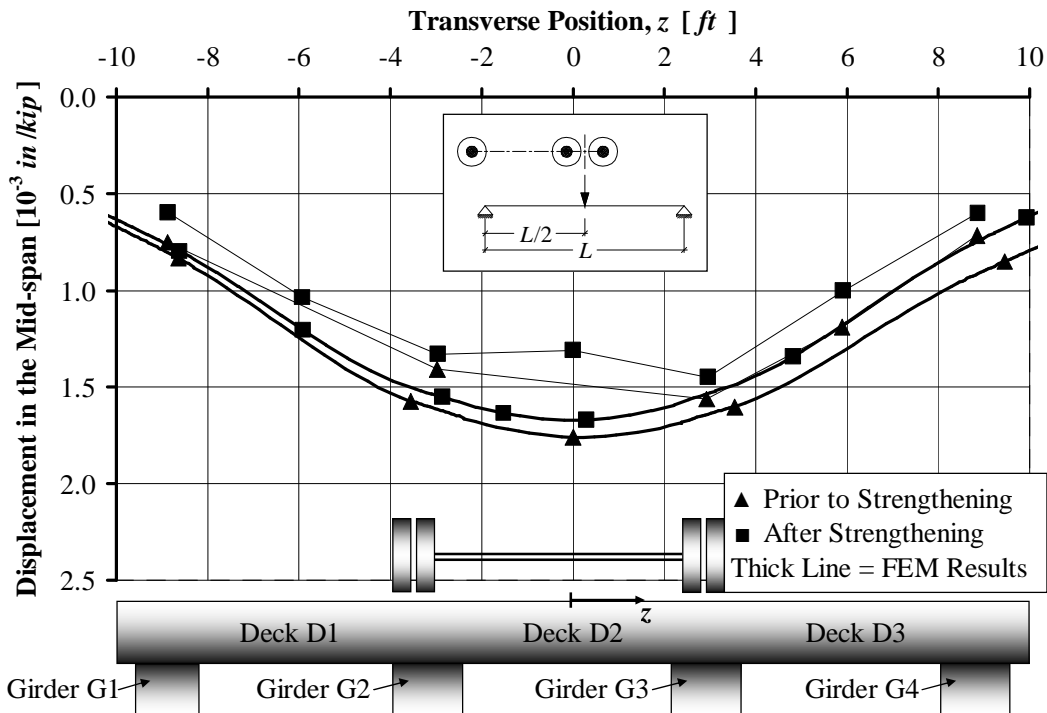


Figure 5.11. Comparison of Experimental and Analytical Results for Mid-span Displacement, Pass #3 and Rear Axle in the Mid-span

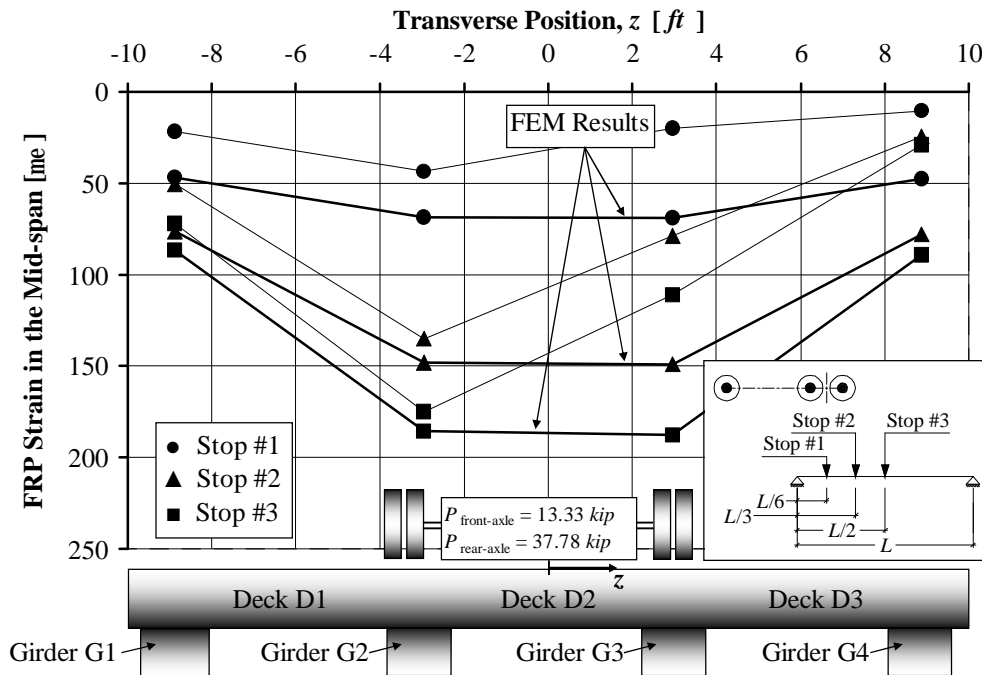


Figure 5.12. Comparison of Experimental and Analytical Results for Strain in the FRP Fastened on the Girders at Mid-span, Pass #3 and Stops #1, #2 and #3

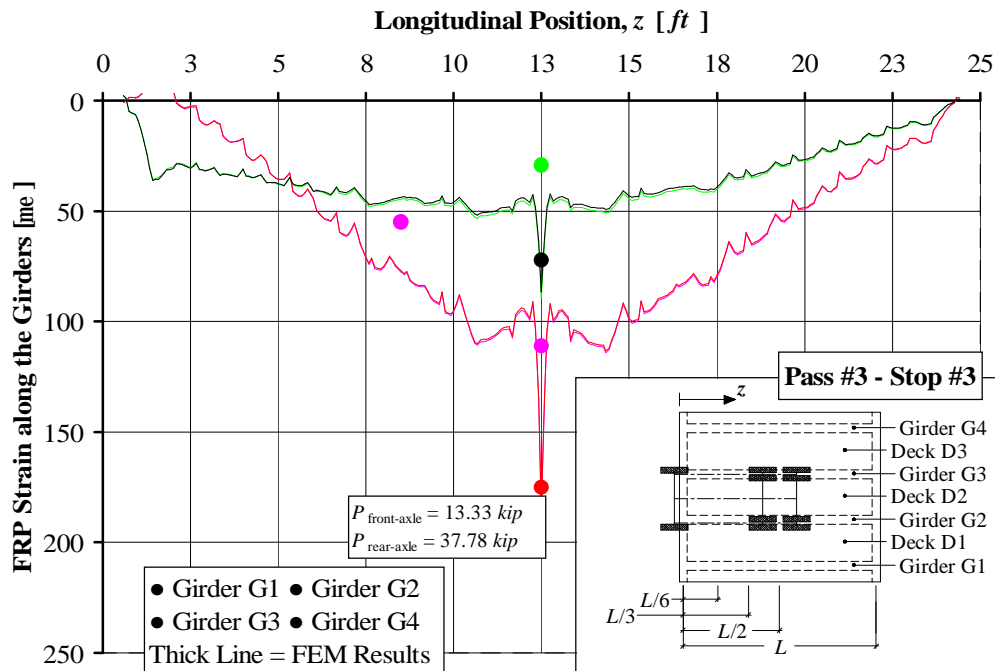


Figure 5.13. Comparison of Experimental and Analytical Results for Strain in the Longitudinal Direction in the FRP Fastened on the Girders, Pass #3 Stop #3

## 6. LOAD RATING

Bridge load rating calculations provide a basis for determining the safe load capacity of a bridge. According to the Missouri Department of Transportation (MoDOT), anytime a bridge is built, rehabilitated, or reevaluated for any reason, inventory and operating ratings are required using the Load Factor rating. All bridges should be rated at two load levels, the maximum load level called the Operating Rating and a lower load level called the Inventory Rating. The Operating Rating is the maximum permissible load that should be allowed on the bridge. Exceeding this level could damage the bridge. The Inventory Rating is the load level the bridge can carry on a daily basis without damaging the bridge.

In Missouri, for the Load Factor Method the Operating Rating is based on the appropriate ultimate capacity using current AASHTO specifications (AASHTO, 1996). The vehicle used for the live load calculations in the Load Factor Method is the HS20 truck. If the stress levels produced by this vehicle configuration are exceeded, load posting may be required.

The method for determining the rating factor is that outlined by AASHTO in the Manual for Condition Evaluation of Bridges (AASHTO, 2002). Equation (6.1) was used:

$$RF = \frac{C - A_1 D}{A_2 L (1 + I)} \quad (6.1)$$

where:

$RF$  is the Rating Factor;

$C$  is the capacity of the member;

$D$  is the dead load effect on the member;

$L$  is the live load effect on the member;

$I$  is the impact factor to be used with the live load effect;

$A_1$  is the factor for dead loads;

$A_2$  is the factor for live loads.

Since the load factor method is being used,  $A_1$  is taken as 1.3 and  $A_2$  varies depending on the desired rating level. For Inventory Rating,  $A_2 = 2.17$ , and for Operating Rating,  $A_2 = 1.3$ .

To determine the rating  $RT$  of the bridge, equation (6.2) was used:

$$RT = RF \cdot W \quad (6.2)$$

where  $W$  is the weight of the nominal truck used to determine the live load effect.

For the bridge No. 1330005, the Load Rating was calculated for a number of different trucks, HS20, H20, 3S2 and MO5. Ratings are required at the inventory and operating levels by the load factor method on each bridge for the HS20 truck. The H20 legal vehicle is used to model the load for single unit vehicles. The 3S2 vehicle is used as a model for all other vehicles. The MO5 is used to model the commercial zone loadings.

For each of the different loading conditions, the maximum shear and maximum moment were calculated. Impact factors are also taken into account for Load Ratings. This value is 30% for the bridge No. 1330005. The shear and moment values for the deck and the girders are shown in Table 6.1 and Table 6.2.

Table 6.1. Maximum Shear and Moment due to Live Load for the Deck

Truck	Maximum Shear [kN] ([kip])	Maximum Moment [kN · m] ([kip · ft])	Maximum Shear with Impact [kN] ([kip])	Maximum Moment with Impact [kN · m] ([kip · ft])
HS20	5.83 (1.31)	4.38 (3.23)	7.56 (1.70)	5.69 (4.20)
MO5	3.07 (0.69)	2.39 (1.76)	4.00 (0.90)	3.10 (2.29)
H20	3.07 (0.69)	2.39 (1.76)	4.00 (0.90)	3.10 (2.29)
3S2	4.36 (0.98)	3.23 (2.38)	5.65 (1.27)	4.19 (3.09)

Table 6.2. Maximum Shear and Moment due to Live Load for the Girders

Truck	Maximum Shear [kN] ([kip])	Maximum Moment [kN · m] ([kip · ft])	Maximum Shear with Impact [kN] ([kip])	Maximum Moment with Impact [kN · m] ([kip · ft])
HS20	102.18 (22.97)	140.14 (103.36)	132.82 (29.86)	182.18 (134.37)
MO5	90.30 (20.30)	161.45 (119.08)	117.39 (26.39)	209.88 (154.80)
H20	72.02 (16.19)	115.82 (85.42)	93.63 (21.05)	150.55 (111.04)
3S2	72.37 (16.27)	116.64 (86.03)	94.12 (21.16)	151.62 (111.83)

Table 6.3 and Table 6.4 give the results of the Load Rating pertaining to moment and shear respectively for the deck.

Table 6.3. Rating Factor for the Deck (Bending Moment)

Truck	Rating Factor <i>RF</i>	Rating <i>RT</i> [ton]	Rating Type
HS20	2.140	69.9 (77.0)	Operating
HS20	1.282	41.9 (46.2)	Inventory
MO5	3.924	130.4 (143.8)	Operating
H20	3.375	61.2 (67.5)	Posting
3S2	2.500	83.1 (91.6)	Posting

Table 6.4. Rating Factor for the Deck (Shear)

Truck	Rating Factor <i>RF</i>	Rating <i>RT</i> [ton]	Rating Type
HS20	2.498	81.6 (89.9)	Operating
HS20	1.496	48.9 (53.9)	Inventory
MO5	4.725	157.1 (173.1)	Operating
H20	4.064	73.7 (81.3)	Posting
3S2	2.872	95.5 (105.2)	Posting

Table 6.5 and Table 6.6 give the results of the Load Rating pertaining to moment and shear respectively for the girders.

Table 6.5. Rating Factor for the Girders (Bending Moment)

Truck	Rating Factor <i>RF</i>	Rating <i>RT</i> [ton]	Rating Type
HS20	1.157	37.8 (41.7)	Operating
HS20	0.693	22.6 (25.0)	Inventory
MO5	1.004	33.4 (36.8)	Operating
H20	1.204	21.8 (24.1)	Posting
3S2	1.195	39.7 (43.8)	Posting
HS20	1.157	37.8 (41.7)	Operating

Table 6.6. Rating Factor for the Girders (Shear)

Truck	Rating Factor <i>RF</i>	Rating <i>RT</i> [ton]	Rating Type
HS20	1.803	58.9 (64.9)	Operating
HS20	1.080	35.3 (38.9)	Inventory
MO5	2.041	67.8 (74.8)	Operating
H20	2.200	39.9 (44.0)	Posting
3S2	2.189	72.8 (80.2)	Posting

In Missouri, load posting is established using the H20 and 3S2 vehicles. Therefore, according to Table 6.5, the bridge should be posted at  $21.8 \text{ ton}_{SI}$  ( $24.1 \text{ ton}$ ). But, since the legal loads established for Missouri are defined as  $20.9 \text{ ton}_{SI}$   $23.0 \text{ ton}$  for single unit vehicles and  $36.3 \text{ ton}_{SI}$  ( $40.0 \text{ ton}$ ) for all others, the existing load posting can be removed.

## 7. Conclusions

Conclusions based on the retrofitting of the bridge utilizing FRP materials can be summarized as follows:

- The mechanically fastened (MF) FRP system showed to be a feasible solution for the strengthening of the bridge;
- In-situ load testing has proven to be useful and convincing;
- The FEM analysis has shown good match with experimental results demonstrating the effectiveness of the strengthening technique;
- As a result of FRP strengthening, the load posting of the bridge can be removed.

## 8. REFERENCES

- AASHTO (1996). "LRFD bridge design specifications." Second Edition, Published by the American Association of State Highway and Transportation Officials, Washington D.C.
- AASHTO (2002). "Standard specifications for highway bridges." 17<sup>th</sup> Edition, Published by the American Association of State Highway and Transportation Officials, Washington D.C.
- ACI Committee 318 (1999). "Building code requirements for structural concrete and commentary." ACI 318R-99, Published by the American Concrete Institute, Farmington Hills, MI.
- ACI Committee 318 (2002). "Building code requirements for structural concrete and commentary." ACI 318R-02, Published by the American Concrete Institute, Farmington Hills, MI.
- ACI Committee 440 (1996). "State-of-the-art report on FRP for concrete structures." ACI 440R-96, Manual of Concrete Practice, ACI, Farmington Hills, MI, 68 pp.
- ACI Committee 440 (2002). "Guide for the design and construction of externally bonded FRP systems for strengthening concrete structures." ACI 440.2R-02, Published by the American Concrete Institute, Farmington Hills, MI.
- Alkhrdaji, T., Nanni, A., Chen, G., and Barker, M. (1999). "Upgrading the transportation infrastructure: solid RC decks strengthened with FRP." Concrete International, American Concrete Institute, Vol. 21, No. 10, October, pp. 37-41.
- ANSYS User's Manual for Revision 6.1 (2000). Volume I Procedure and Volume III Elements, Swanson Analysis Systems, Inc.
- Arora, D. (2003). "Rapid strengthening of reinforced concrete bridge with mechanically fastened fiber-reinforced polymer strips." M.Sc. Thesis, University of Wisconsin – Madison.
- Bank, L. C., Lamanna A. J., Ray, J. C., and Velásquez G. I. (2002). "Rapid strengthening

of reinforced concrete beams with mechanically fastened, fiber-reinforced polymeric composite materials.” US Army Corps of Engineers, Washington D.C.

Bank, L. C., Borowicz D. T., Lamanna A. J., Ray J. C., and Velásquez G. I. (2002). “Rapid strengthening of full-sized concrete beams with powder-actuated fastening systems and Fiber-Reinforced Polymer (FRP) composite materials.” US Army Corps of Engineers, Washington D.C.

Borowicz, D. T. (2002). “Rapid strengthening of concrete beams with powder-actuated fastening systems and Fiber-Reinforced Polymer (FRP) composite materials.” M.Sc. Thesis, University of Wisconsin – Madison.

Lamanna, A.J. (2002). “Flexural strengthening of reinforced concrete beams with mechanically fastened fiber reinforced polymer strips.” PhD Thesis, University of Wisconsin – Madison.

## **APPENDICES**

## **APPENDIX**

### **A. Prior to Strengthening Test Results**

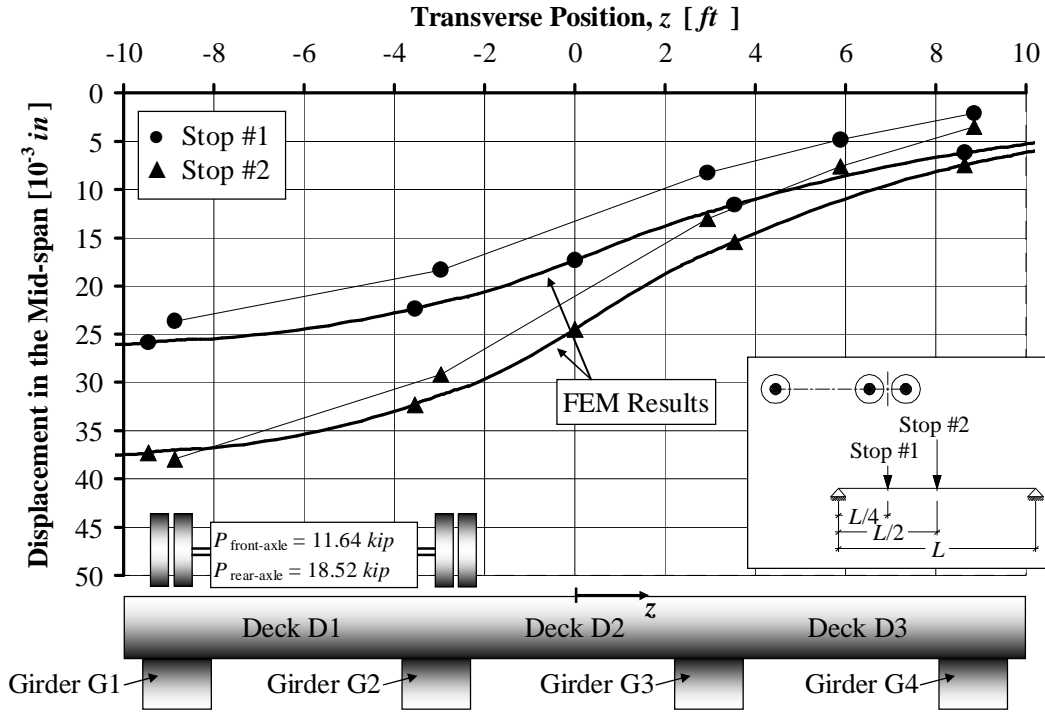


Figure A. 1. Prior to Strengthening Mid-span Displacement, Pass #1

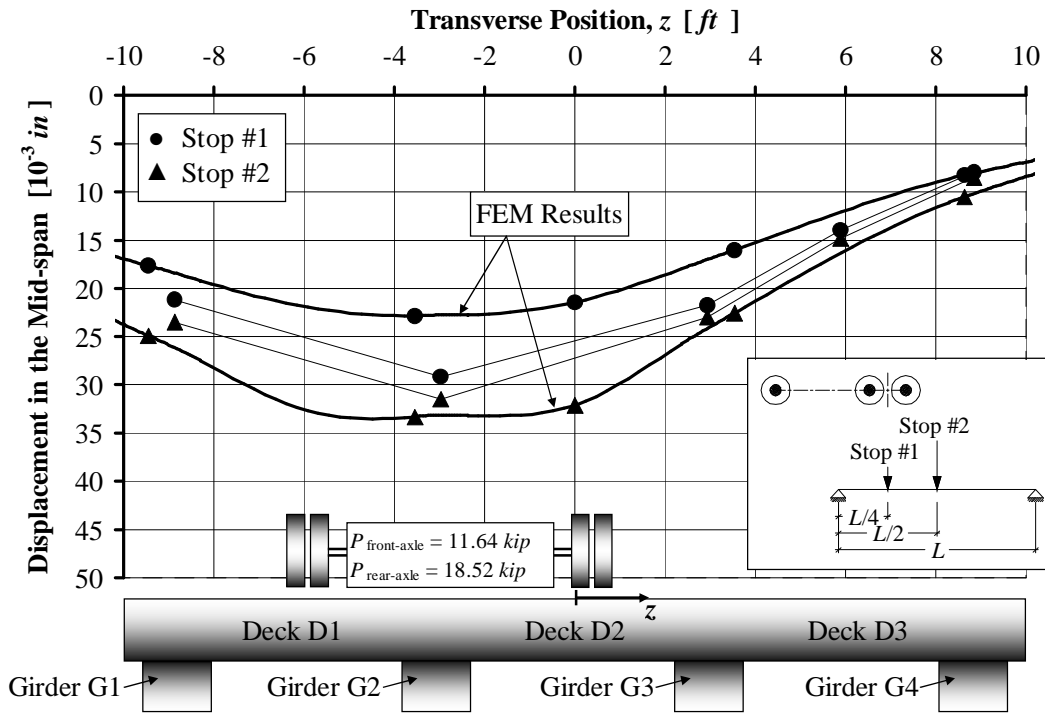


Figure A. 2. Prior to Strengthening Mid-span Displacement, Pass #2

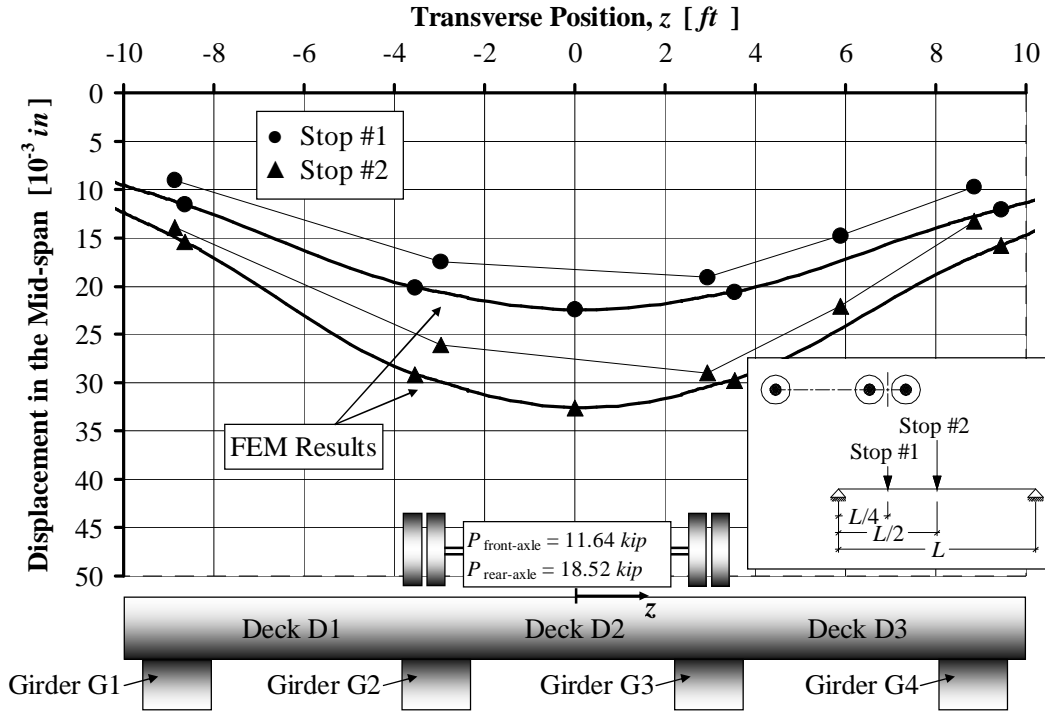


Figure A. 3. Prior to Strengthening Mid-span Displacement, Pass #3

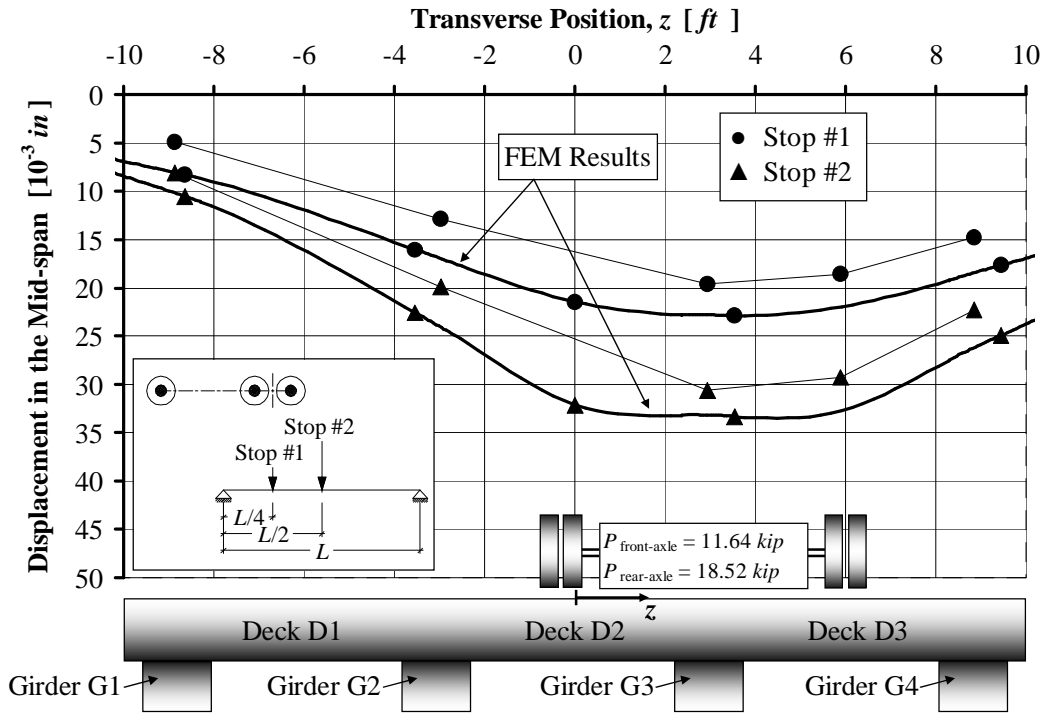


Figure A. 4. Prior to Strengthening Mid-span Displacement, Pass #4

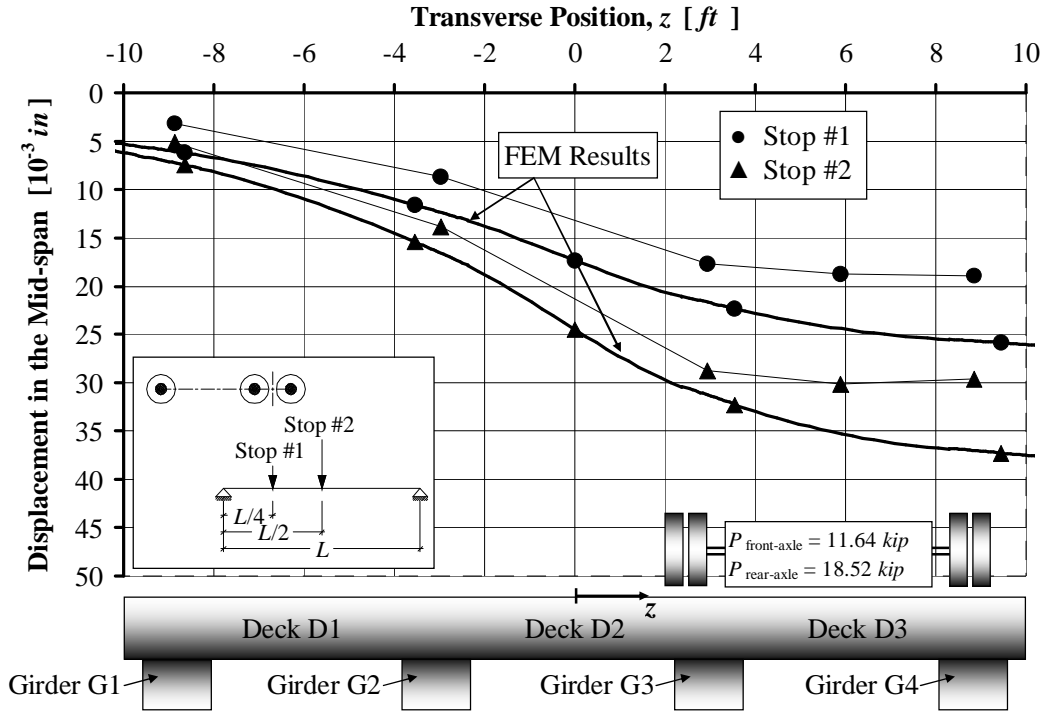


Figure A. 5. Prior to Strengthening Mid-span Displacement, Pass #5

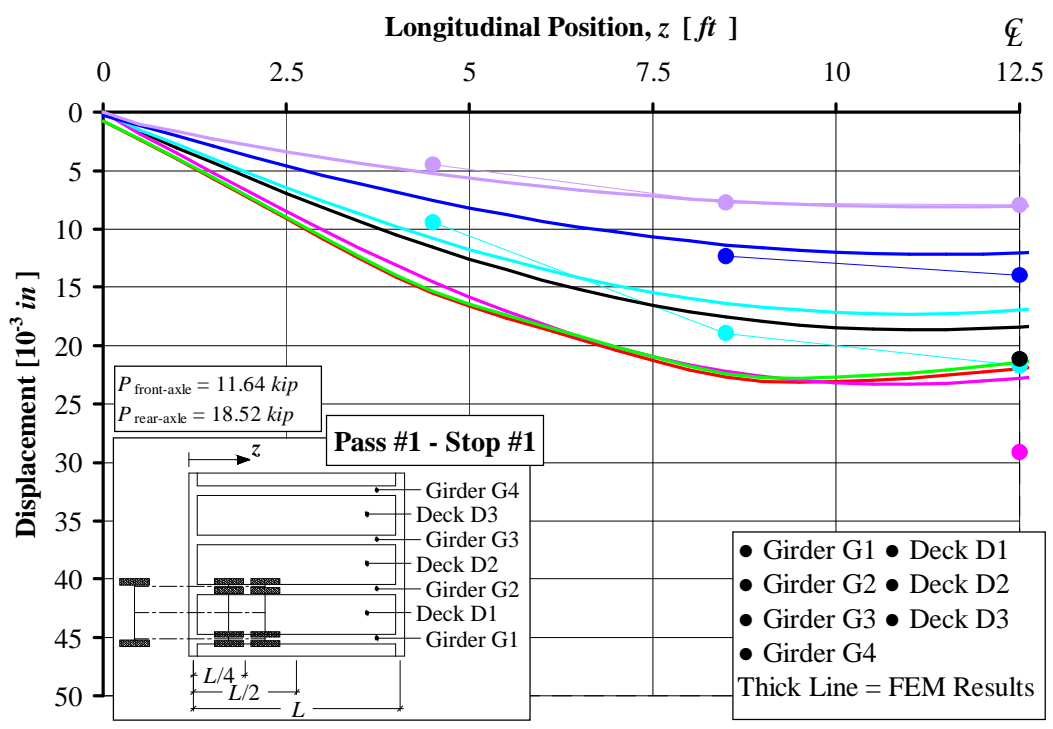


Figure A. 6. Prior to Strengthening Displacement Distribution, Pass #1 Stop #1

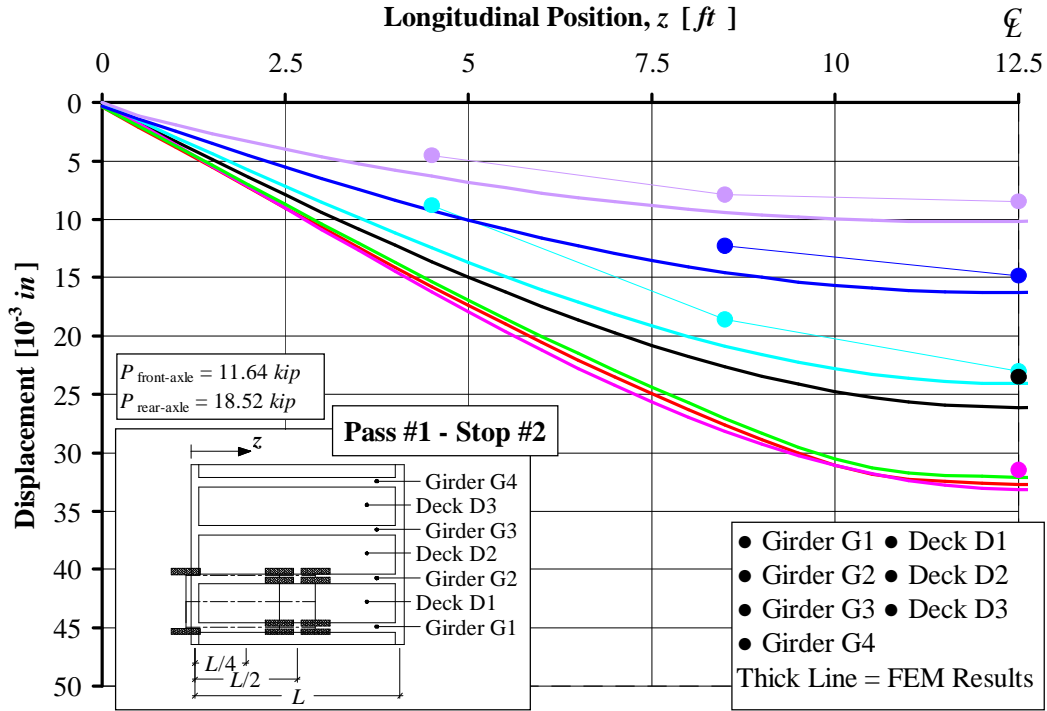


Figure A. 7. Prior to Strengthening Displacement Distribution, Pass #1 Stop #2

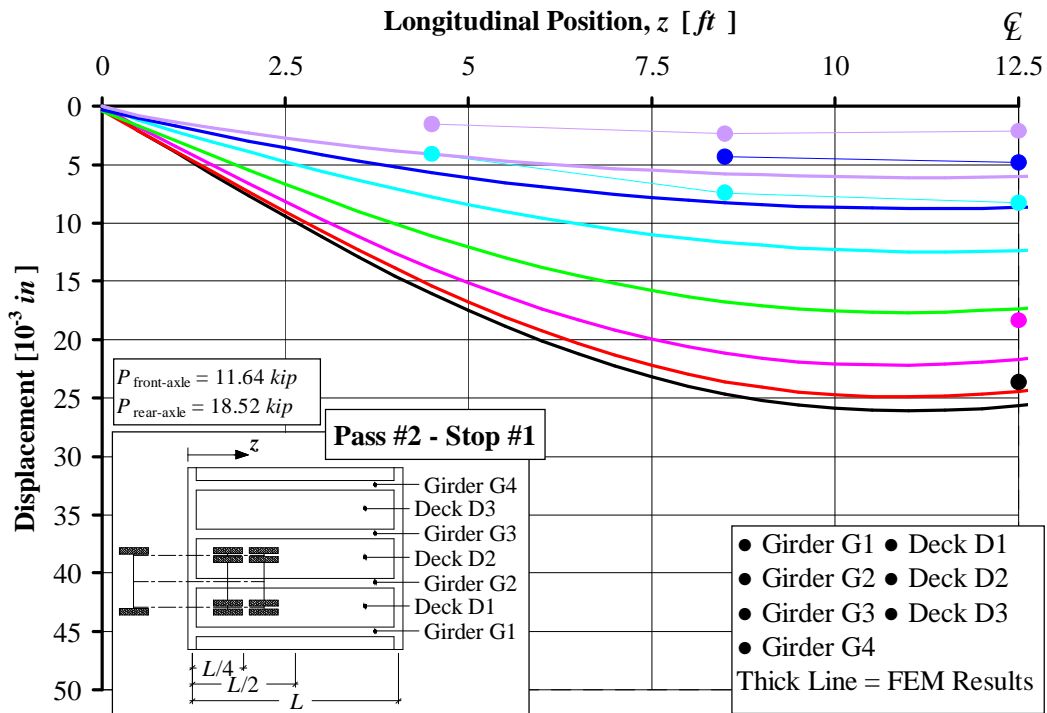


Figure A. 8. Prior to Strengthening Displacement Distribution, Pass #2 Stop #1

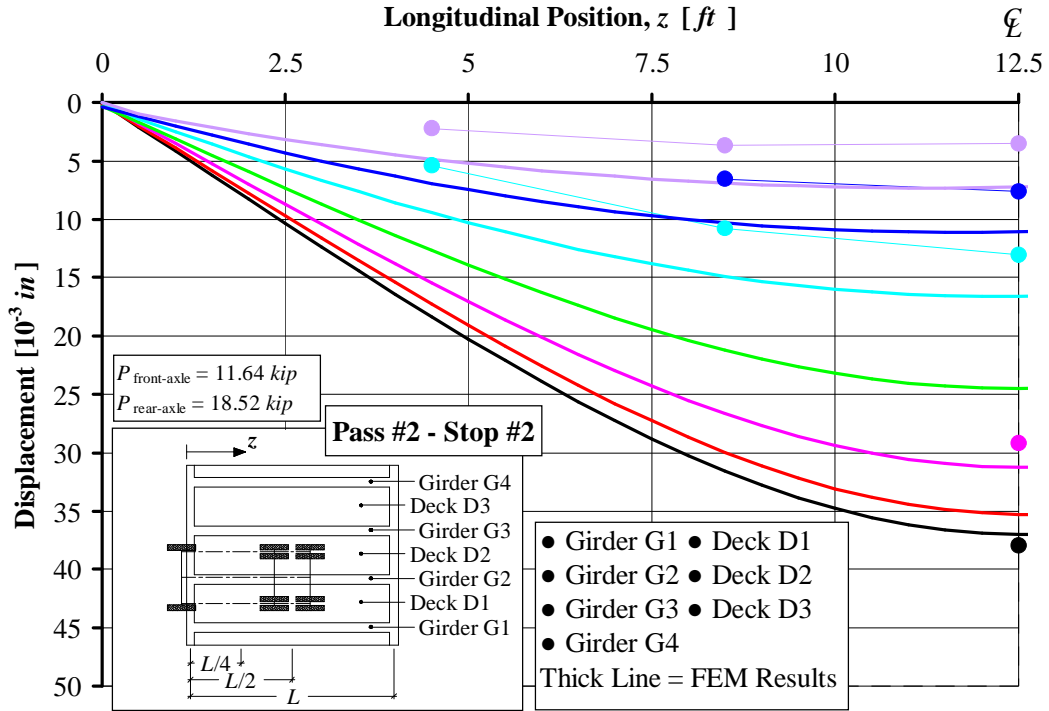


Figure A. 9. Prior to Strengthening Displacement Distribution, Pass #2 Stop #2

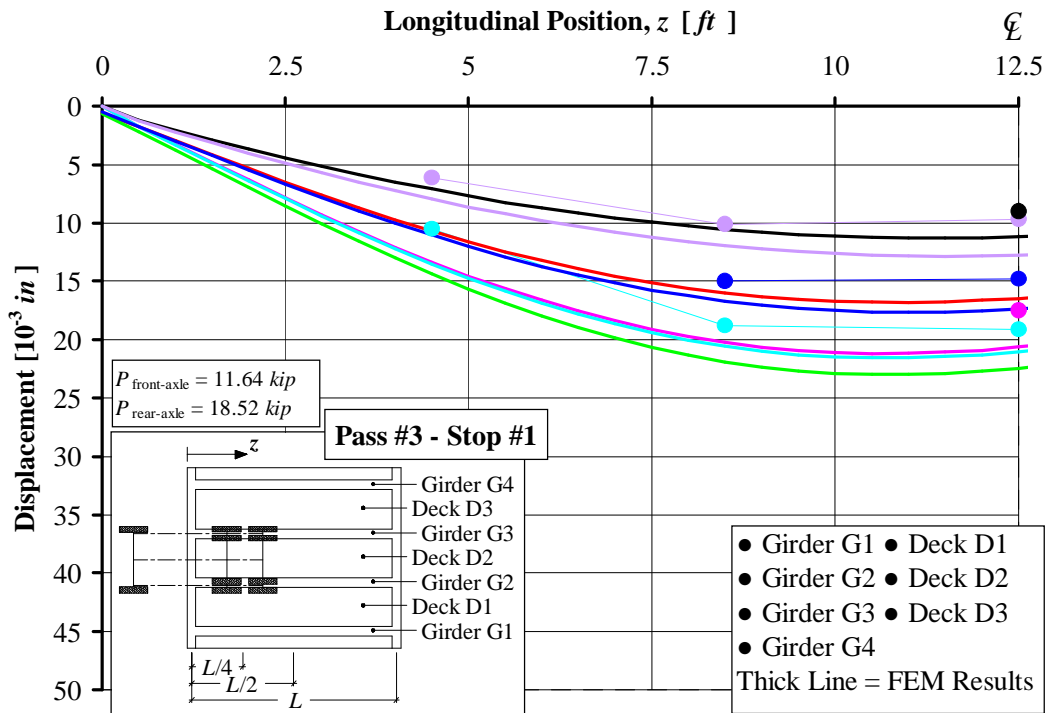


Figure A. 10. Prior to Strengthening Displacement Distribution, Pass #3 Stop #1

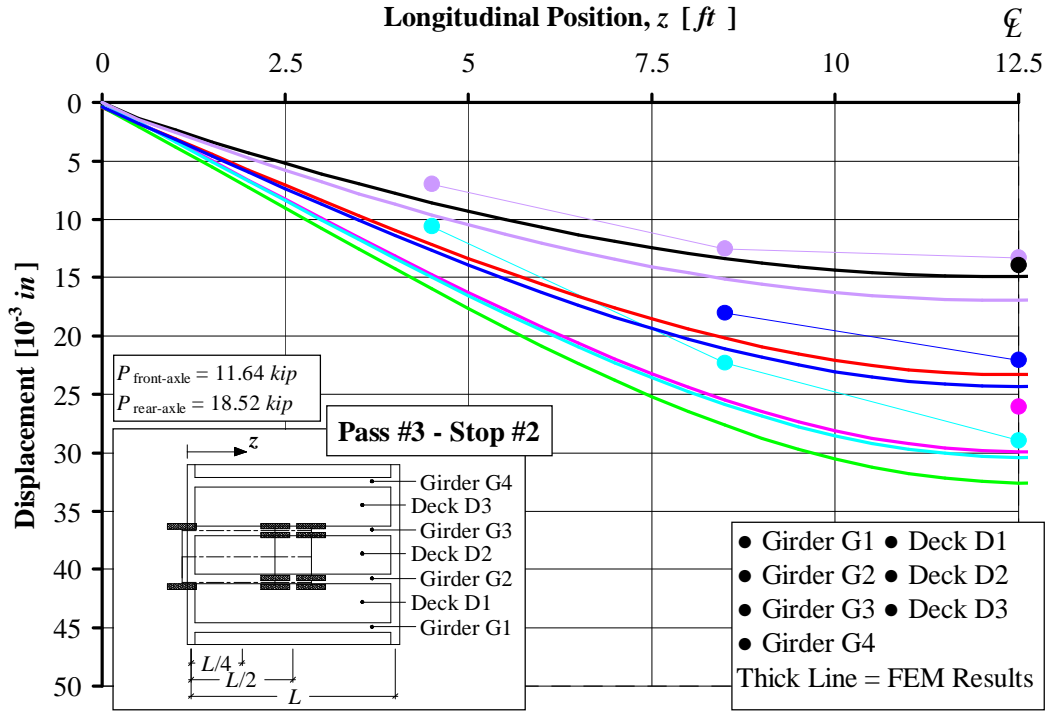


Figure A.11. Prior to Strengthening Displacement Distribution, Pass #3 Stop #2

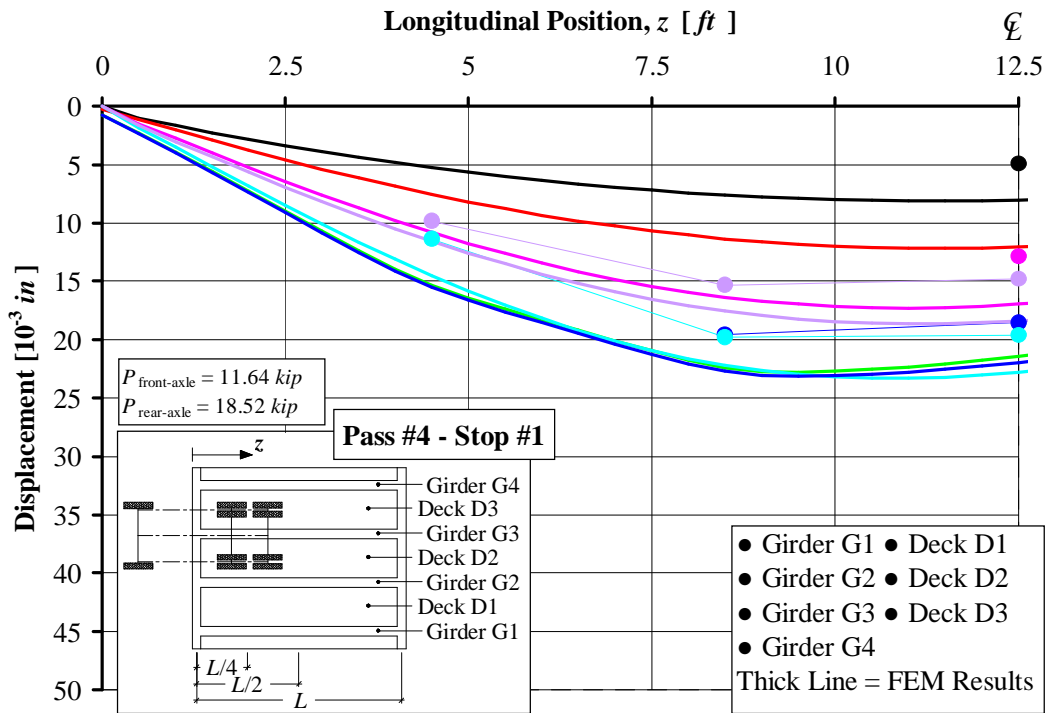


Figure A.12. Prior to Strengthening Displacement Distribution, Pass #4 Stop #1

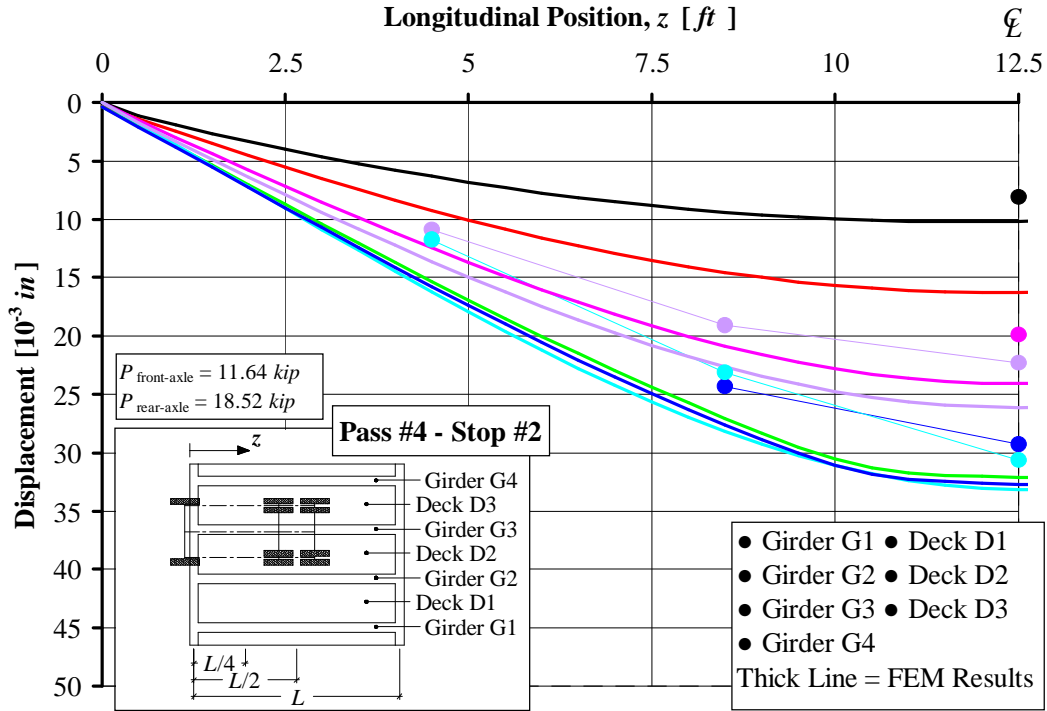


Figure A. 13. Prior to Strengthening Displacement Distribution, Pass #4 Stop #2

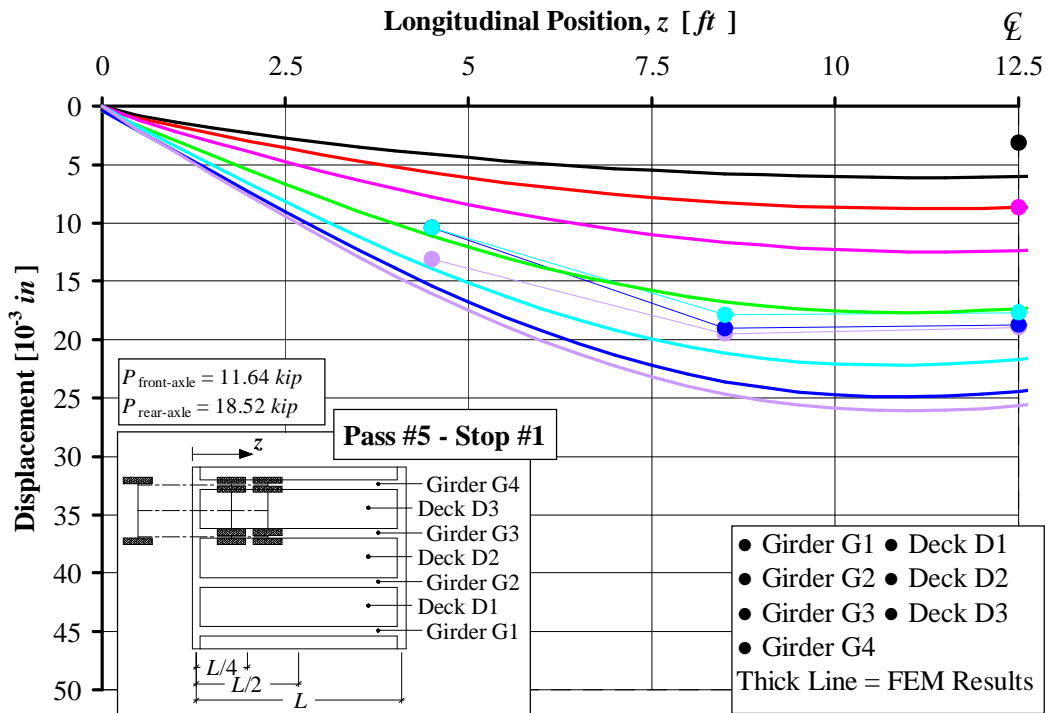


Figure A. 14. Prior to Strengthening Displacement Distribution, Pass #5 Stop #1

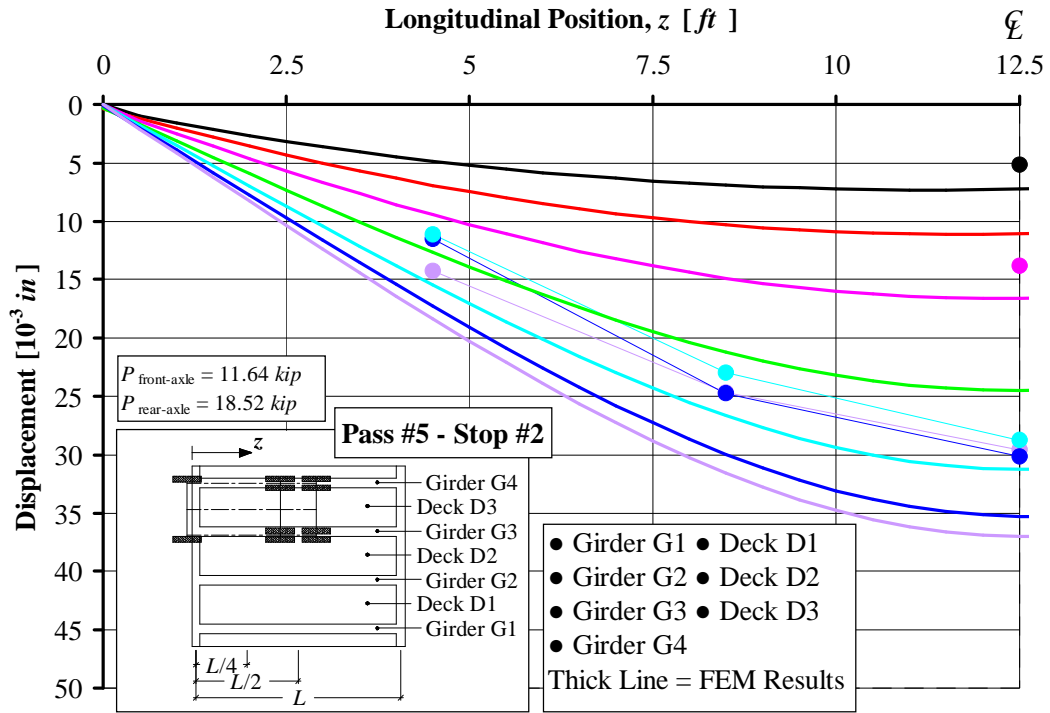


Figure A. 15. Prior to Strengthening Displacement Distribution, Pass #5 Stop #2

## **APPENDIX**

### **B. After Strengthening Test Results**

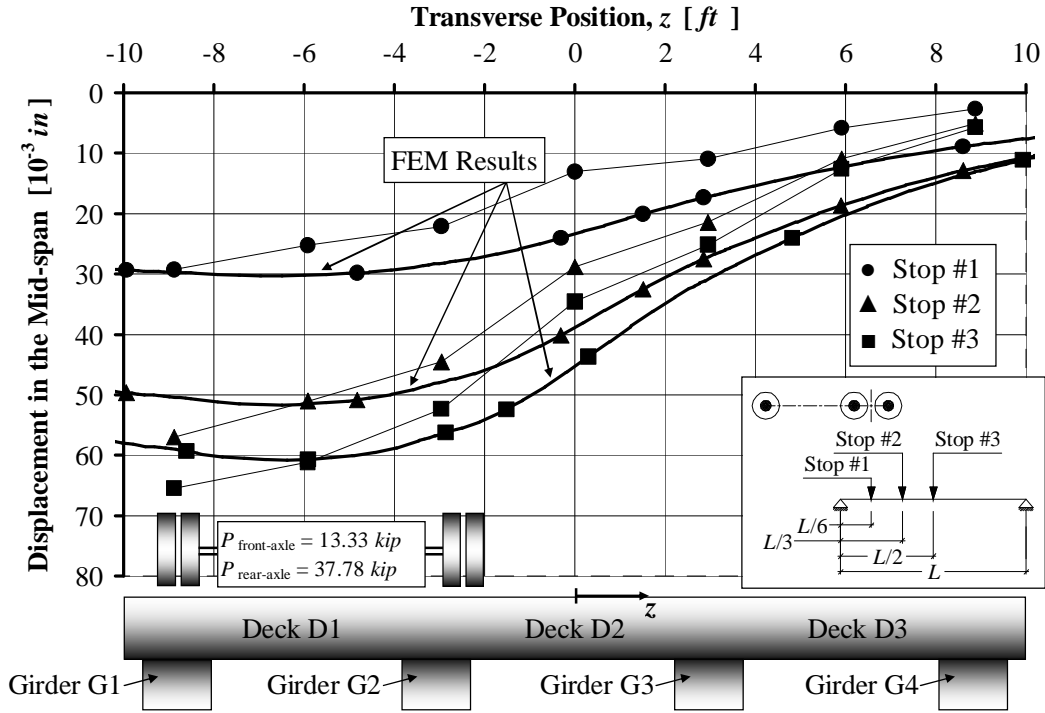


Figure B. 1. After Strengthening Mid-span Displacement, Pass #1

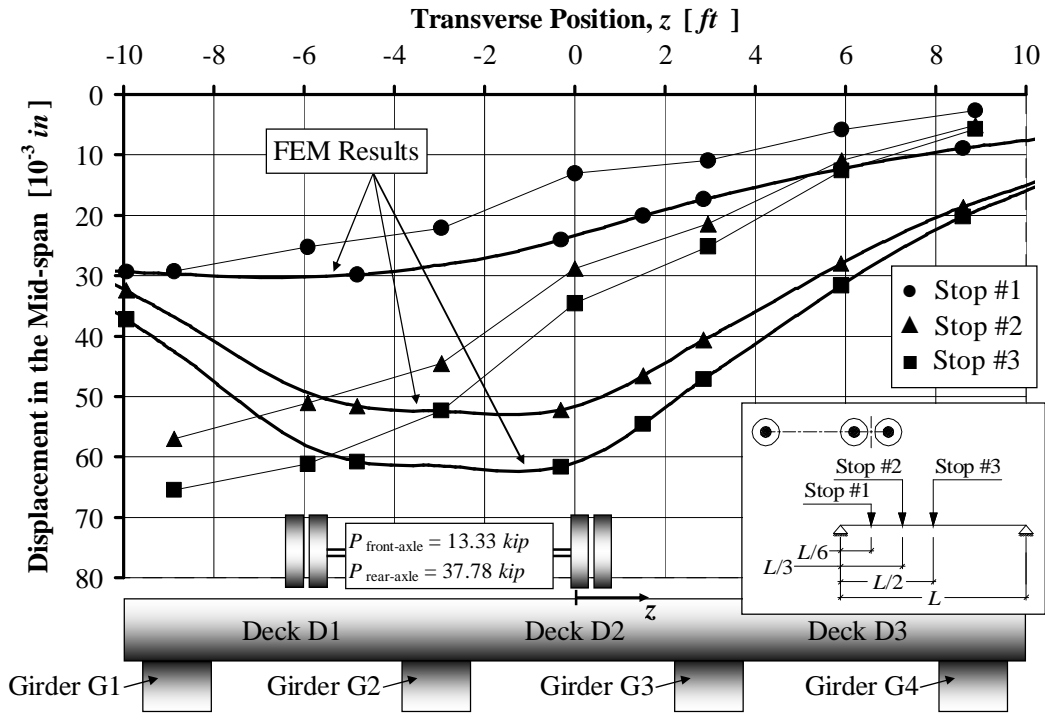
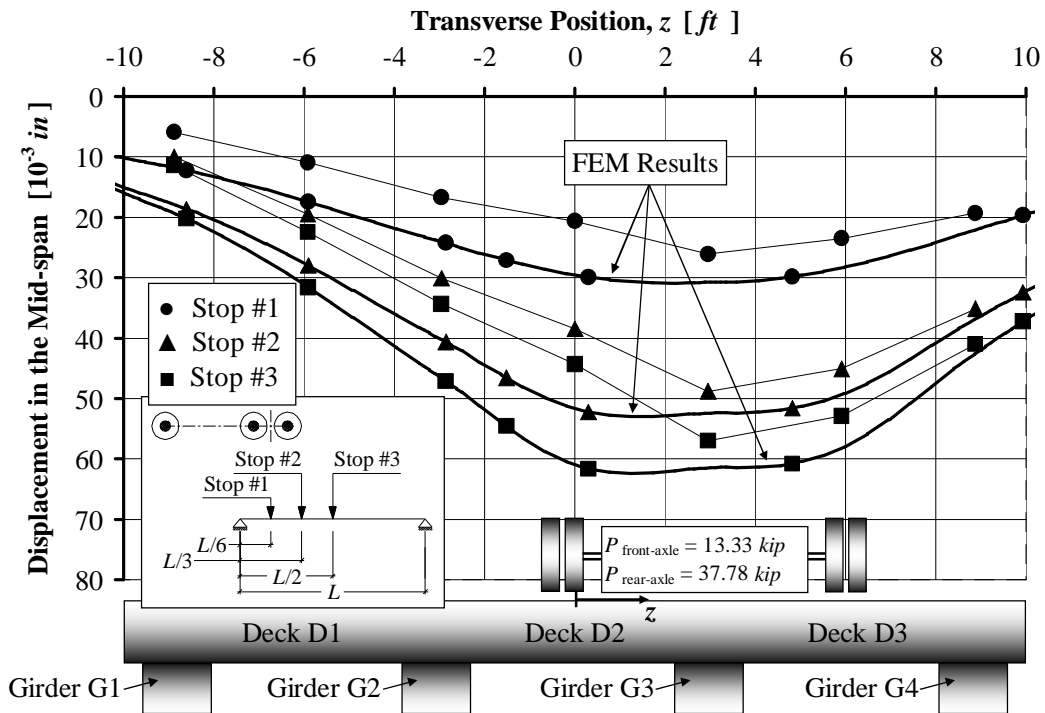
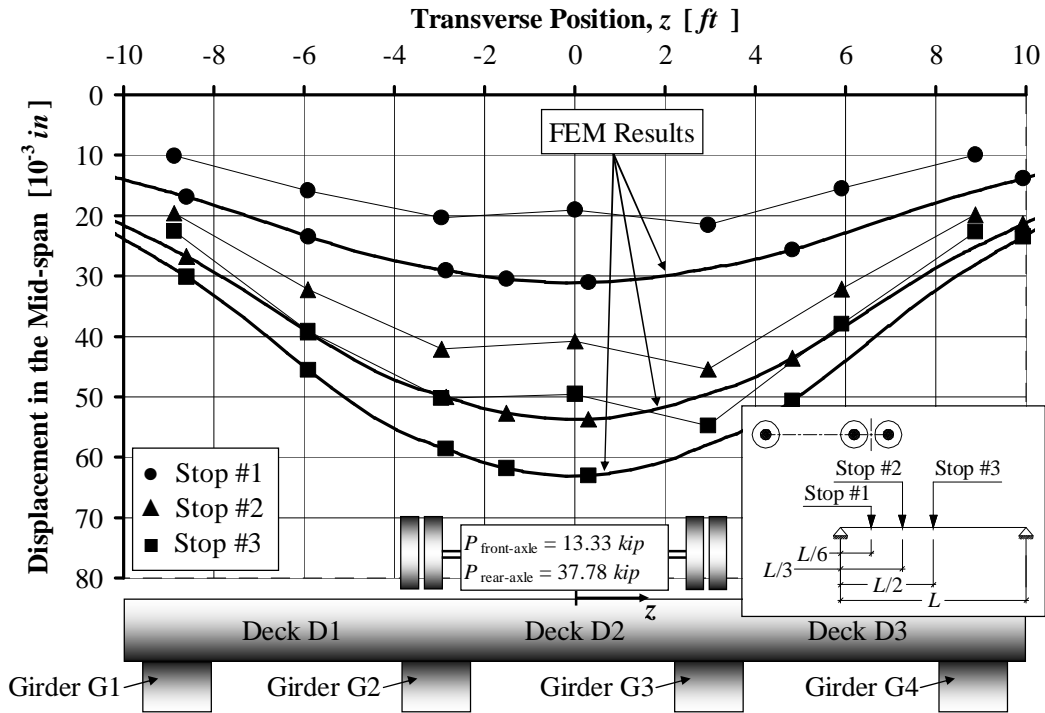


Figure B. 2. After Strengthening Mid-span Displacement, Pass #2



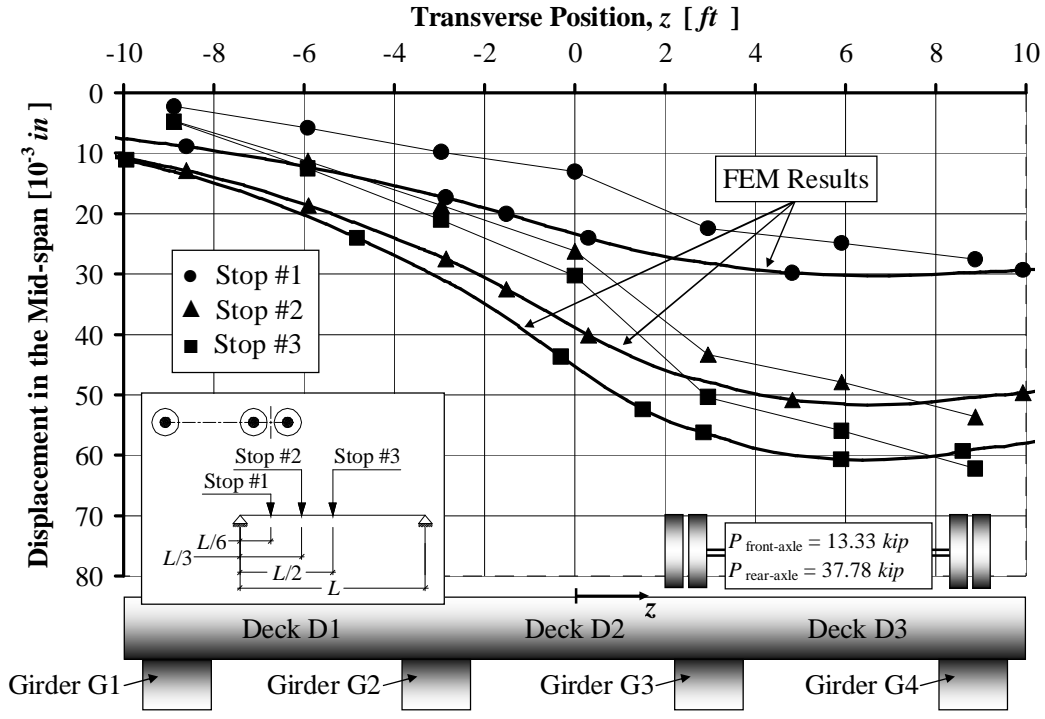


Figure B. 5. After Strengthening Mid-span Displacement, Pass #5

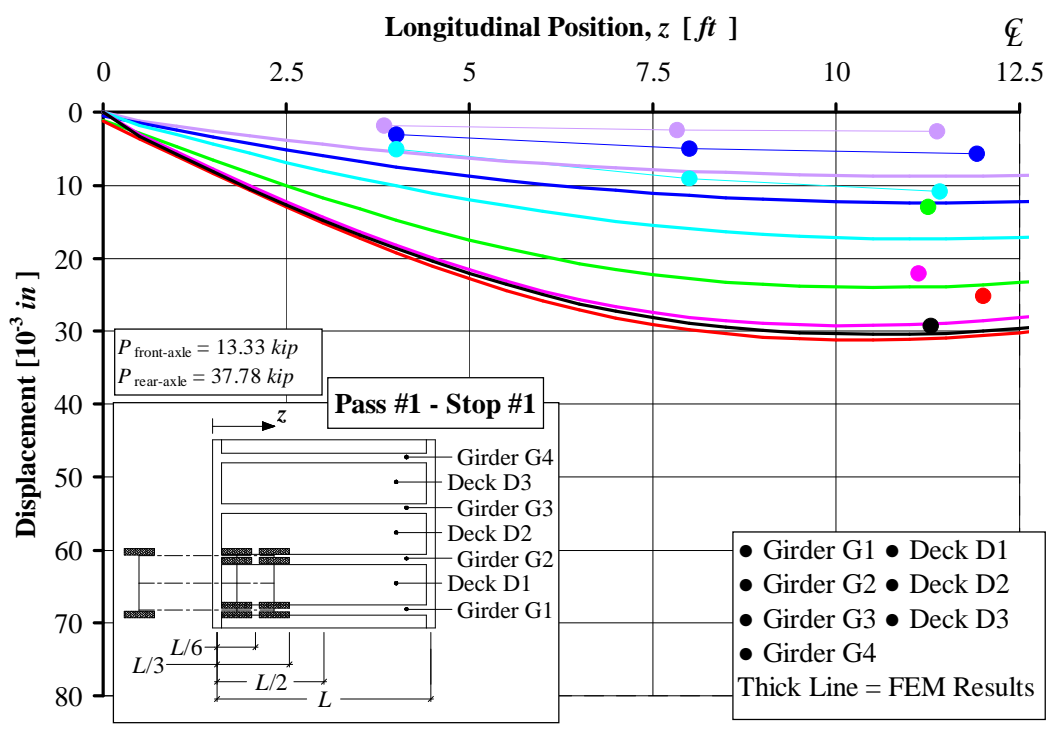


Figure B. 6. After Strengthening Displacement Distribution, Pass #1 Stop #1

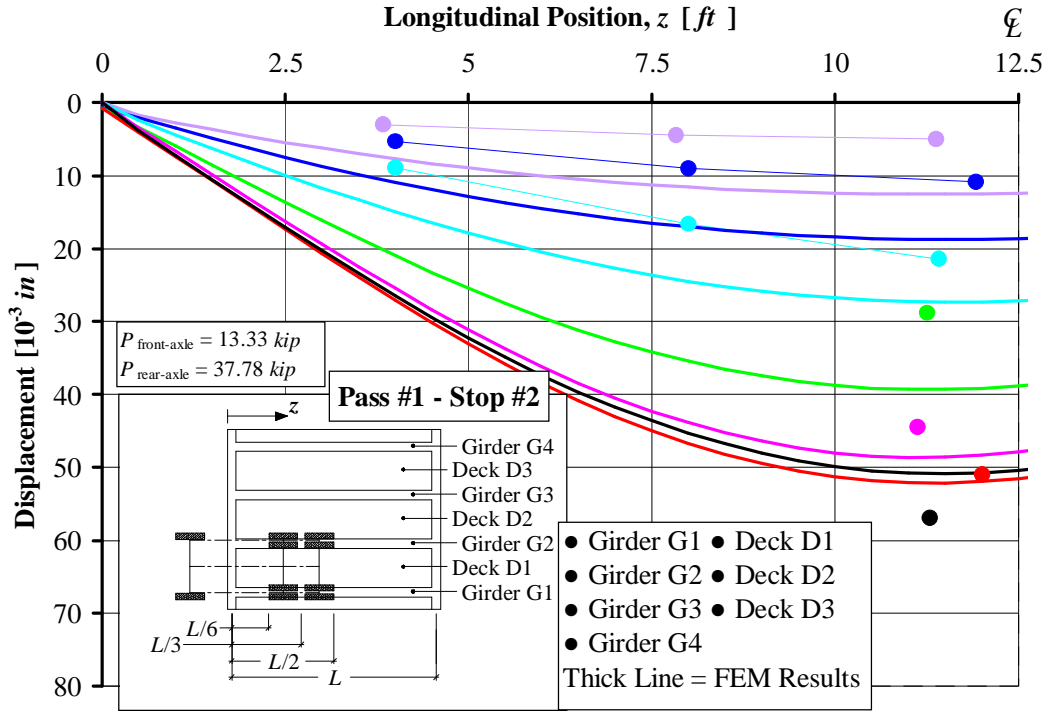


Figure B. 7. After Strengthening Displacement Distribution, Pass #1 Stop #2

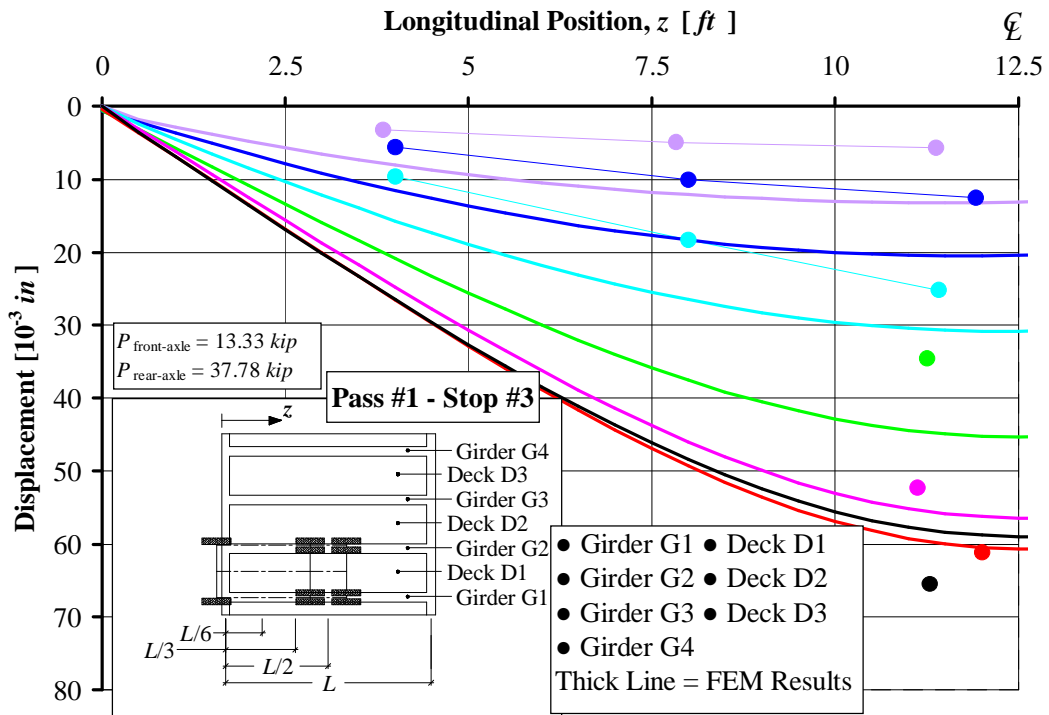


Figure B. 8. After Strengthening Displacement Distribution, Pass #1 Stop #3

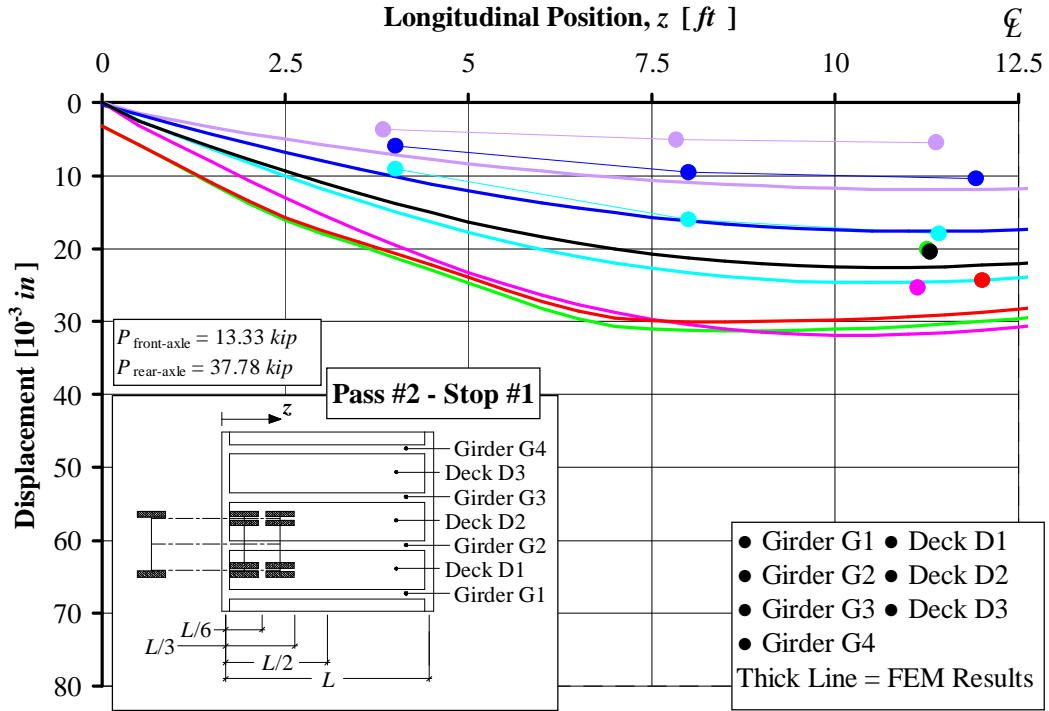


Figure B. 9. After Strengthening Displacement Distribution, Pass #2 Stop #1

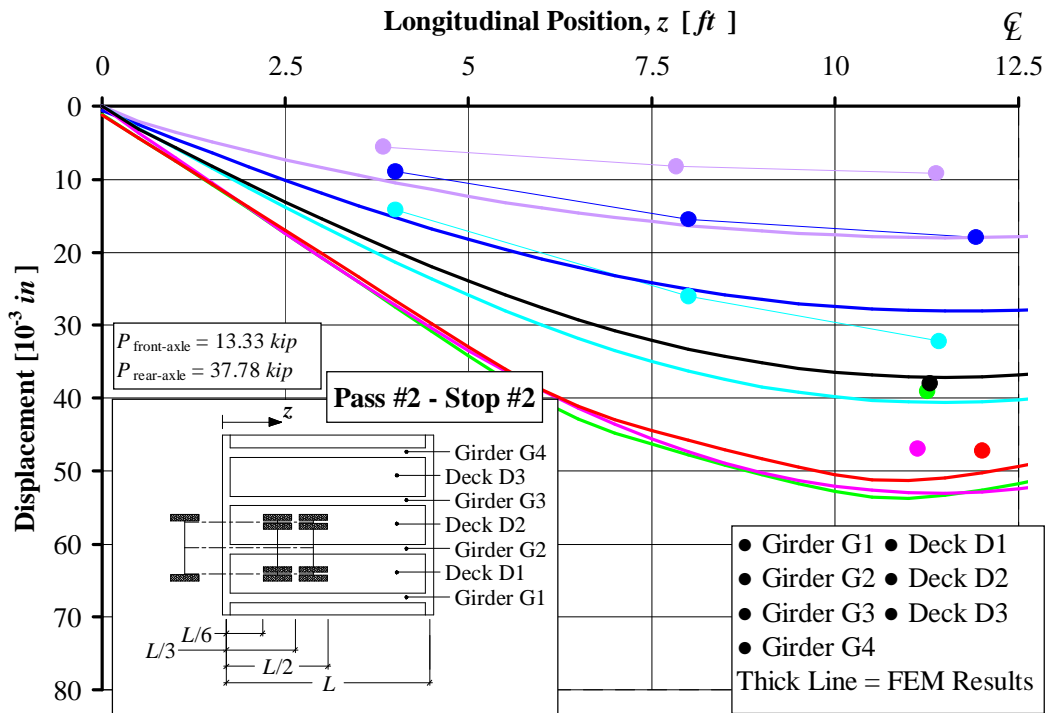


Figure B. 10. After Strengthening Displacement Distribution, Pass #2 Stop #2

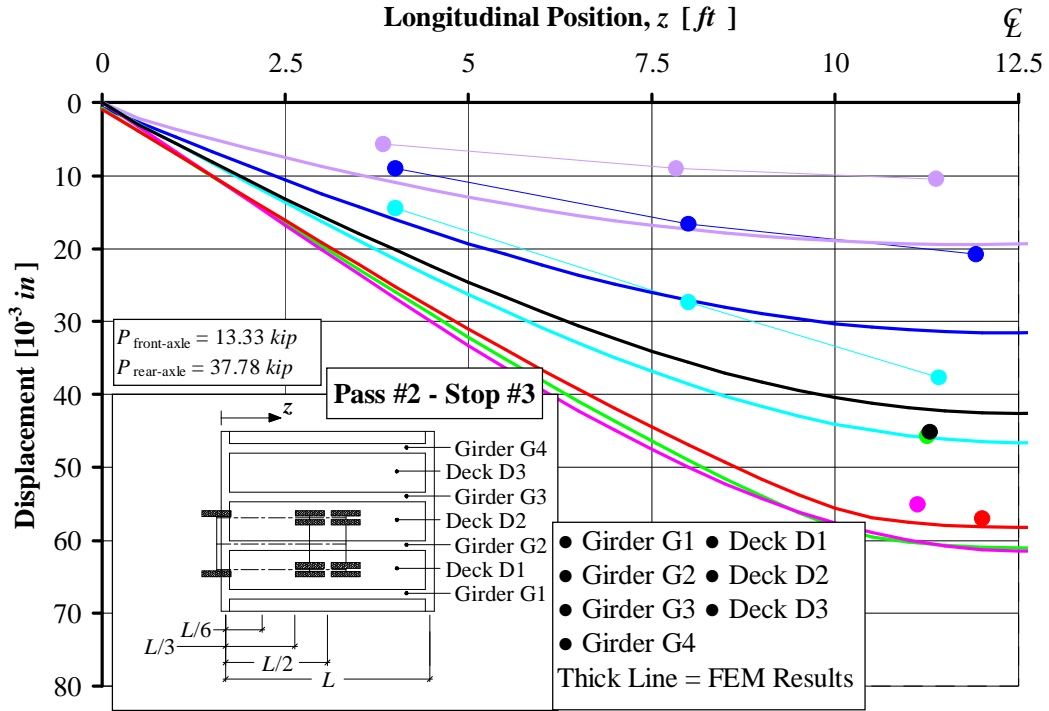


Figure B. 11. After Strengthening Displacement Distribution, Pass #2 Stop #3

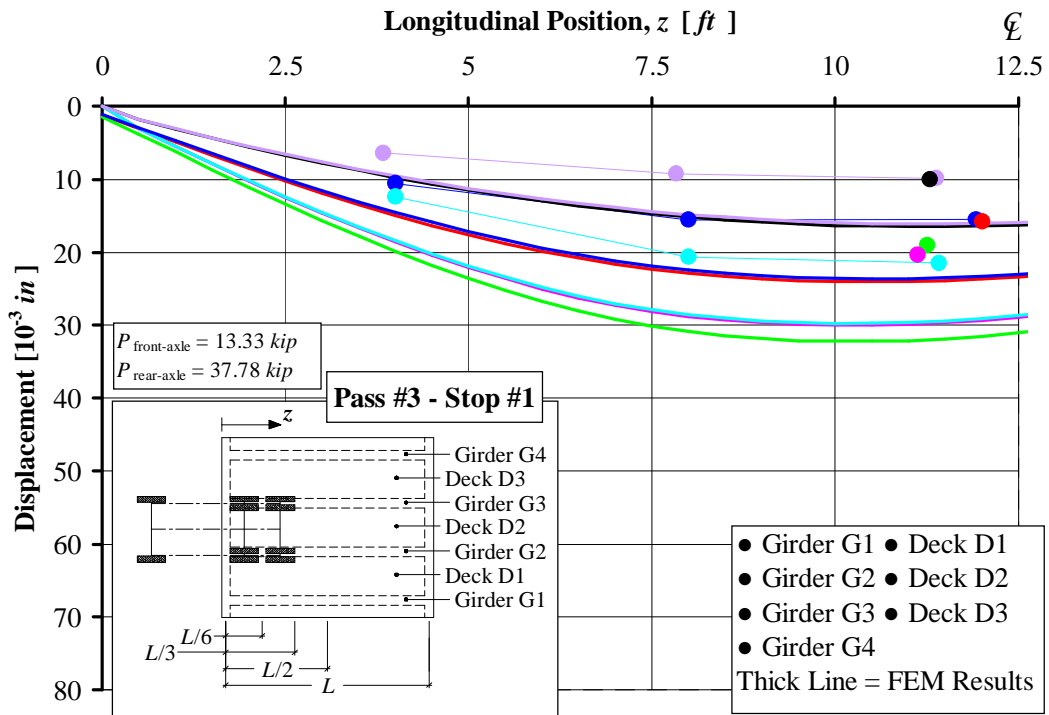


Figure B. 12. After Strengthening Displacement Distribution, Pass #3 Stop #1

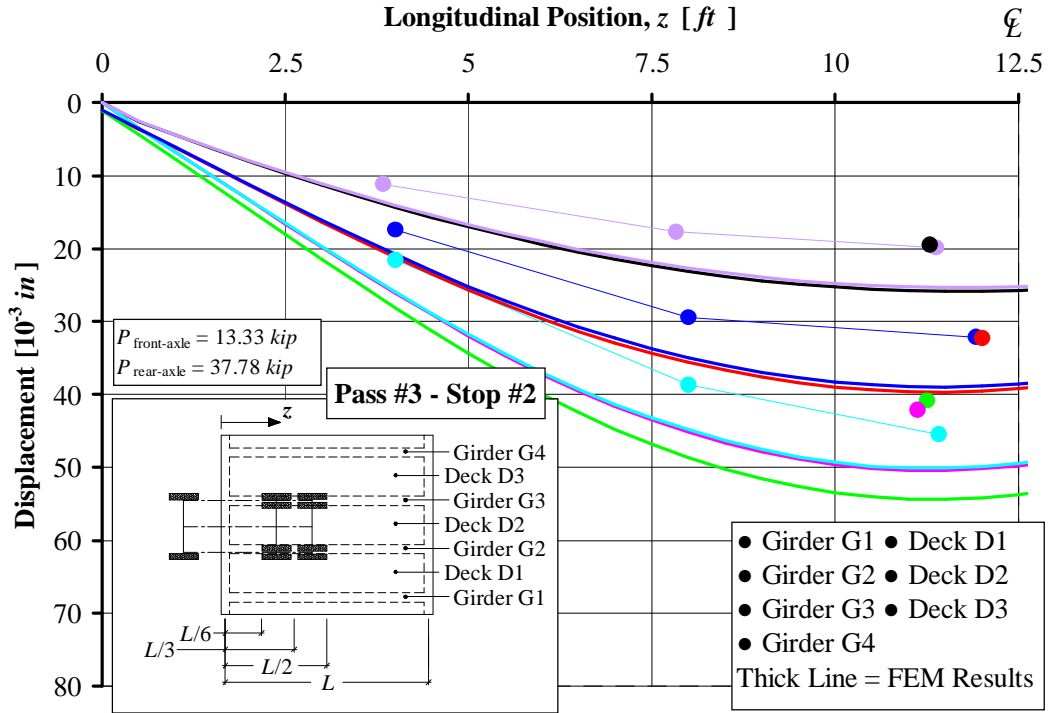


Figure B. 13. After Strengthening Displacement Distribution, Pass #3 Stop #2

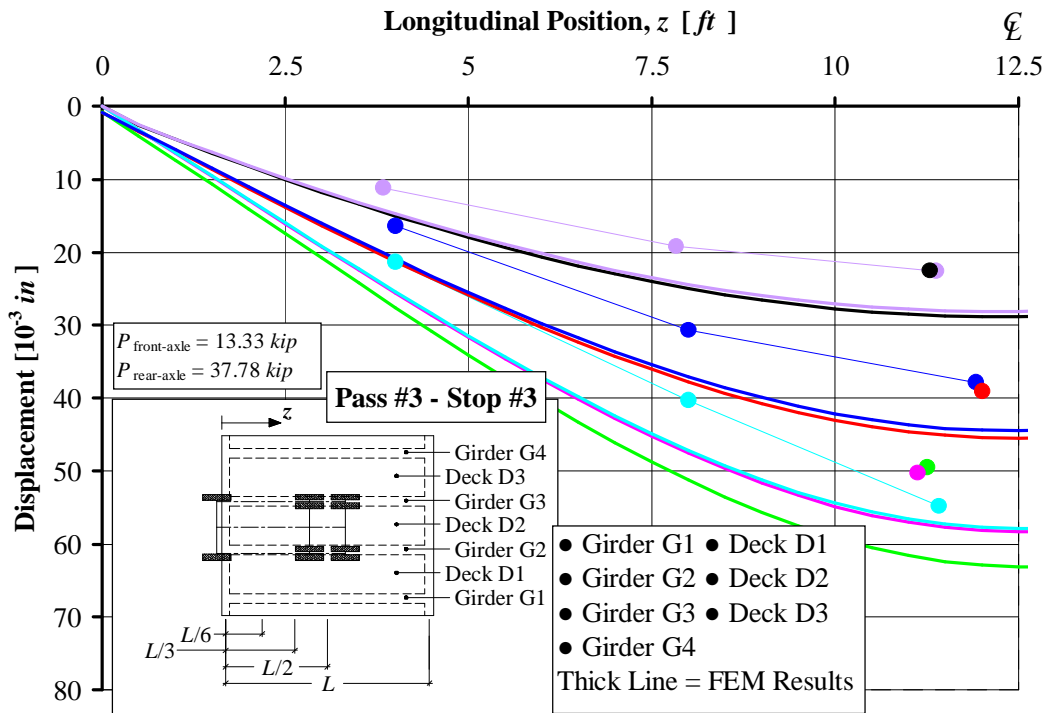


Figure B. 14. After Strengthening Displacement Distribution, Pass #3 Stop #3

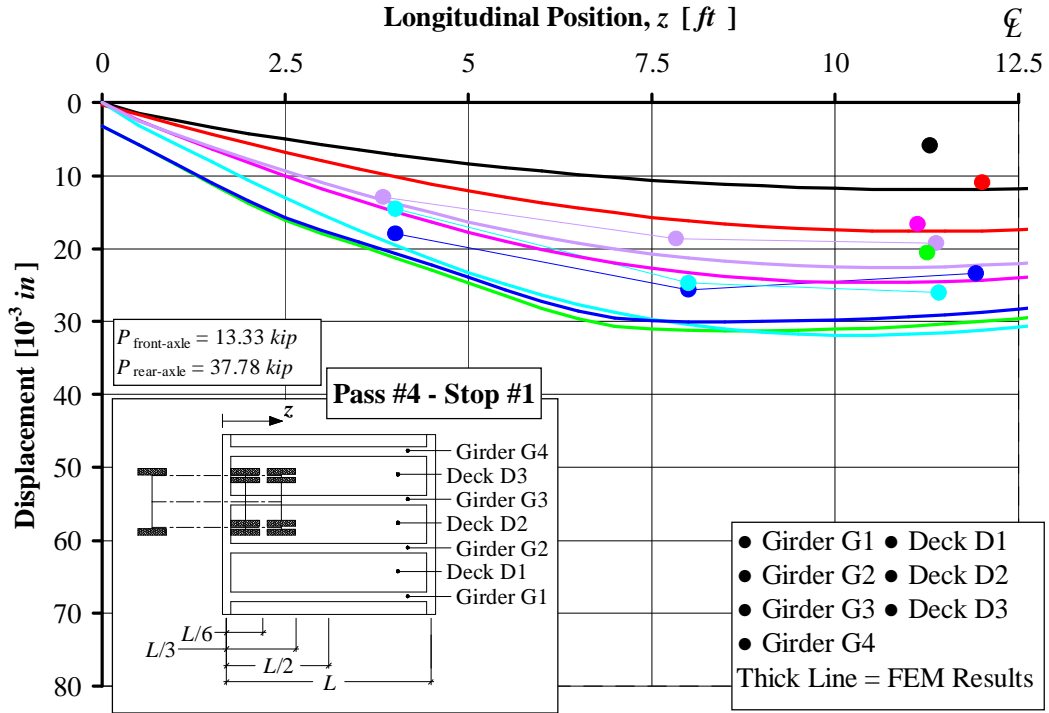


Figure B. 15. After Strengthening Displacement Distribution, Pass #4 Stop #1

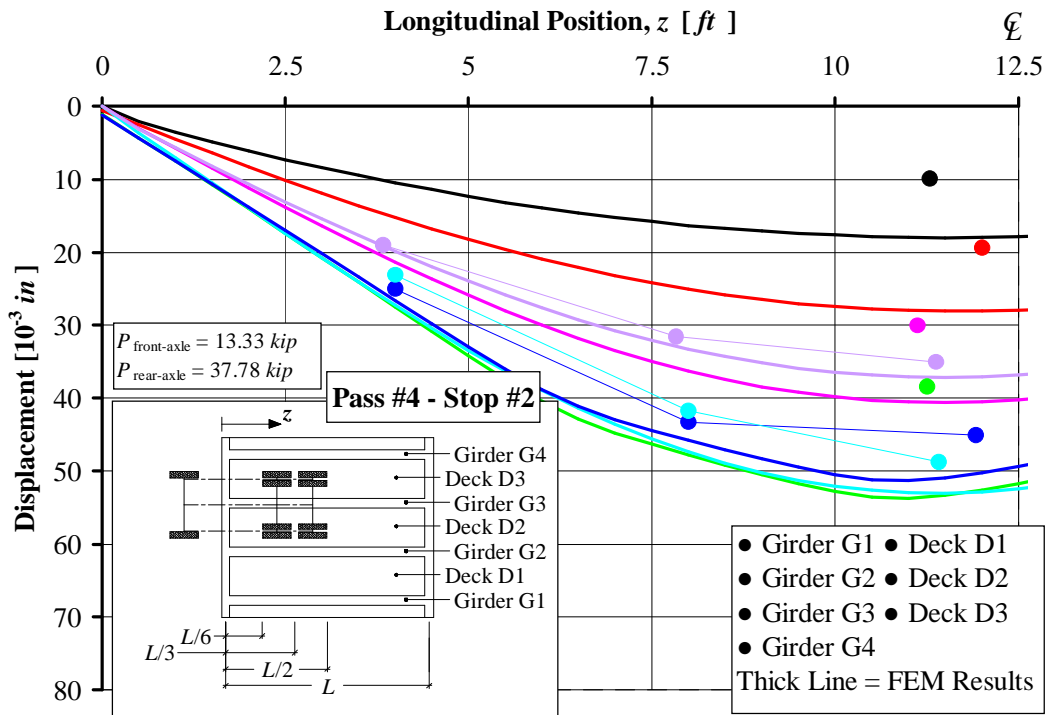


Figure B. 16. After Strengthening Displacement Distribution, Pass #4 Stop #2

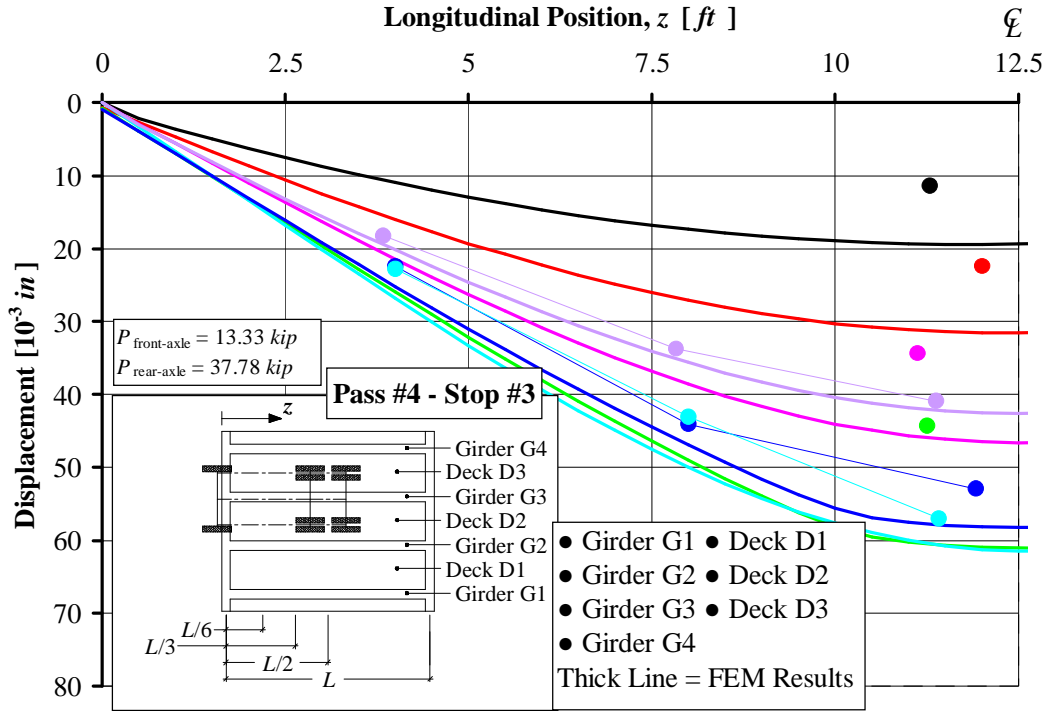


Figure B. 17. After Strengthening Displacement Distribution, Pass #4 Stop #3

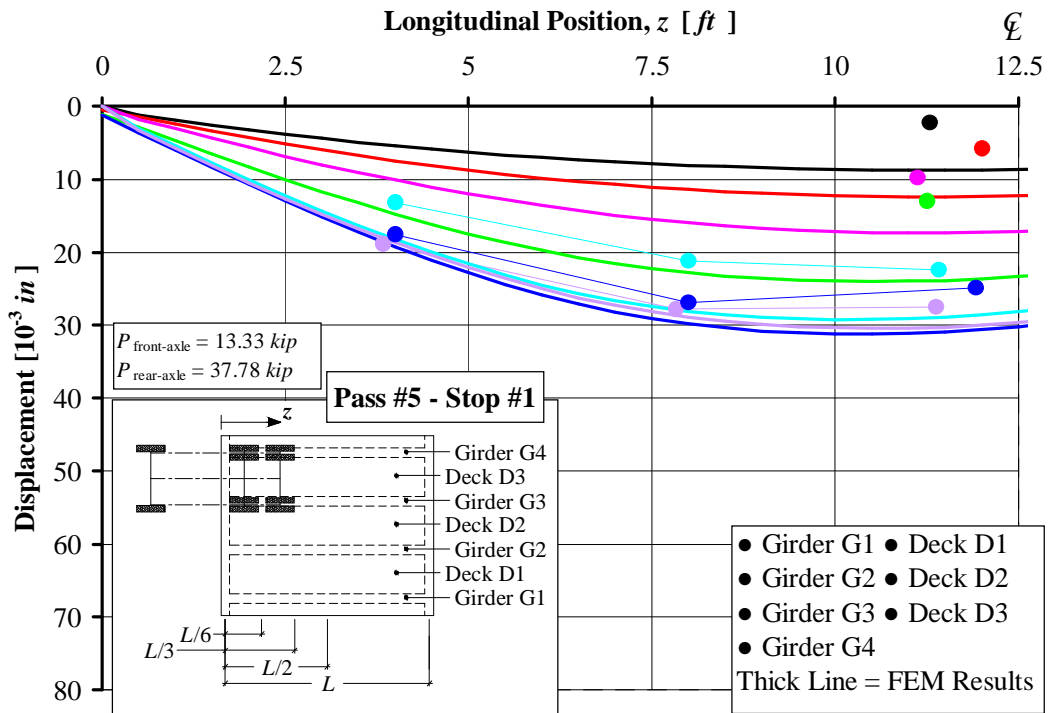


Figure B. 18. After Strengthening Displacement Distribution, Pass #5 Stop #1

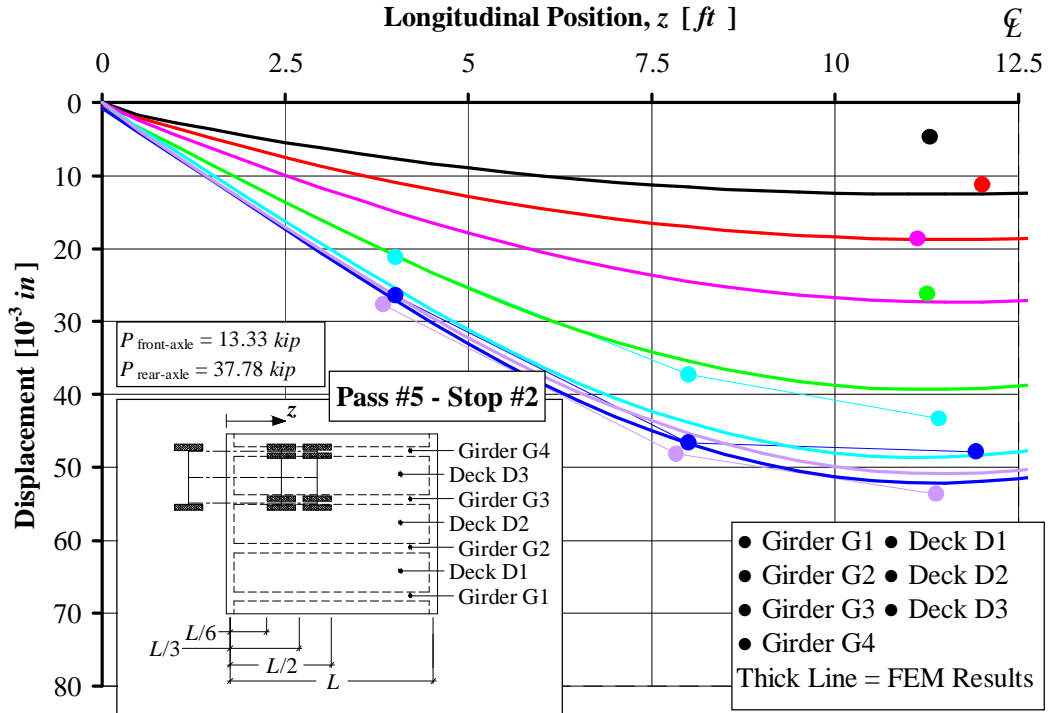


Figure B. 19. After Strengthening Displacement Distribution, Pass #5 Stop #2

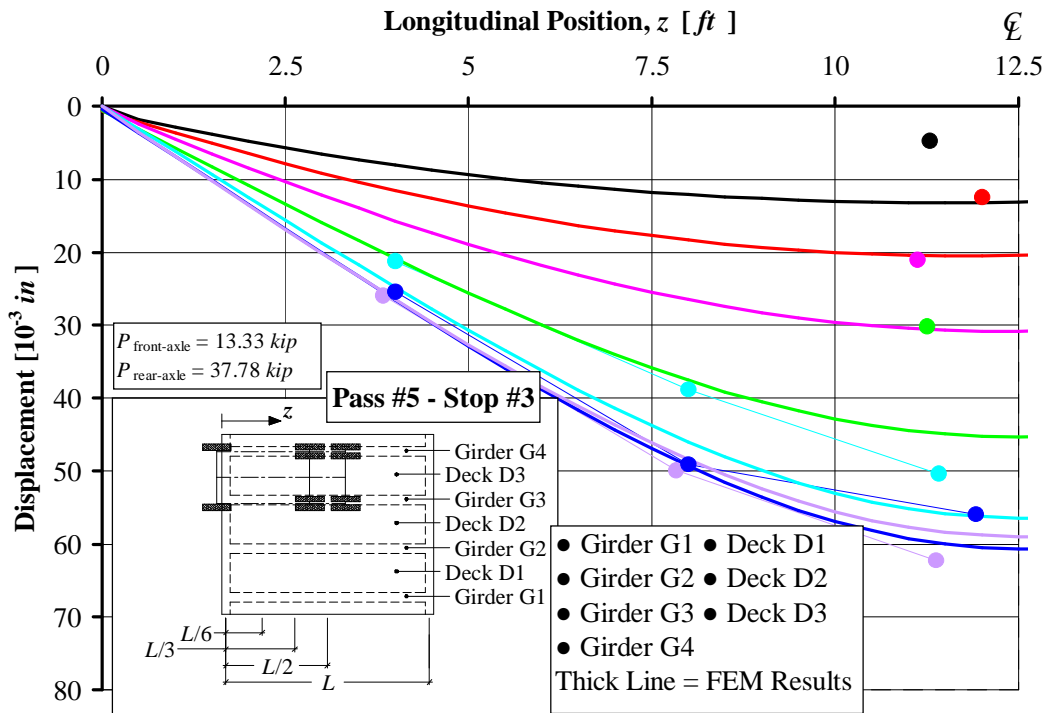


Figure B. 20. After Strengthening Displacement Distribution, Pass #5 Stop #3

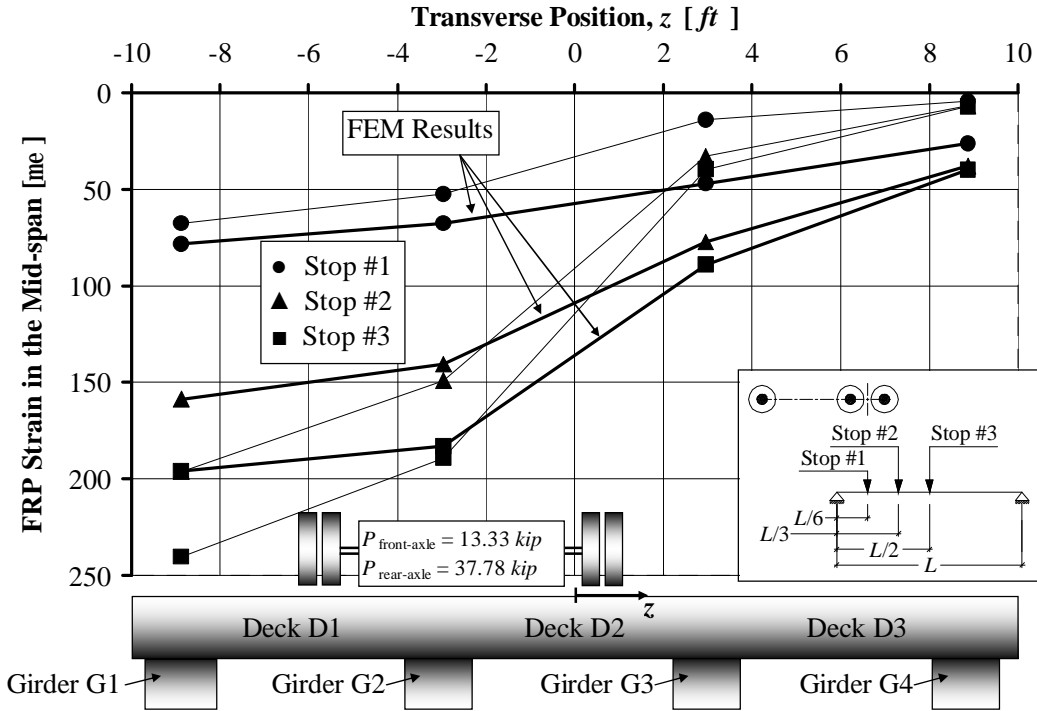


Figure B. 21. Strain in the FRP Strengthening on the Girders at Mid-span, Pass #1

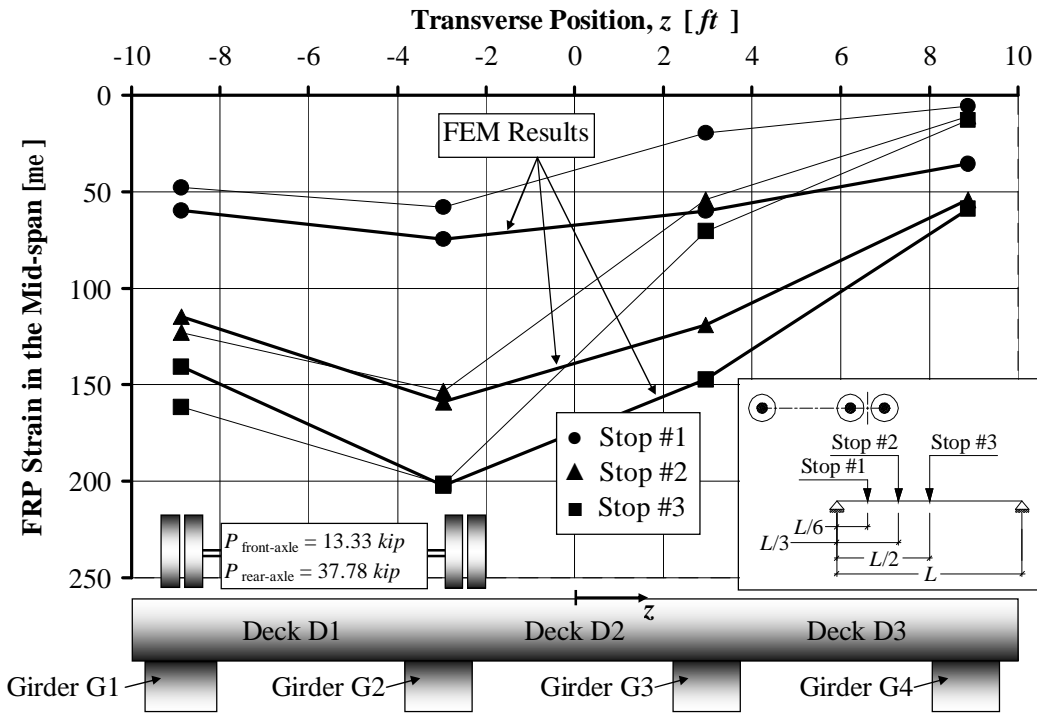


Figure B. 22. Strain in the FRP Strengthening on the Girders at Mid-span, Pass #2

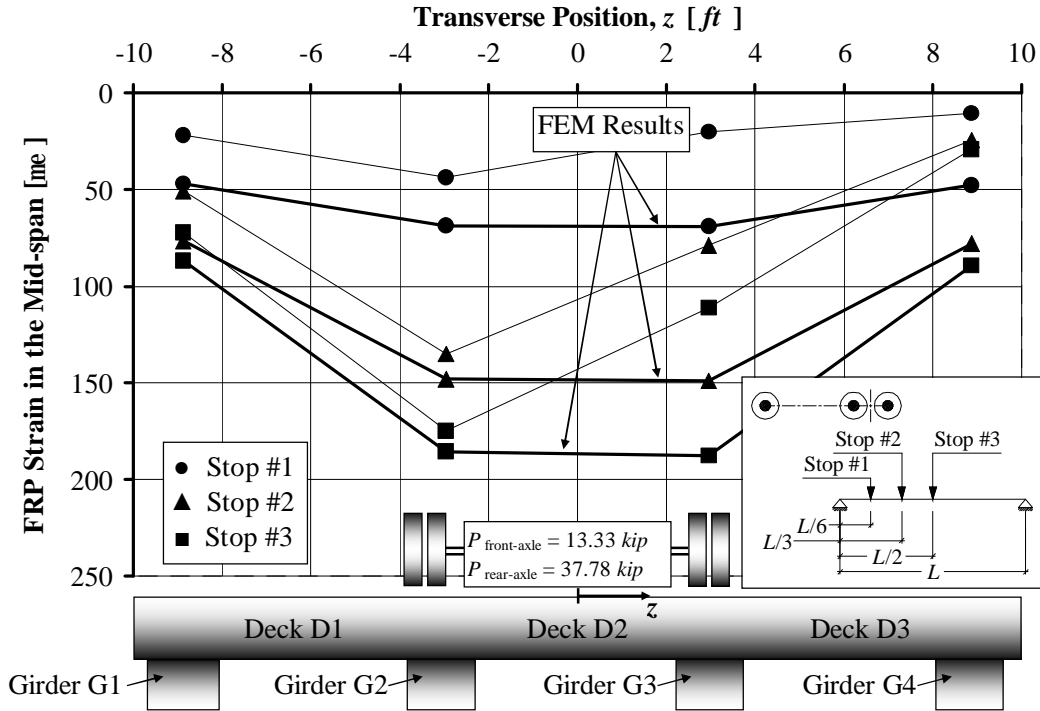


Figure B. 23. Strain in the FRP Strengthening on the Girders at Mid-span, Pass #3

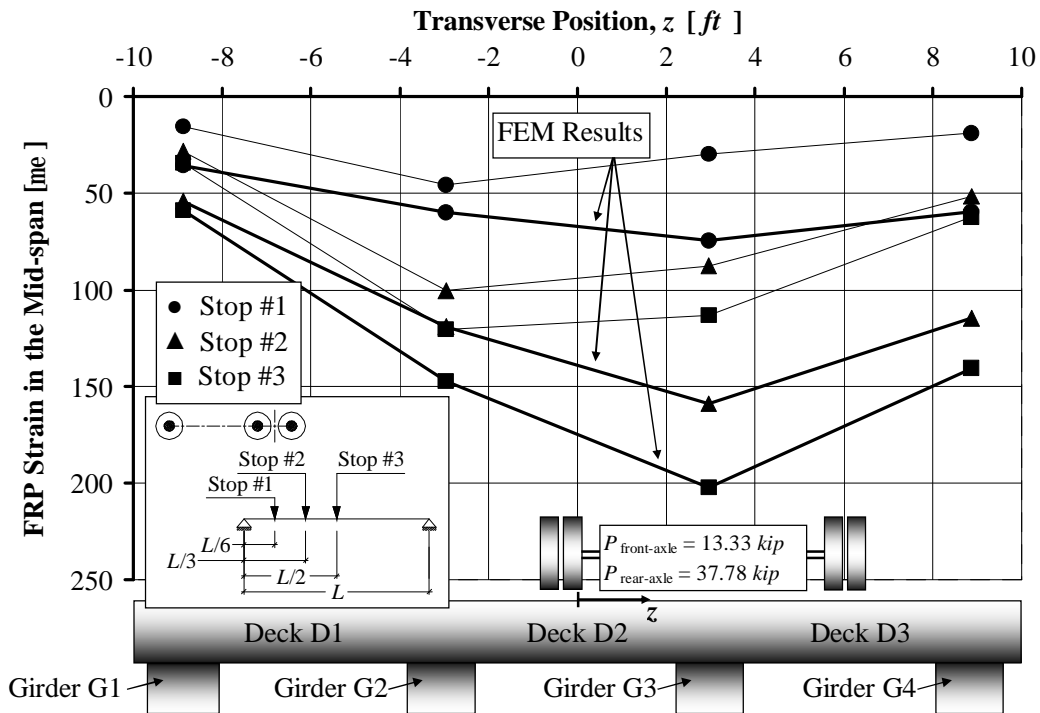


Figure B. 24. Strain in the FRP Strengthening on the Girders at Mid-span, Pass #4

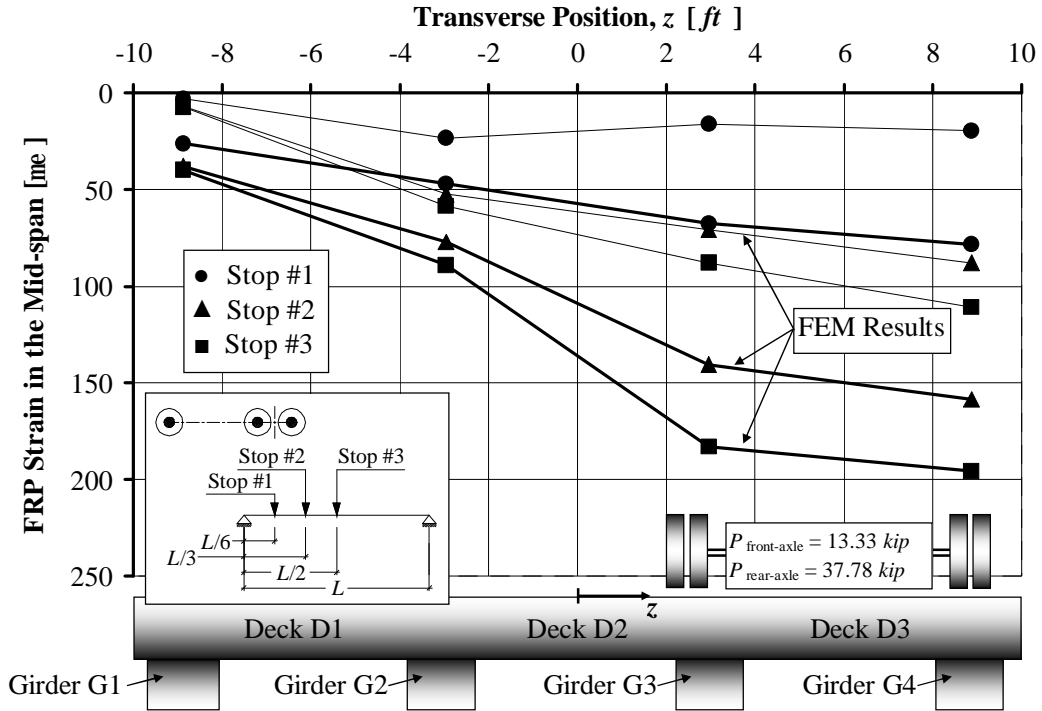


Figure B. 25. Strain in the FRP Strengthening on the Girders at Mid-span, Pass #5

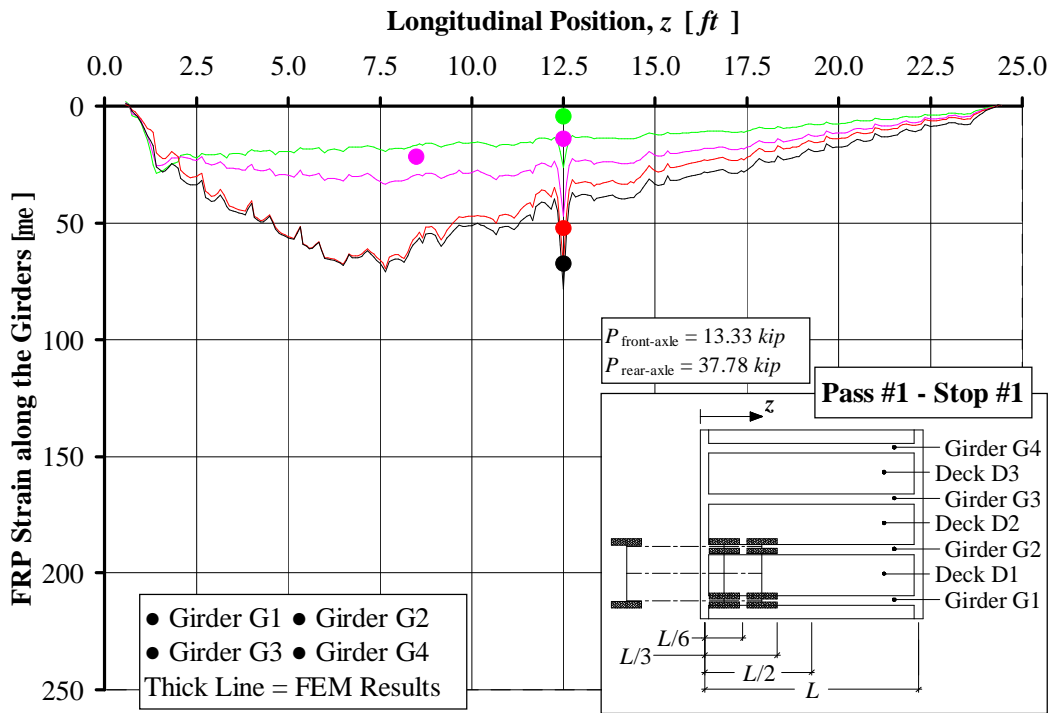


Figure B. 26. Strain Distribution in the FRP along the Girders, Pass #1 Stop #1

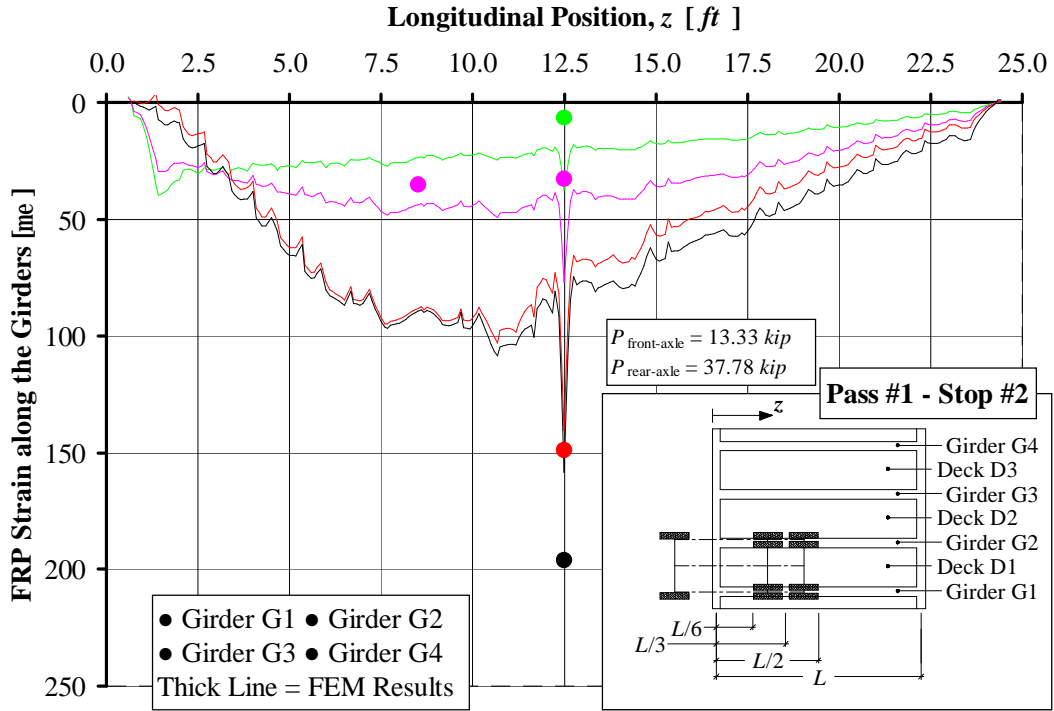


Figure B. 27. Strain Distribution in the FRP along the Girders, Pass #1 Stop #2

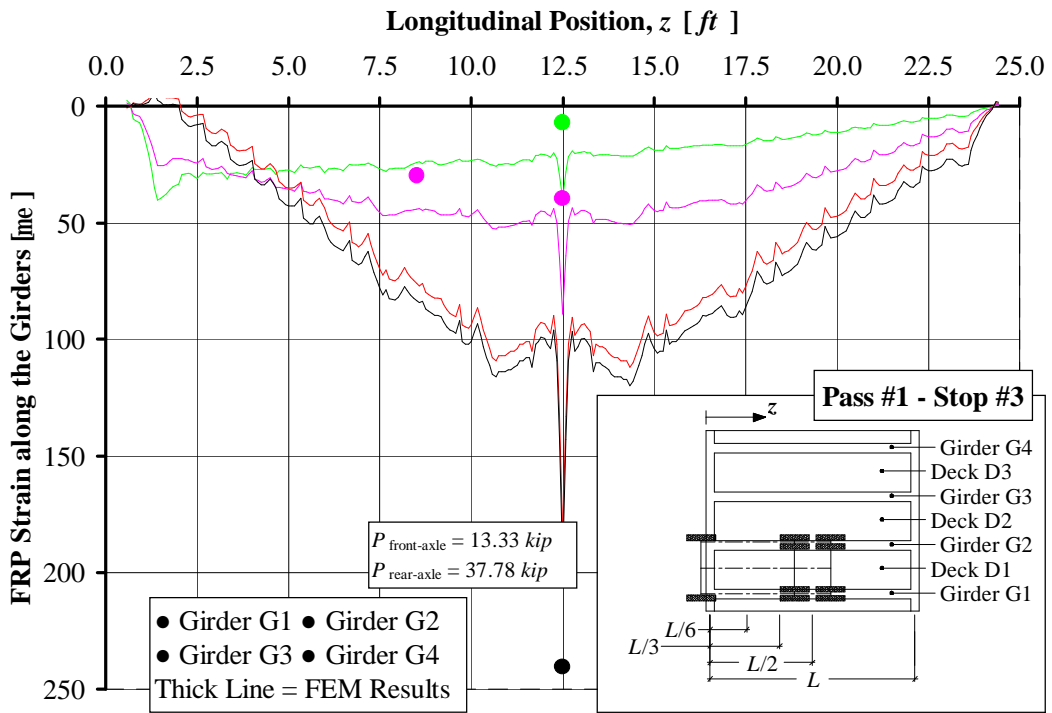


Figure B. 28. Strain Distribution in the FRP along the Girders, Pass #1 Stop #3

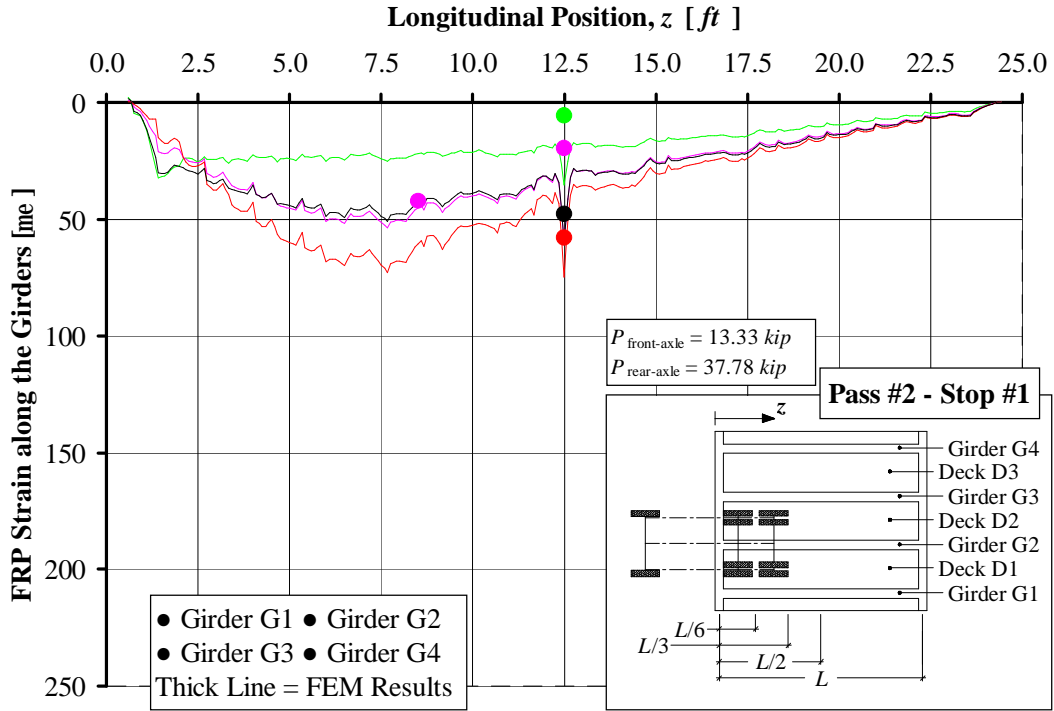


Figure B. 29. Strain Distribution in the FRP along the Girders, Pass #2 Stop #1

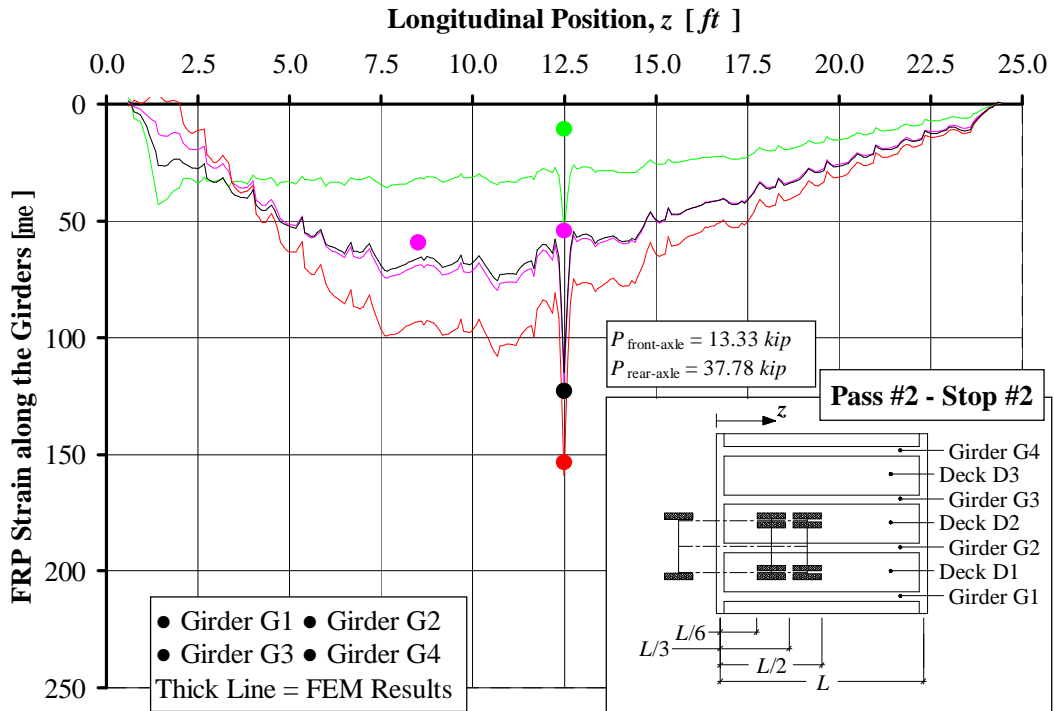


Figure B. 30. Strain Distribution in the FRP along the Girders, Pass #2 Stop #2

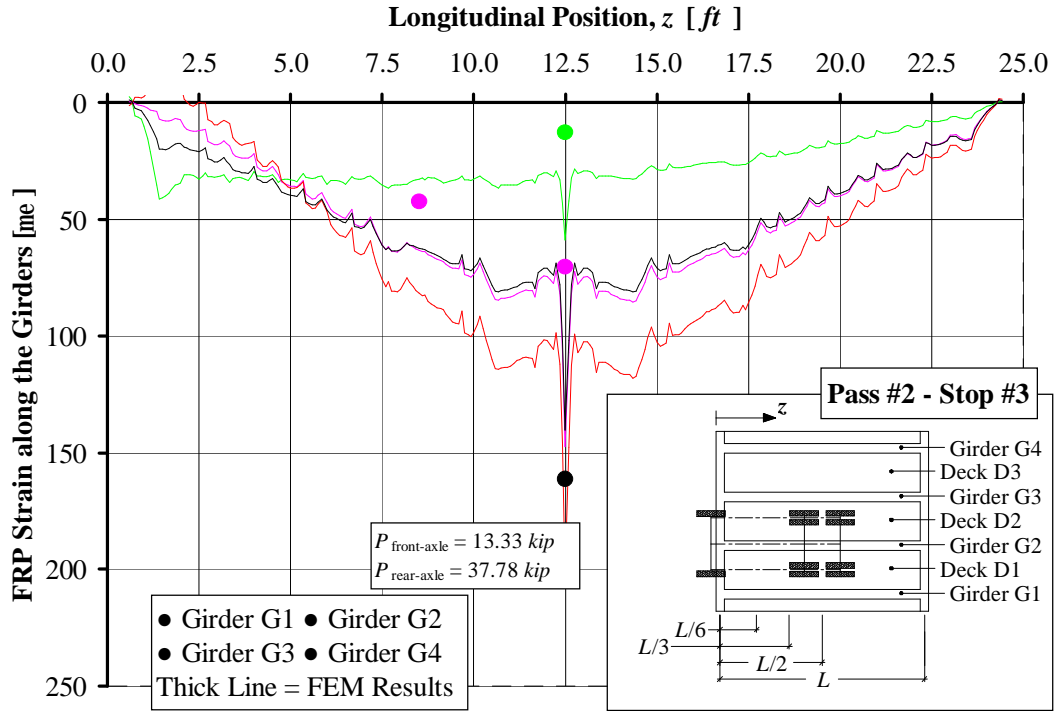


Figure B. 31. Strain Distribution in the FRP along the Girders, Pass #2 Stop #3

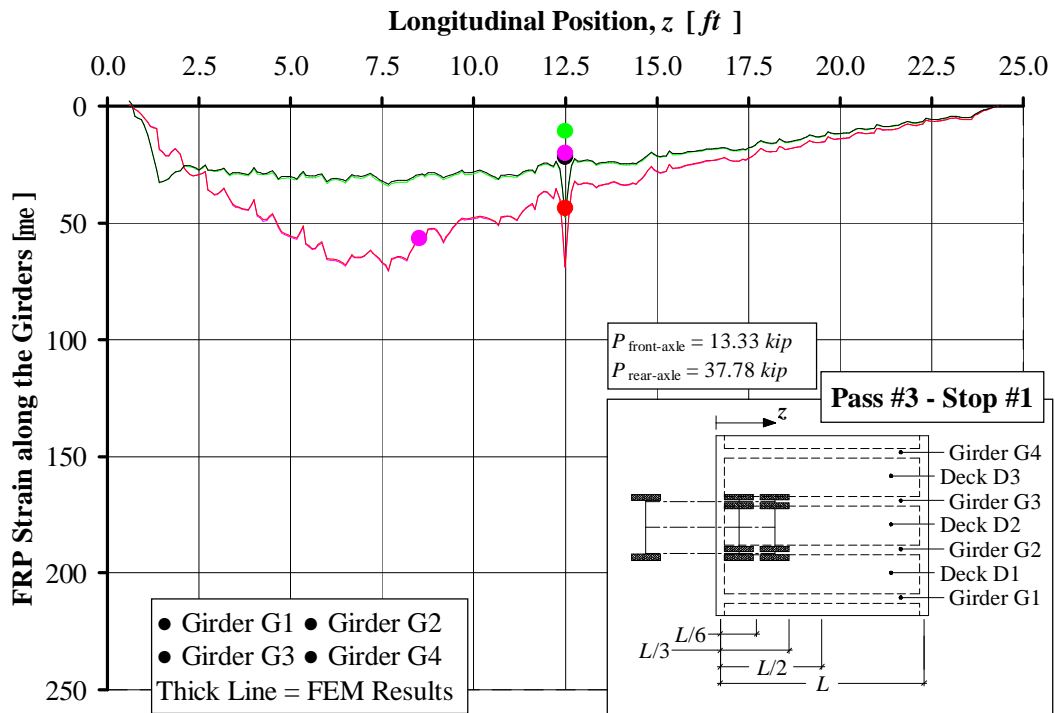


Figure B. 32. Strain Distribution in the FRP along the Girders, Pass #3 Stop #1

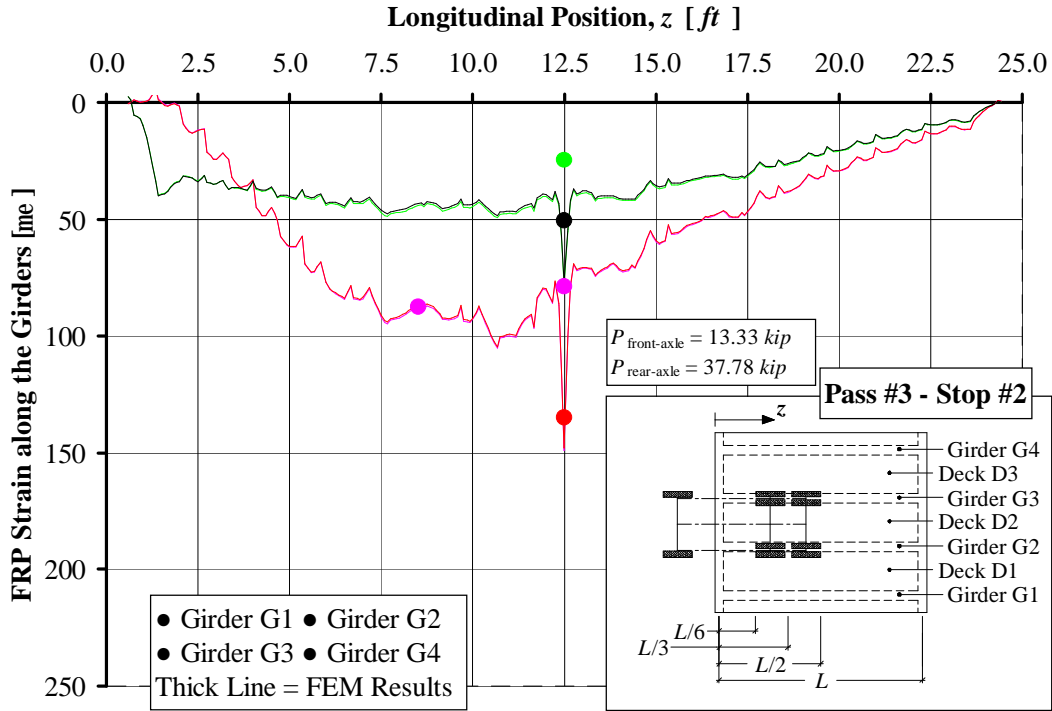


Figure B. 33. Strain Distribution in the FRP along the Girders, Pass #3 Stop #2

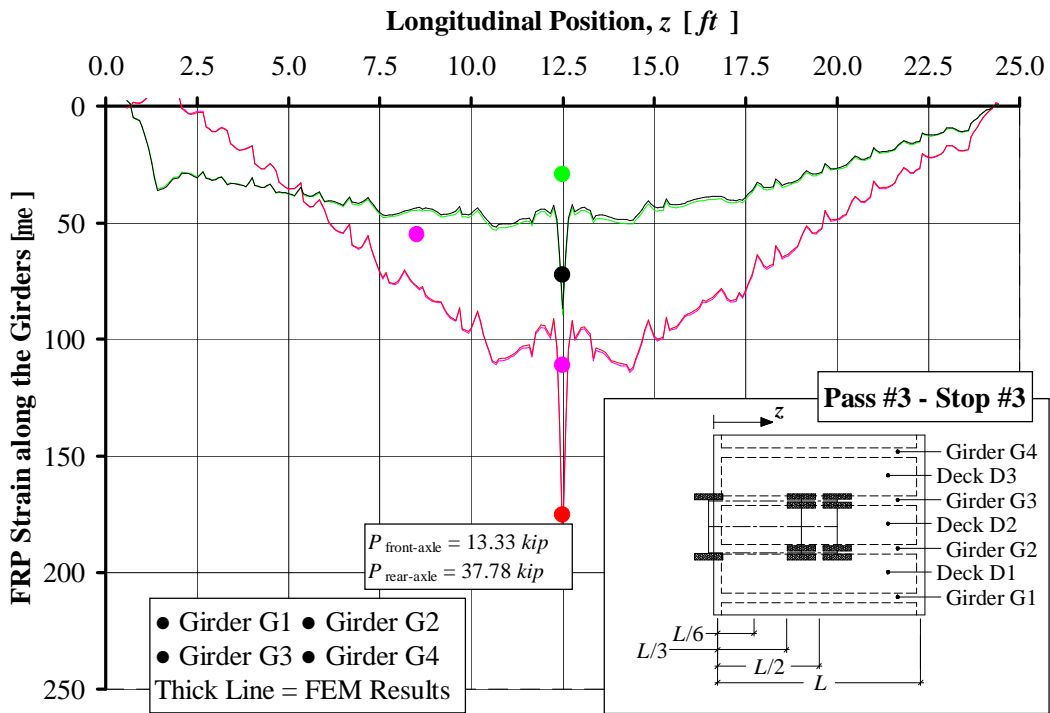


Figure B. 34. Strain Distribution in the FRP along the Girders, Pass #3 Stop #3

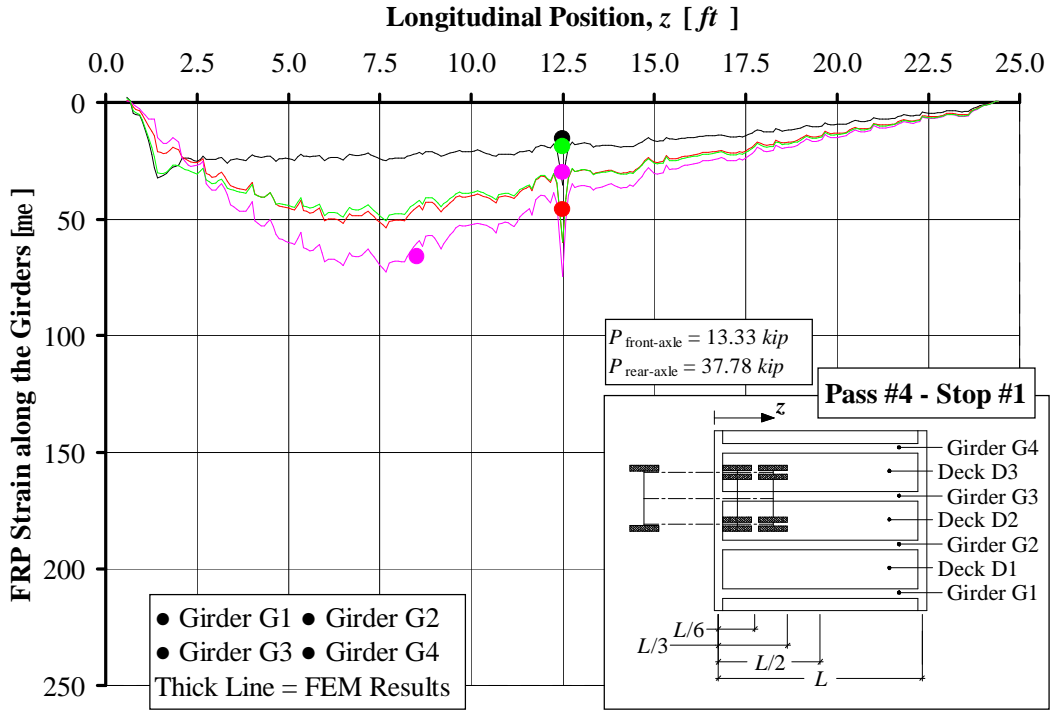


Figure B. 35. Strain Distribution in the FRP along the Girders, Pass #4 Stop #1

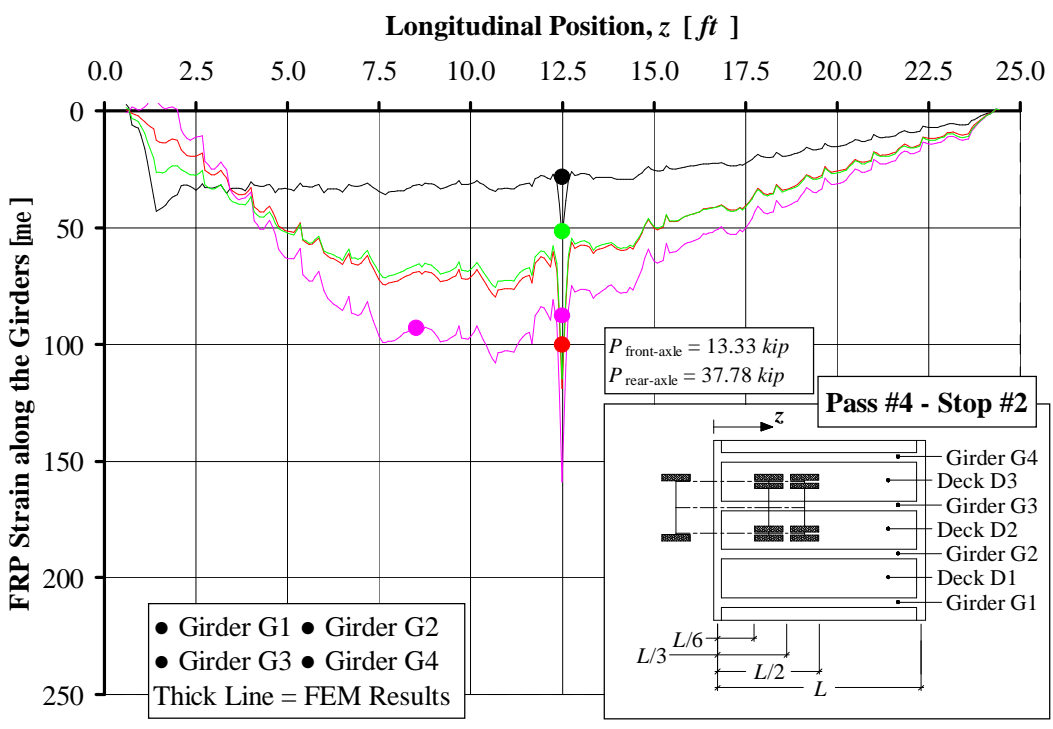


Figure B. 36. Strain Distribution in the FRP along the Girders, Pass #4 Stop #2

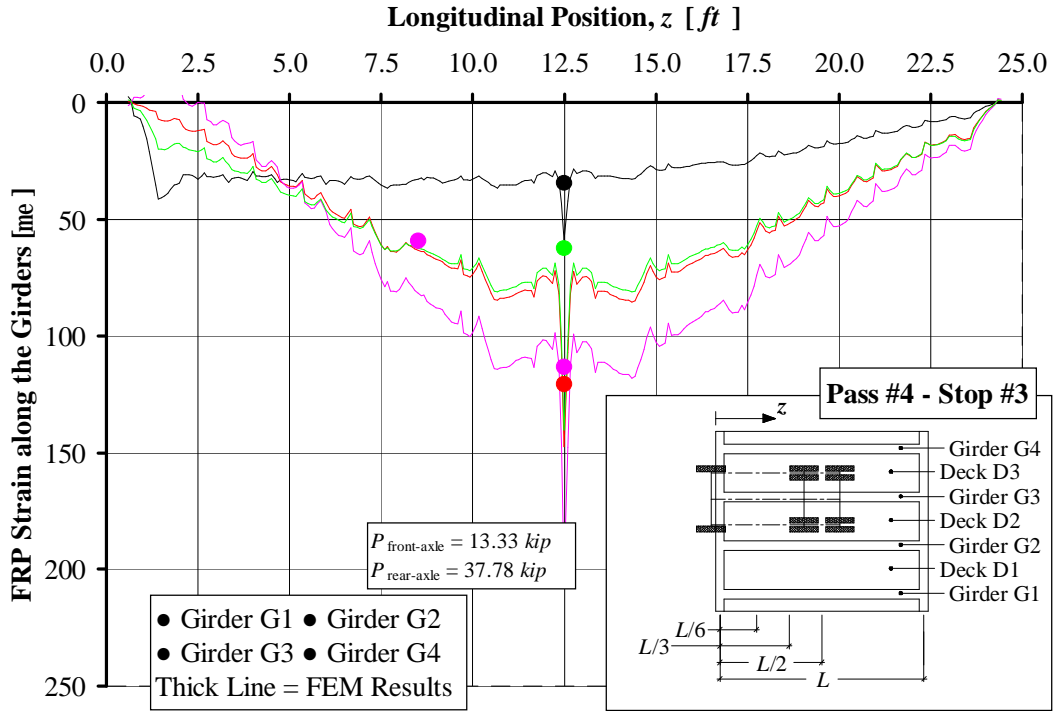


Figure B. 37. Strain Distribution in the FRP along the Girders, Pass #4 Stop #3

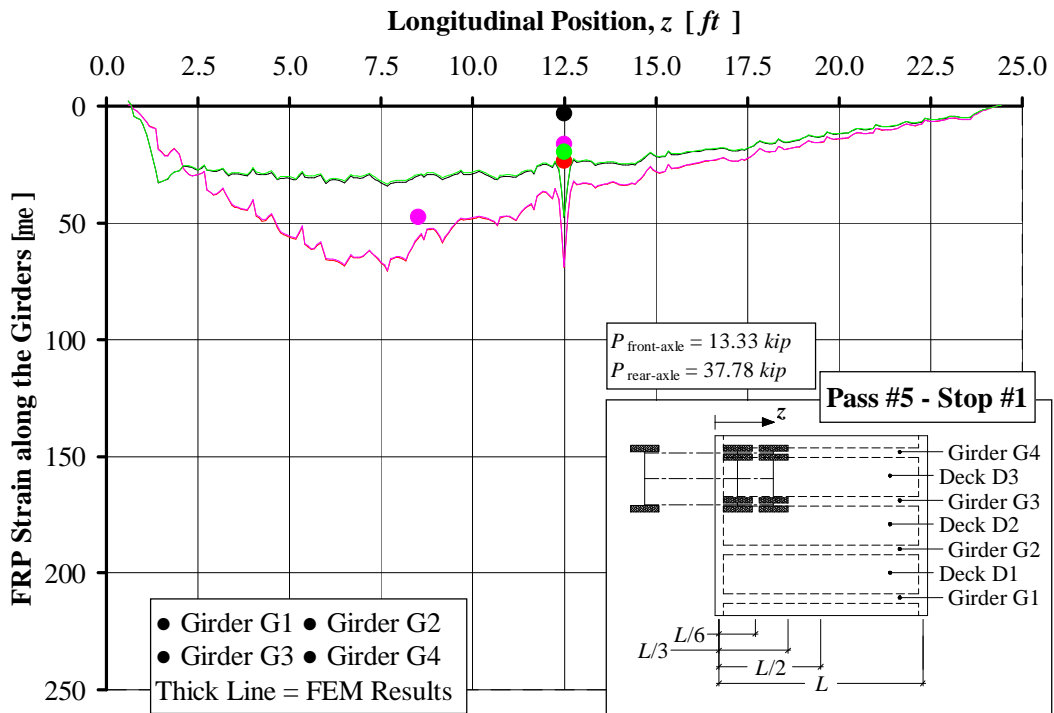


Figure B. 38. Strain Distribution in the FRP along the Girders, Pass #5 Stop #1

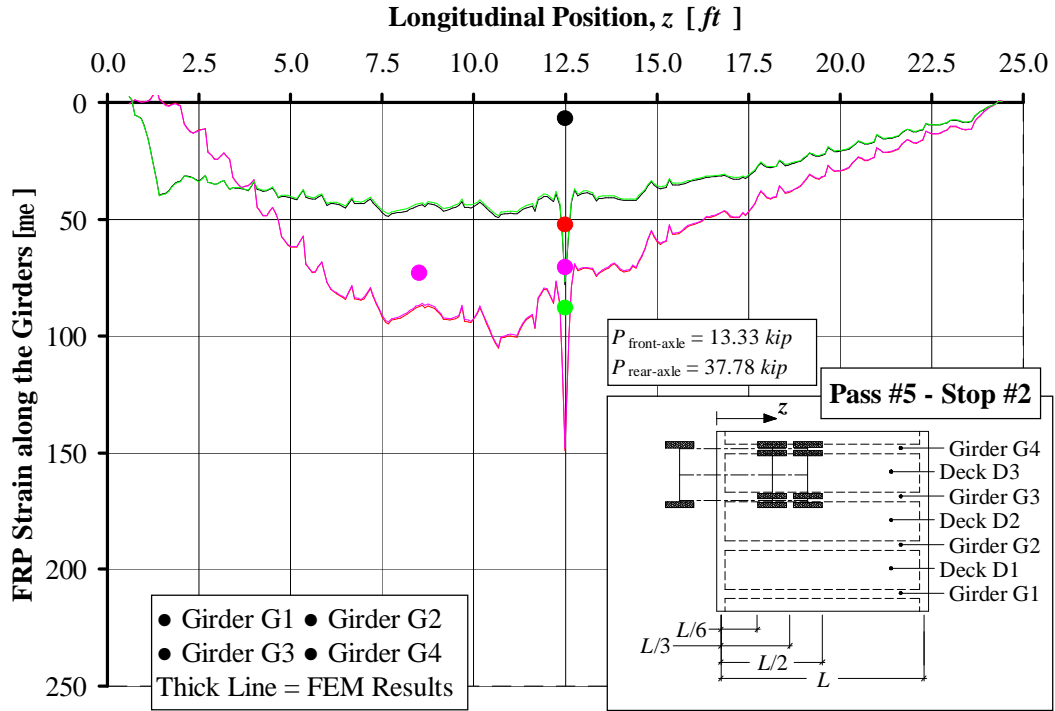


Figure B. 39. Strain Distribution in the FRP along the Girders, Pass #5 Stop #2

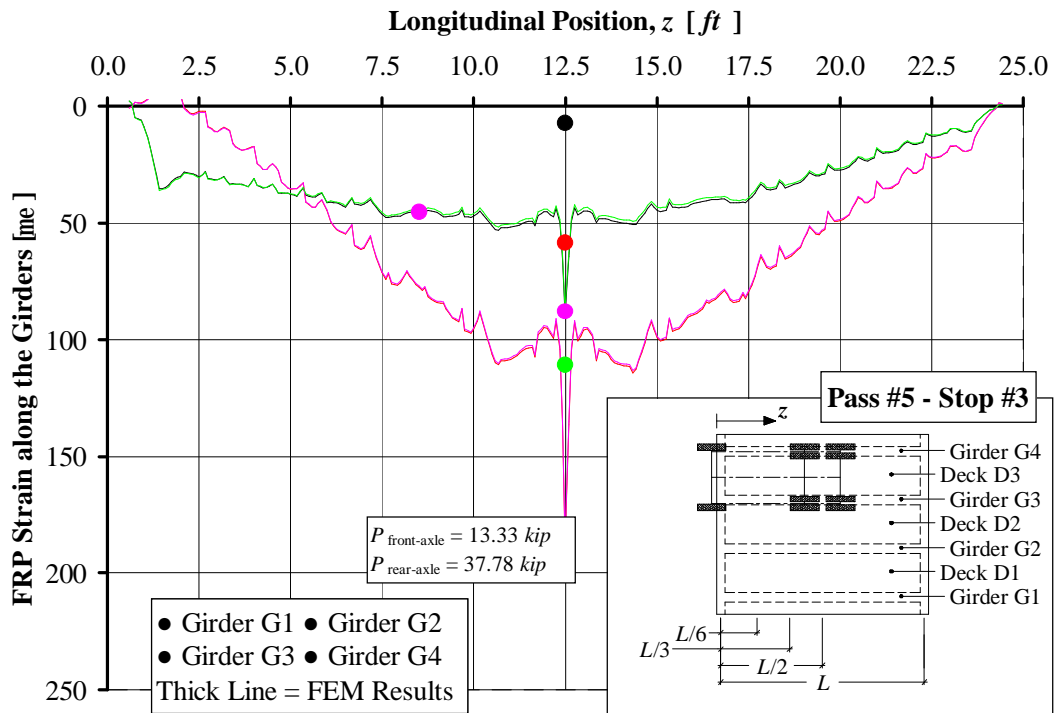


Figure B. 40. Strain Distribution in the FRP along the Girders, Pass #5 Stop #3

## **APPENDIX**

### **C. Comparison between prior to and after Strengthening Normalized Results**

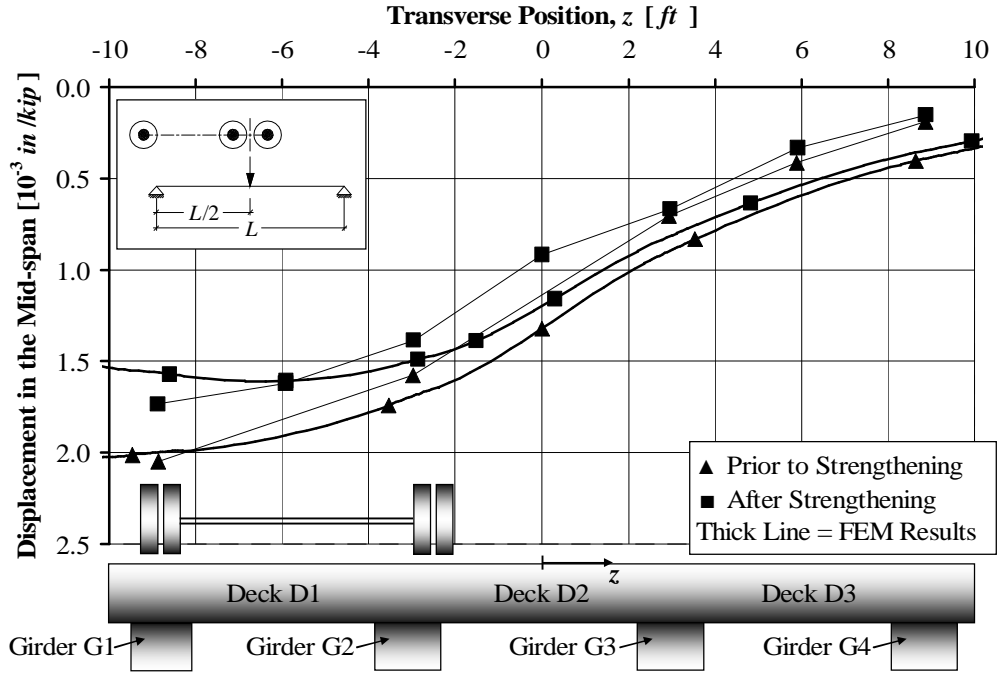


Figure C. 1. Mid-span Displacement prior to and after the Strengthening, Pass #1 and Rear Axle in the Mid-span

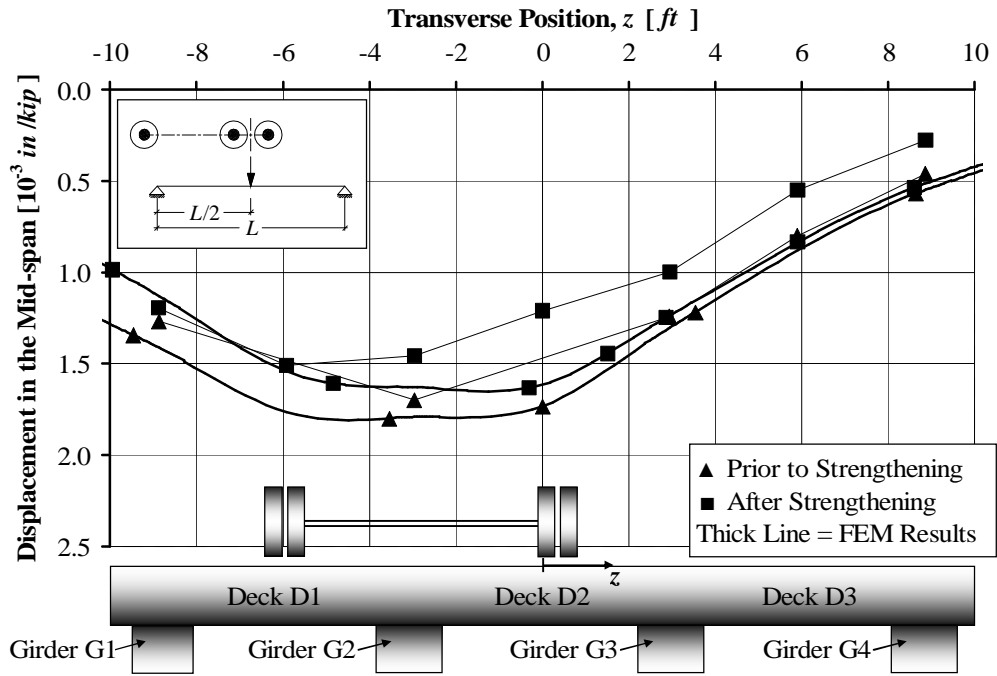


Figure C. 2. Mid-span Displacement prior to and after the Strengthening, Pass #2 and Rear Axle in the Mid-span

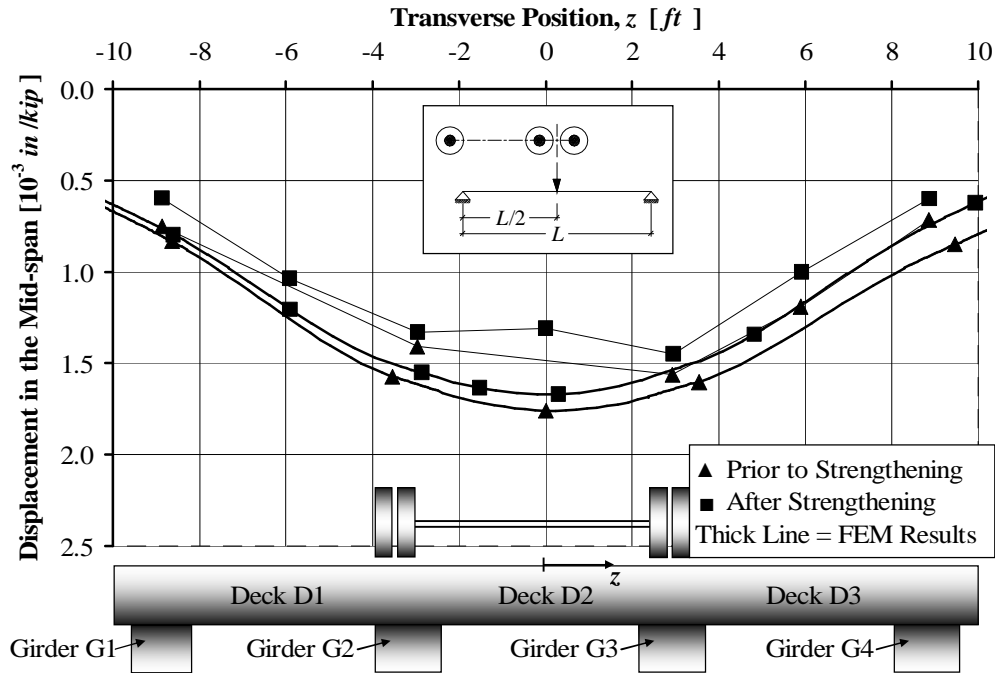


Figure C. 3. Mid-span Displacement prior to and after the Strengthening, Pass #3 and Rear Axle in the Mid-span

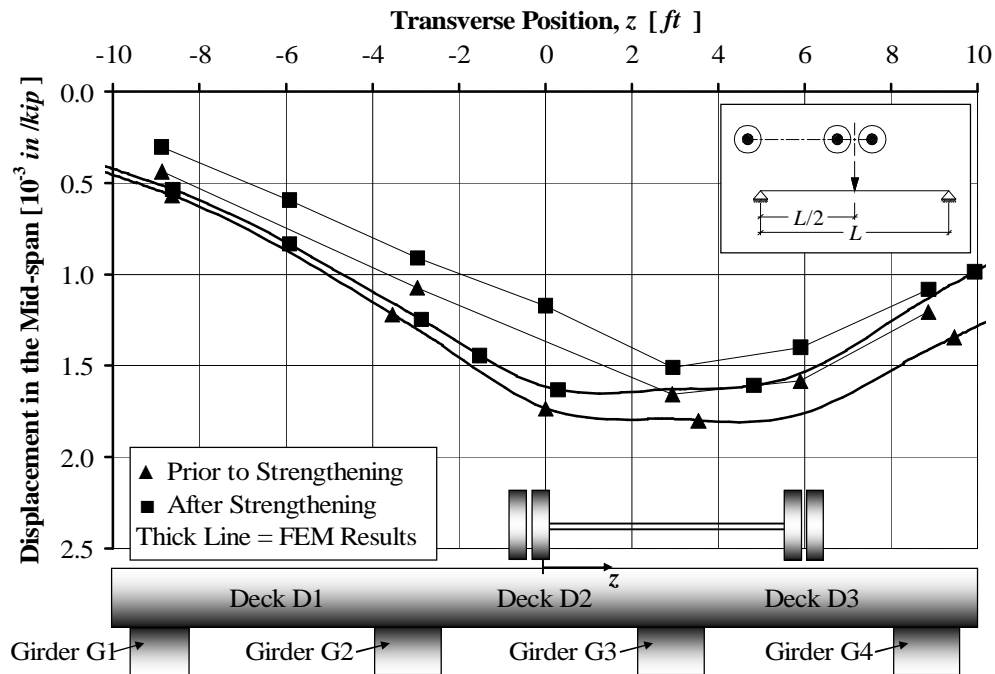


Figure C. 4. Mid-span Displacement prior to and after the Strengthening, Pass #4 and Rear Axle in the Mid-span

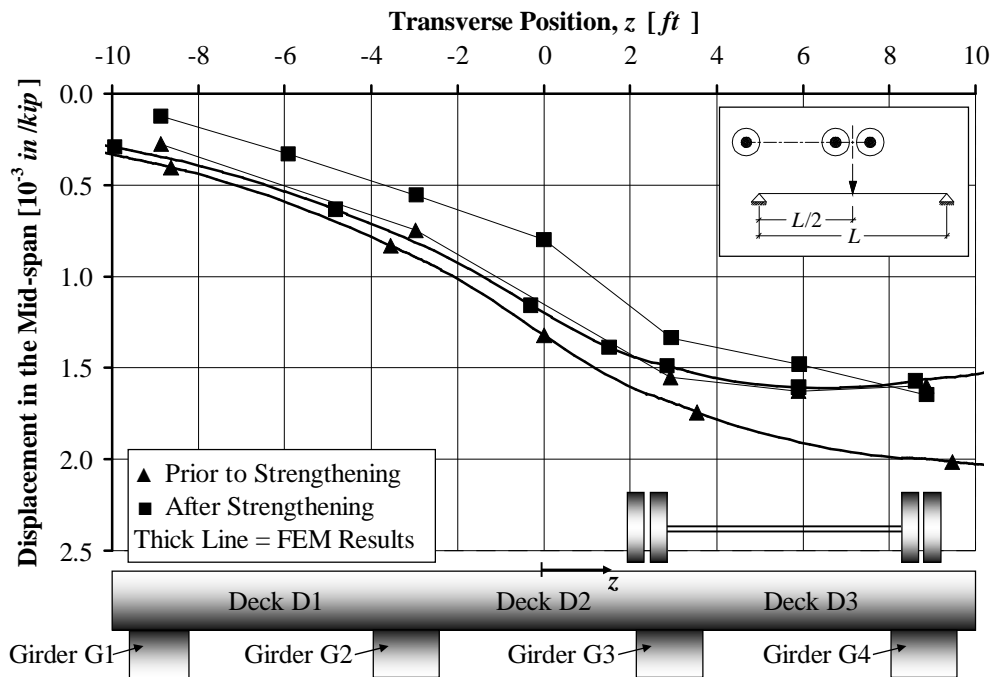


Figure C. 5. Mid-span Displacement prior to and after the Strengthening, Pass #5 and Rear Axle in the Mid-span

## **APPENDIX**

### **D. Dynamic Test Results**

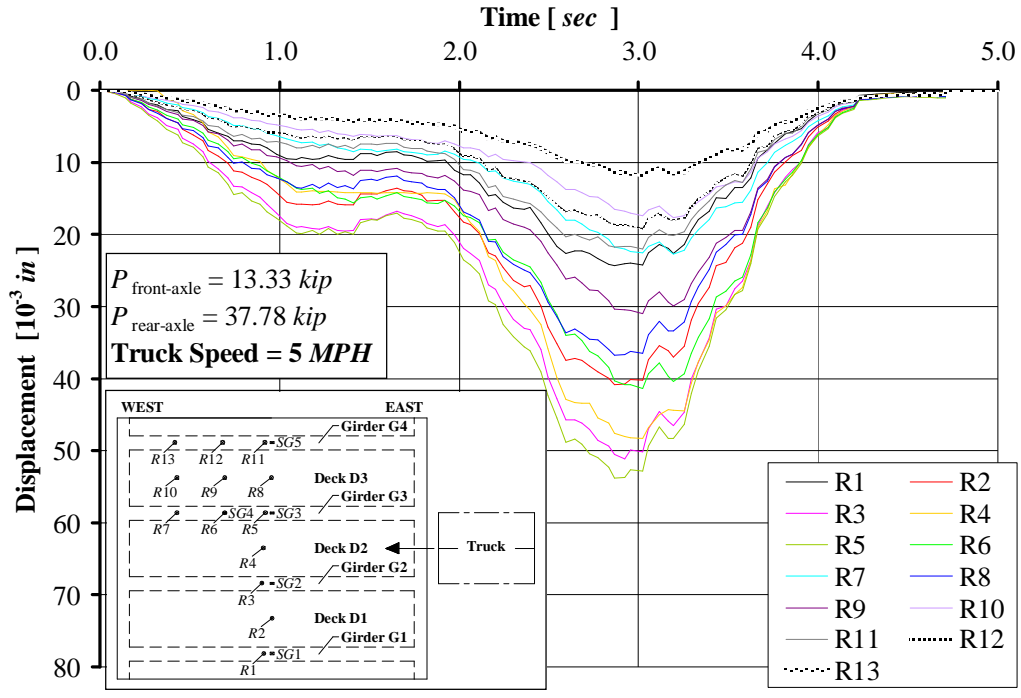


Figure D. 1. After Strengthening Displacements at 2.2 m/s (5 MPH)

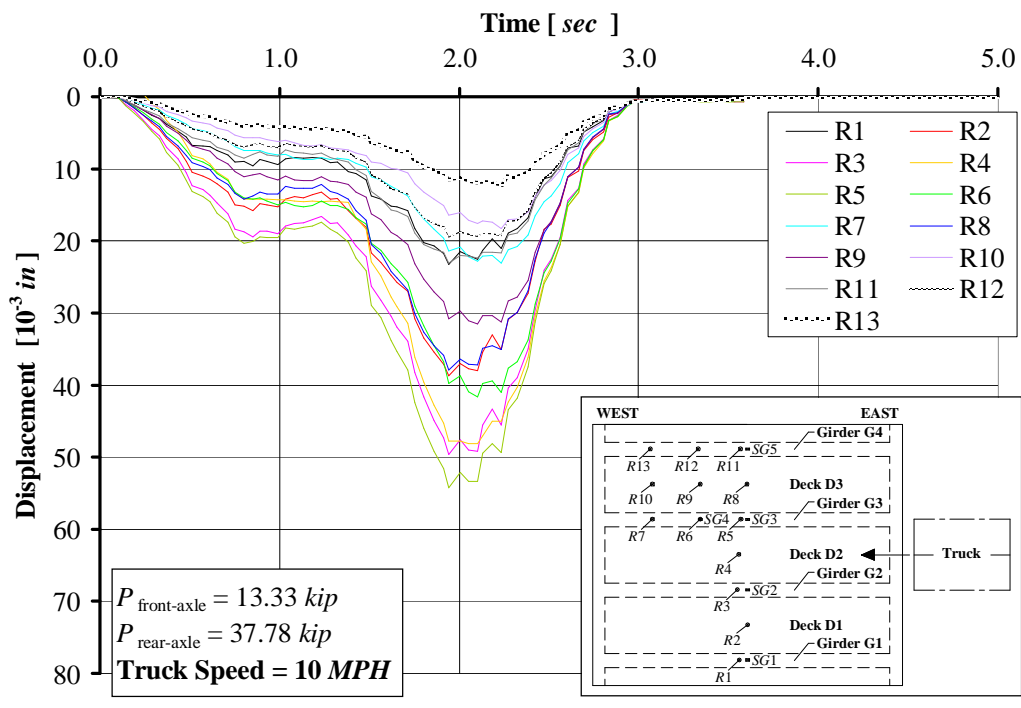


Figure D. 2. After Strengthening Displacements at 4.5 m/s (10 MPH)

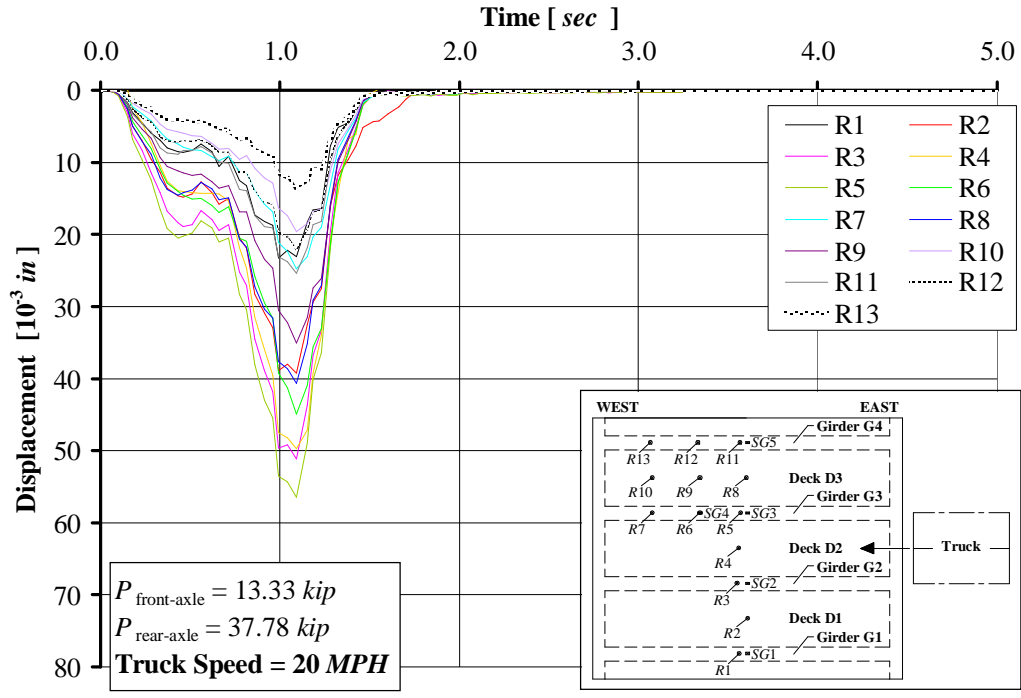


Figure D. 3. After Strengthening Displacements at 8.9 m/s (20 MPH)

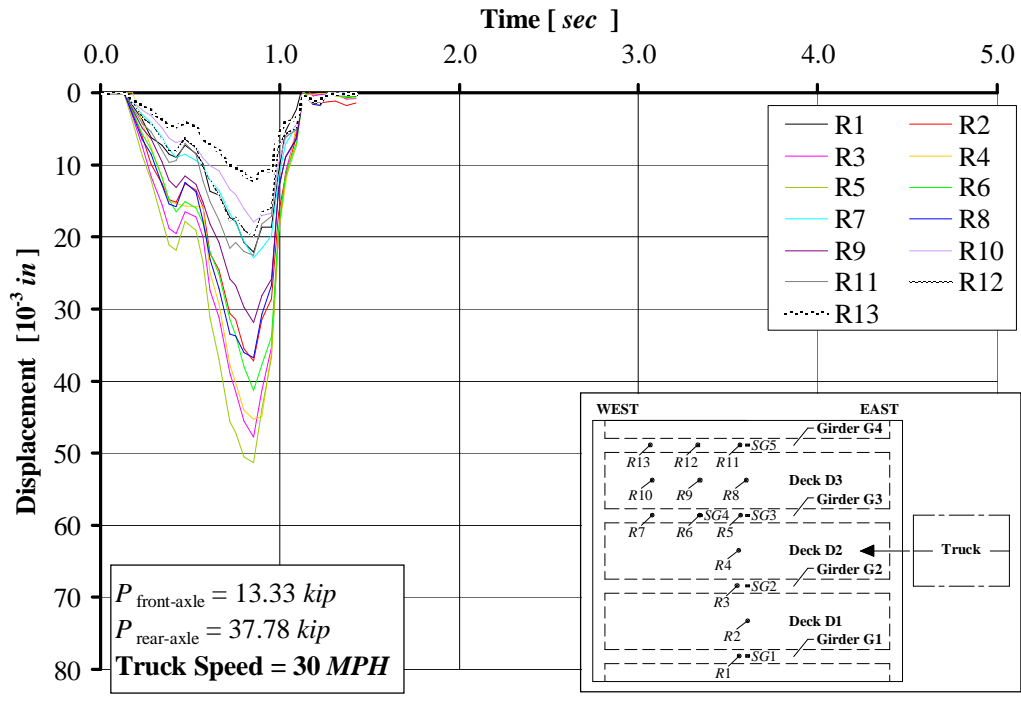


Figure D. 4. After Strengthening Displacements at 13.4 m/s (30 MPH)

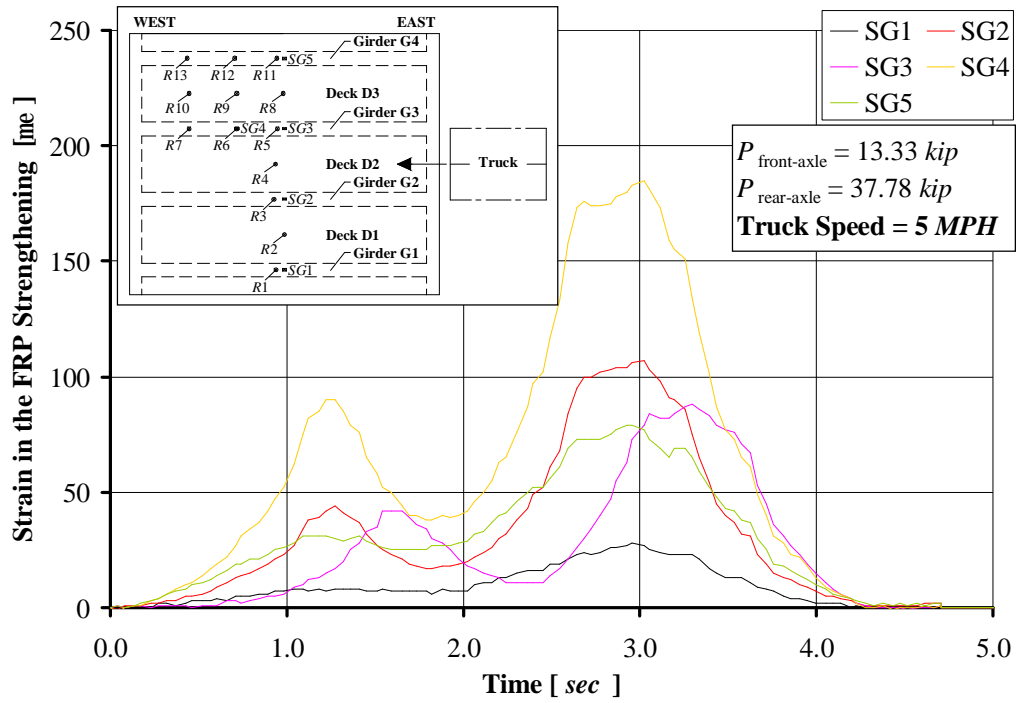


Figure D. 5. After Strengthening Strain in the FRP Laminates at 2.2 m/s (5 MPH)

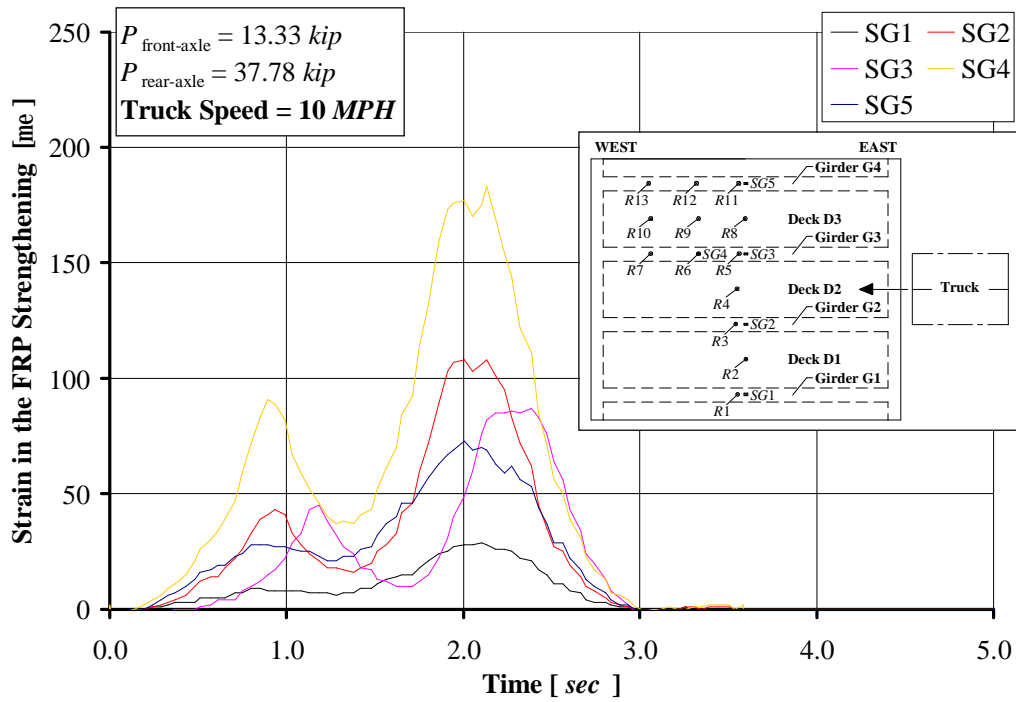


Figure D. 6. After Strengthening Strain in the FRP Laminates at 4.5 m/s (10 MPH)

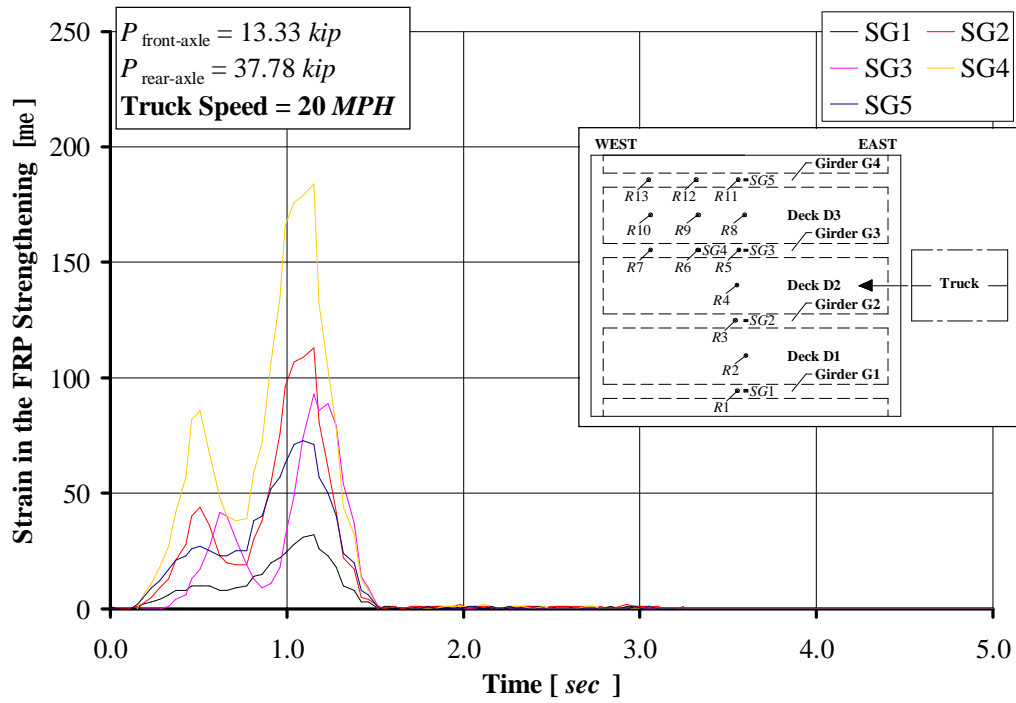


Figure D. 7. After Strengthening Strain in the FRP Laminates at 8.9 m/s (20 MPH)

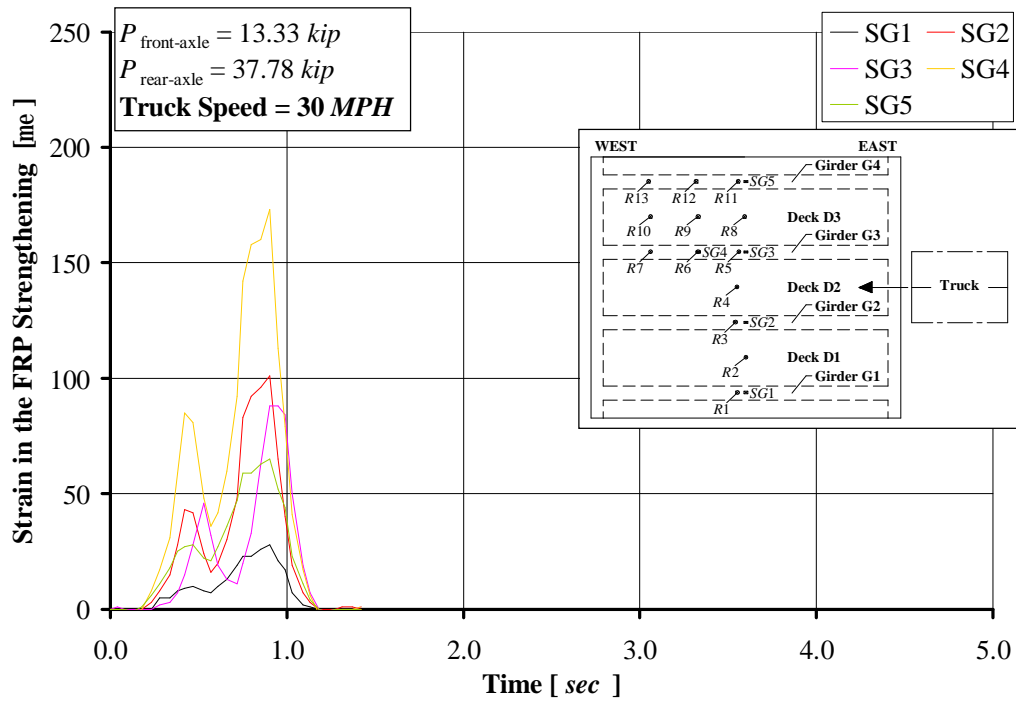


Figure D. 8. After Strengthening Strain in the FRP Laminates at 13.4 m/s (30 MPH)

## **APPENDIX**

### **E. Installation of the MF-FRP Strengthening System**



Figure E. 1. Drilling of the Pre-cured FRP Laminates



Figure E. 2. Positioning of the Pre-cured FRP Laminates



Figure E. 3. Drilling of the Holes in the Concrete



a) Hole Filling with Epoxy



b) Bolt Hammering



c) Torque Control Clamping

Figure E. 4. Fastening Procedure



Figure E. 5. Bridge No. 1330005 after Strengthening